

In presenting the dissertation as a partial fulfillment of the requirements for an advanced degree from the Georgia Institute of Technology, I agree that the Library of the Institute shall make it available for inspection and circulation in accordance with its regulations governing materials of this type. I agree that permission to copy from, or to publish from, this dissertation may be granted by the professor under whose direction it was written, or, in his absence, by the Dean of the Graduate Division when such copying or publication is solely for scholarly purposes and does not involve potential financial gain. It is understood that any copying from, or publication of, this dissertation which involves potential financial gain will not be allowed without written permission.

7/25/68

A DIFFERENTIAL-INTEGRAL APPROACH TO DETERMINE  
THERMALLY INDUCED FLOW OSCILLATIONS

A THESIS

Presented to

The Faculty of the Graduate Division

by

Joachim Teichmann

In Partial Fulfillment  
of the Requirements for the Degree  
Master of Science in Mechanical Engineering

Georgia Institute of Technology

September, 1971

A DIFFERENTIAL-INTEGRAL APPROACH TO DETERMINE  
THERMALLY INDUCED FLOW OSCILLATIONS

Approved:

Chairman

Date Approved by Chairman:

Aug 6, 1971

## ACKNOWLEDGMENTS

The author expresses his appreciation to Dr. Novak Zuber, his thesis advisor, for expert guidance, constant help, and encouragement throughout this research.

Dr. A. E. Bergles and Dr. G. M. Rentzepis are due a special note of thanks for their sincere interest and constructive comments as readers.

Finally the author is grateful to Mamoru Ishii and Gunol Kocamustafaogullari for the many stimulating discussions.

This research program was performed under National Science Foundation grant no. GK-16023 at the Georgia Institute of Technology and the cooperation of the Fulbright Commission/Germany. The author gratefully acknowledges the assistance extended by the above organizations.

## TABLE OF CONTENTS

	Page
ACKNOWLEDGMENTS . . . . .	ii
LIST OF ILLUSTRATIONS . . . . .	v
NOMENCLATURE . . . . .	viii
SUMMARY . . . . .	xii
Chapter	
I. INTRODUCTION . . . . .	1
1. Significance of the Problem	
2. Previous Work	
2.1. Experimental Studies	
2.2. Theoretical Investigations	
3. Purpose and Outline of the Analysis	
II. INSTABILITIES IN TWO-PHASE FLOW SYSTEMS--GENERAL CONSIDERATIONS . . . . .	9
1. The System and Its Thermodynamic Behavior	
2. Kinematics of the System	
3. Dynamics of the System	
4. Method of Solution	
4.1. The Differential Method	
4.2. The Integral Method	
4.3. Stability Analysis	
III. DYNAMICS OF THE SINGLE-PHASE REGION . . . . .	23
1. The Governing Equations	
2. The Equation of Continuity and the Divergence of the Velocity	
3. The Energy Equation	
3.1. Determination of the Boiling Boundary	
3.2. The Dynamic Behavior of the Boiling Boundary	
4. The Momentum Equation	
IV. DYNAMICS OF THE TWO-PHASE REGION . . . . .	45
1. The Governing Equations	
2. The Equation of State	

## Table of Contents Continued

Page

3. The Equation of Continuity and the Divergence of the Velocity	
4. The Density Distribution	
5. Steady State Relations in the Two-Phase Region	
6. The Momentum Equation	
6.1. The Inertia Term	
6.2. The Convective Acceleration Term	
6.3. The Gravitational Term	
6.4. The Frictional Pressure Drop	
6.5. The Exit Pressure Drop	
6.6. The Integrated Momentum Equation	
6.7. Pressure Drop Variations of the Entire System	
V. ANALYSIS OF TWO-PHASE FLOW INSTABILITIES BY MEANS OF AN INTEGRAL METHOD . . . . .	92
1. General Considerations	
2. The Integrated Density Variations in the Two-Phase Region	
2.1. Integral Approach Methods	
2.2. Overall Density Variations by Means of Energy and Constitutive Equations	
2.3. Overall Density Variations by Means of Continuity Equation	
2.4. A Simplified Expression for the Overall Density Variations in the Two-Phase Region	
3. The Averaged Momentum Equation	
VI. STABILITY ANALYSIS . . . . .	121
1. General Considerations	
2. A Simplified Stability Analysis	
3. Similarity Groups Governing the System	
3.1. Geometric Similarity	
3.2. Dynamic Similarity	
3.3. Kinematic Similarity	
4. Dimensionless Stability Criterion	
5. The Stability Plane	
6. Parametric Analysis of the System	
7. Evaluation of the Results	
VII. SUMMARY AND RECOMMENDATIONS . . . . .	153
BIBLIOGRAPHY . . . . .	157

## LIST OF ILLUSTRATIONS

Figure	Page
1. Total Pressure Drop vs. Flow Characteristics . . . . .	5
2. The System . . . . .	11
3. Temperature-Specific Volume-Diagram for Water with 2 Isobars and Condensation and Saturation Lines . . . . .	11
4. Density as a Function of Enthalpy, Time and Position-- "Two-Region" Approximation Showing the Time Lag and the Space Lag . . . . .	14
5. Time Lag Between the Variations of Inlet Velocity and Exit Pressure Drop . . . . .	17
6. Phase Lag Between the Variations of Inlet Velocity and Exit Pressure Drop in the Complex Plane and the Stability Boundary . . . . .	17
7. Block Diagram of the System and Its Two Component Subsystems . . . . .	20
8. Temperature - Entropy - Diagram with 1 Isobar and Condensation and Saturation Lines . . . . .	27
9. The Boiling Boundary as a Function of the Inlet Velocity Perturbation for Varying Frequencies and Constant Subcooling . . . . .	33
10. The Boiling Boundary as a Function of the Inlet Velocity Perturbation for Varying Subcooling and Constant Frequencies . . . . .	33
11. Enthalpy Distributions in the Single-Phase Region Before and After a Velocity Step Function Perturbation	35
12. Pressure Drop Variations for Large Inlet Flow Restrictions $k_i$ . . . . .	41
13. Pressure Drop Variations for Small Inlet Flow Restrictions $k_i$ . . . . .	41

## List of Illustrations Continued

Figure	Page
14. Velocity Perturbation in the Two-Phase Region as a Function of the Inlet Velocity Perturbation . . . . .	57
15. Velocity Distribution for Steady State Conditions . . . . .	57
16. Oscillatory Modes of the Velocity Profile for a Sinusoidal Input . . . . .	59
17. Behaviour of the Velocity Profile for an Inlet Step Function Perturbation . . . . .	59
18. Evaluation of the Density Perturbation Out of a Steady State and a Time Dependent Velocity Profile . .	67
19. Density Distribution in a Complex Plane for Small Frequencies at a Specific Time . . . . .	71
20. Density Distribution in a Complex Plane for Large Frequencies at a Specific Time . . . . .	71
21. Density Distribution for Small Frequencies as a Function of Position . . . . .	72
22. Density Distribution for High Frequencies as a Function of Position . . . . .	72
23. Total Pressure Variations for Higher Frequencies . . .	91
24. The Second Term in Equation 5.45 and Equation 5.46 as a Function of the Exit Velocity . . . . .	110
25. Equation 5.52 as a Function of the Exit Velocity . . .	110
26. Block Diagram of the System . . . . .	125
27. Graphical Representation of the Transfer Function Between Inlet Velocity and Pressure Drop Perturbation .	126
28. Tangential Course of the Transfer Function and Its Dependence on the Parameters . . . . .	126
29. Graphical Solution of Equation 6.19 . . . . .	130



## List of Illustrations Continued

Figure		Page
30.	Stability Plane . . . . .	139
31.	Influence of the Subcooling Number and Phase Change Number on the Stability of the System . . . . .	140
32.	Influence of Several Operational Parameters on the Stability of the System . . . . .	141
33.	Comparison with Levy's Experiments and the Theory of Ishii and Zuber (20) . . . . .	142
34.	Comparison with Solberg's Experiments and the Theory of Ishii and Zuber (20) . . . . .	143
35.	Comparison with Solberg's Experiments and the Theory of Ishii and Zuber (20) . . . . .	144
36.	Comparison with FLARE Experiments and the Theory of Ishii and Zuber (20) . . . . .	145

## NOMENCLATURE

Latin

$a$	defined by Equation 3.58
$a_s$	velocity of sound
$A_c$	cross sectional area of the system
$b$	defined by Equation 3.58
$c$	defined by Equation 3.58
$c_p, c_v$	specific heats
$c_m$	coefficient for friction factor defined by Equation 6.53
$C_r^*$	ratio of exit to inlet velocity
$D$	hydraulic diameter
$f$	friction factor
$f_s$	liquid friction factor
$f_m$	mixture friction factor
$g$	gravitational constant
$G$	mass flux density
$h$	heat transfer coefficient
$i$	enthalpy
$\Delta i_{12}$	subcooling
$\Delta i_s$	maximum subcooling
$\Delta i_{fg}$	latent heat
$k$	variable axial coordinate in the two-phase region
$k_i, k_e$	inlet and exit orifice coefficients
$l$	length of heated channel

## Nomenclature Continued

Latin

$N_{pch}$	phase change number
$N_{\rho}$	density number (ratio)
$N_{Fr}$	Froude number
$N_{sub}$	subcooling number
$N_{Re}$	Reynolds number for the liquid at saturation (flow is entirely liquid)
$P$	pressure
$\Delta P$	pressure drop
$q$	heat flux
$Q(s)$	characteristic function
$R$	gas constant
$s = i\omega$	perturbation variable ( $i = \sqrt{-1}$ )
$\omega$	frequency
$T$	temperature
$t$	time
$u$	velocity
$u_{fi}$	velocity at the inlet of the heated channel
$v$	specific volume
$x$	vapor quality
$x_e$	exit quality
$z$	axial coordinate

## Nomenclature Continued

Greek

$\alpha$	isothermal compressibility
$\alpha_s$	adiabatic compressibility
$\beta$	isobaric expansivity
$\gamma$	ratio of specific heats
$\delta u_1$	inlet velocity perturbation
$\epsilon$	perturbation magnitude ( $\ll \bar{u}_{fl}$ )
$\lambda$	heated region non-boiling length
$\mu$	viscosity
$\Sigma$	heated perimeter
$\rho$	density
$\Delta\rho$	density difference between two phases
$\tau$	time variable
$\tau_b = \tau_{l2}$	residence time in the liquid region
$\phi$	angle between inlet velocity perturbation and pressure response
$\omega$	frequency of oscillation
$\Omega$	reaction of frequency

Subscript

e	exit
f	liquid
g	vapor
i	inlet
m	mixture
I	inlet

## Nomenclature Continued

Subscript

2	saturation
3	exit
12	subcooled region
23	two-phase region

Symbols and Operators

*	dimensionless
$\delta A$	perturbed part of variable A
$\bar{A}$	steady state part of variable A

## SUMMARY

This investigation presents a differential-integral analysis of thermally induced instabilities in two-phase flow systems. The differential method was applied to study the physical behavior of the system and was limited to the evaluation of the total pressure drop of the system. The graphical representation of the results so obtained showed that at high frequencies the pressure drop variations become very large. As this is not in agreement with the derived equations of state, the present investigation was limited to the study of low frequency instabilities.

The simplifying integral method was used exclusively in the treatment of the energy and momentum equation of the second phase. For the first phase and the velocity profile in the second phase exact solutions, previously derived by other investigators, were applied, in order to avoid additional inaccuracies. The overall density variations in the two-phase region were evaluated in two different ways: by means of energy and constitutive equation and directly through the continuity equation. From the results, obtained by these two methods, a very simple expression for the density was found.

The pressure drop variations were determined by simply averaging the momentum equation and introducing in this expression the velocity distribution and the equation for the density.

When the corresponding formulas for the single and the two-phase region were added, overall pressure drop variations of the entire system followed and the characteristic equation was determined. Then, using a simple stability criteria, a stability plane was set up to show the effects which various parameters have on flow stability. A comparison with previous work allowed a careful judgement of the integral method presented in this analysis.

## CHAPTER I

### INTRODUCTION

#### 1.1. Significance of the Problem

The problem of instabilities in two-phase flow systems became relevant in the last few decades with the advent of new technologies, like for example, nuclear and chemical reactors, and sea water desalination processes. Since then this problem has increasingly occupied the attention and interest of scientists and research engineers in the areas of heat transfer, fluid dynamics, and control systems.

Initially a great number of purely experimental investigations were carried out with the purpose of studying these flow and pressure oscillations. The results revealed that, for specific operational conditions of the system, considerable temperature and pressure variations appeared. It is understandable that such oscillations are considered undesirable and harmful. For example, in nuclear or chemical reactors large variations in temperature and pressure can seriously endanger the safety of the reaction process and may even lead to the rupture of the entire operating system.

As it is expected that the application of two-phase flow systems in engineering will increase in the future, the idea of studying in detail through experimental and theoretical analysis the physical nature of flow instabilities should be of considerable use. Moreover, in order to avoid these instabilities and guarantee reliable operating conditions,



fundamental studies on the dependence of these detrimental oscillations on the system parameters appear to be of eminent importance.

The particular objective of this work is to present a theoretical investigation of the measured and observed oscillations in numerous experimental analysis. In addition by using a simplifying integral method, this work attempts to approximate the dependence of these oscillations on the system parameters as well as to prove the validity of the integral method itself.

## 1.2. Previous Work

### 1.2.1. Experimental Studies

In the past, as mentioned, a great deal of largely experimental work has been performed in the area of two-phase flow instabilities. In his theoretical analysis, which was the basic reference for the present work, Zuber (1) gives a very detailed enumeration of the research made so far, indicating also the most interesting results the different authors obtained.

In general the extensive experimental investigations showed that mainly two types of oscillations seem to lead to major flow instabilities: acoustical and chugging oscillations. Hines and Wolf (2) describe the first one audible as a clear and steady scream of high frequency (3000 - 75000 Hz) and the second one as an oscillation with a lower frequency (600 - 2400 Hz) audible as a pulsating noise.

Cornelius and Parker (3,4) specify the dependence of these two prevalent oscillations on the temperature: the frequency of the acoustical oscillations decreases, whereas for chugging oscillations it increases

with temperature.

Scientists and research engineers who have been working on this very complex problem of instabilities in two-phase flows generally admit that the incipience of flow and pressure oscillations occur because of the large variations of the thermodynamic and transport properties of the fluid in the super- and subcritical thermodynamic region. Therefore several of their reports include interesting efforts to find qualitative explanations of the phenomena generating instabilities.

So for example, Firstenberg (5) makes the heat transfer coefficient dependence on the various flow regimes responsible for the oscillations. Thurston (6) and Shitzman (7,8) note that the large variations of the specific heat at the "pseudocritical" or the "transposed" critical temperatures (note: these are at supercritical pressures, the temperatures for which certain thermodynamic properties reach a maximum) lead to the appearance of critical flow conditions. Hines and Wolf (2) consider the strong temperature dependence of the viscosity at supercritical temperatures to be the reason for the oscillations occurring. Cornelius and Parker (3) argue that acoustical as well as chugging oscillations have their origin in the pressure dependent heat transfer rate. In addition to these observations, other investigators cite several more physical phenomena for these undesirable flow conditions (9, 10).

#### 1.2.2. Theoretical Investigations

Because of its complexity, relatively little analytical work has been done to date on the problem of instabilities in two-phase flow systems. In the following only the more important investigations will

be briefly discussed.

Although the main purpose of this analysis is to investigate dynamic or oscillatory instabilities, a brief reference will be made to the early studies of Ledinegg (11), who first treated static or excursive instabilities. These are only possible at relatively low flow rates and low pressure levels. The criterion which he formulated is that a system operates at unstable conditions if the steady-state pressure drop curve as a function of the flow rate has a negative slope ( $\Delta P / \Delta G < 0$ ). For such conditions a sudden change in flow pattern and flow rate would always lead to conditions where  $\Delta P / \Delta G > 0$  and a return to the original state is impossible. This instability is therefore called aperiodic or excursive. Figure 1 shows qualitatively the flow rate domain in which stable operation is not possible.

Later on Ledinegg (12) and Profos (13, 14, 15) analyzed the transient behavior of once-through boilers for higher flow rates. These investigations describe several physical phenomena rather well; however they do not consider dynamic instabilities. It should also be mentioned that both authors introduce graphical methods in their mathematical procedures, which makes understanding the problem rather difficult.

Early in the sixties, Wallis and Heasley (13) published a mathematical analysis, which since then has been repeatedly used as a reference in subsequent reports.

About the same time Quandt (17) presented an analytical solution of the problem by utilizing the technique of small perturbations. This method again is exclusively mathematical, but does not present a

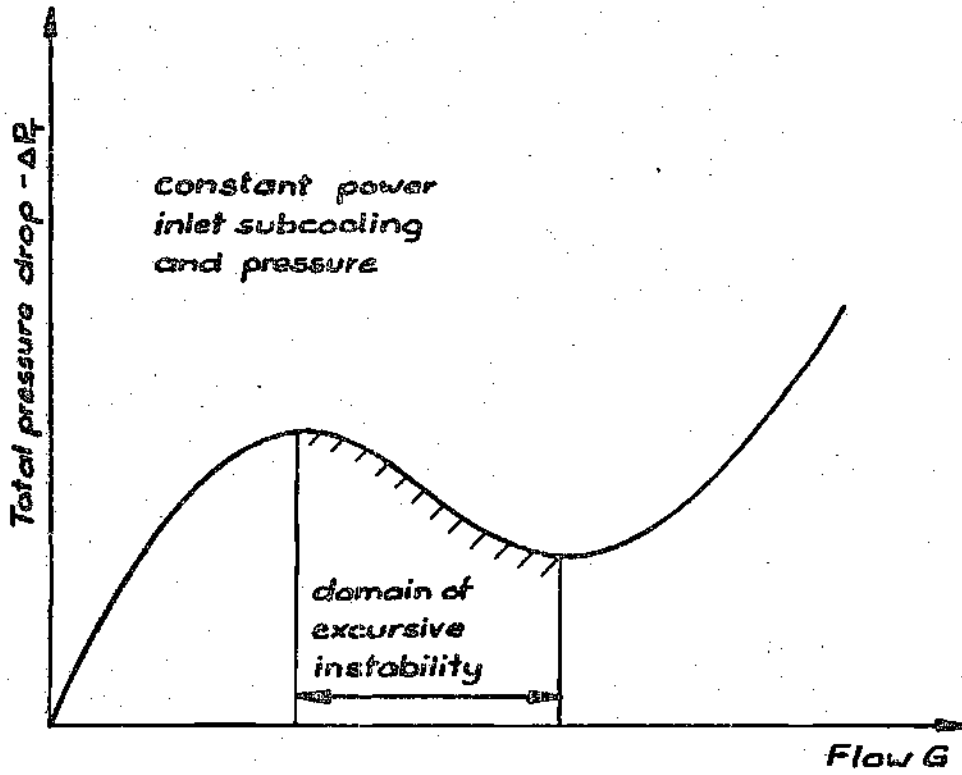


Figure I. Total Pressure Drop vs. Flow Characteristics

physical discussion of the problem. Moreover, the mathematical procedure itself is rather complicated.

Recently Mayinger (18) made a study on instabilities in two-phase flow systems. His analysis is basically a solution of the fundamental differential mass, momentum, and energy equations by converting these into difference equations and solving them numerically by computers.

A very extensive analytical and experimental solution of the problem has been presented by Yadigaroglu and Bergles (19). The report investigates in detail the influence of several phenomena. In the single phase region, for example, the dynamics of the heated wall, variable heat transfer, and the dependence of the boiling boundary on the pressure were considered. In the two-phase region account is taken of the variations of saturation temperature and other properties with pressure in space, by making use of a reference pressure profile. Furthermore an enthalpy trajectory model was introduced, to predict the pressure drop in the two-phase region with oscillating flow. At the end of their analysis, the authors present stability maps and the theoretically predicted stability threshold, which exhibits also a correct behavior.

Finally, Ishii and Zuber (20) made extensive studies in this area. In the two-phase flow region the analysis takes into account the effects of the relative velocity of the two phases by formulating the problem in terms of the center of mass of the mixture. It thus eliminates confusing theories based on different expressions for the velocity "slip" ratio, which were introduced by various authors previously. The set of four partial differential equations

(continuity, momentum, and energy for the mixture and continuity for the vapor) was integrated for the case of thermodynamic equilibrium, from which they obtain a characteristic equation for the system. The investigations present a detailed discussion of appropriate scaling criteria, which the authors apply in the evaluation of the characteristic equation. Its solution is a stability plane, which shows the effects the various parameters (such as mass flow rate, subcooling, power input, etc.) have on flow stability. The theoretically obtained results are in remarkably good agreement with experimental data, which makes this analysis one of the most significant in this area. Extensive use of this reference will be made in the present report.

### 1.3. Purpose and Outline of the Analysis

Most of the theoretical studies, which were briefly discussed so far in the previous section have in common that the mathematical treatment is very lengthy. The main purpose of this analysis will be to study the usefulness of the integral method in the investigation of two-phase flow instabilities. The integral approach has found wide application in the area of momentum, heat, and mass transfer. Its main advantage is that it shortens considerably the computational procedures. On the other side it requires a deep understanding of the physical phenomena in the system. Therefore, this work will also present a thorough study of the differential method, which will be mainly based on previous investigations of Serov, Smirnov, Teletov and Boure (21, 22, 23, 24, 25, 26, 27). These authors formulate the

problem as follows: the two-phase flow system consists of two regions, a single phase and a two-phase flow region, both divided by a boiling boundary. For each region a constitutive equation and the three field equations describing the conservation of mass, momentum, and energy are established. In order to decouple the momentum equation from the energy and the continuity equation, the density of the medium is assumed only to be a function of the enthalpy.

The report will mainly follow the mathematical outline of Zuber (1). Its most significant contributions will be the graphical interpretations of the transfer functions, a simplified mathematical procedure in evaluating an expression for the density perturbation as a function of space and time, and the application of an integral method to shorten the entire theoretical analysis.

The investigation can be summarized as follows: the present Chapter I is an extensive introduction to the problem. In Chapter II the system, its thermodynamic behavior, its kinematics and dynamics and the method of solution will be discussed. Chapters III and IV will be devoted to the exact solution of the problem and in Chapter V the integral method will be treated. In Chapter VI the stability analysis will be performed and the report will conclude with an outline of the results in Chapter VII.

## CHAPTER II

## INSTABILITIES IN TWO-PHASE FLOW SYSTEMS--GENERAL CONSIDERATIONS

2.1. The System and Its Thermodynamic Behavior

As the extensive literature in this field shows, the thermo-hydrodynamics in two-phase flow systems are of a very complex nature. Therefore, to make a stability analysis accessible, a simplification of the system by introducing an appropriate model appears to be a necessity. A model that takes into account all possible effects very easily can result to be mathematically inextricable. On the other hand, a too-simplified formulation can endanger the accuracy of the analysis itself and consequently limit its applicability.

The present work will use, as was stated in Chapter I, the same model Serov and Teletov (22, 25) apply in their investigations. The two-phase flow system will be therefore simplified in the following way:

(1) It will operate at constant pressure as well in the supercritical as in the subcritical region.

(2) Heat addition will be constant along the duct. This implies that the product of the varying heat transfer coefficient  $h$  and the temperature difference  $\Delta T = T_{WALL} - T_{LIQUID}$  will also remain constant.

(3) There will be no radial temperature distributions. This presupposes very high heat conductivity and constant temperature for every cross sectional area.



(4) Boiling will start at the so called boiling boundary at which the medium will always have saturation conditions. This boundary represents a separation of the two-phase region from the single-phase region. Both will be treated separately.

(5) In the two-phase region, the vapor and the liquid phase will move with no relative velocity to each other.

(6) The fluid will have to pass two flow restrictions, one located at the entrance, the other at the exit. It will be one of the purposes of the analysis to determine the dependence of the operational conditions of the system on these two flow restrictions. Figure 2 shows the system schematically.

Once we have set up the model, the thermodynamic process can be described very easily in a temperature-specific volume plane for sub- and supercritical pressures. As the present analysis is mainly oriented towards its applicability in relation with boiling water reactors, the diagram in Figure 3 is given for water.

At subcritical pressures the fluid behaves as follows: it enters the duct with velocity  $u_1$  at ① and remains in the liquid phase until it reaches the saturation line at ②, whereby its temperature increases considerably at constant specific volume. At ② a phase change occurs. Now the temperature is constant but the specific volume increases. Therefore for the following discussions in the next chapters, we will especially bear in mind that the boiling boundary, which was introduced in our model, represents the transition from the heavy to the light phase and that this transition point corresponds to the saturation enthalpy.

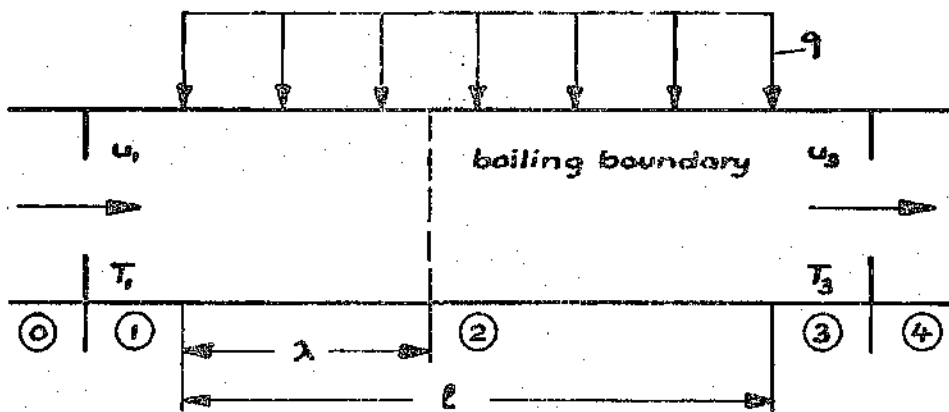


Figure 2. The System

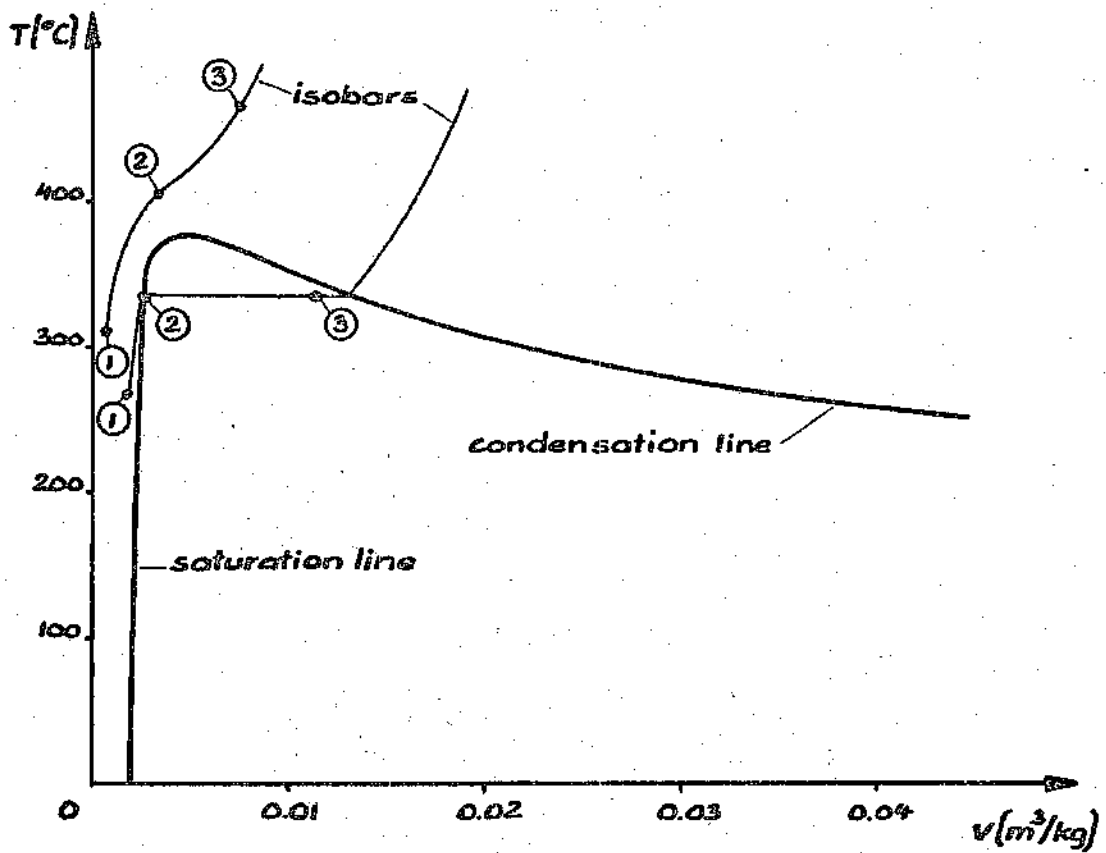


Figure 3. Temperature, Specific Volume-Diagram for Water with 2 Isobars and Condensation and Saturation Lines

At supercritical pressures, as Figure 3 shows, such a transition from the liquid to the gas phase cannot be clearly defined, because at these pressures as well as at the critical one, the interface, the heat of vaporization and the surface energy all vanish. At present there is no general agreement where and how the phase transitions occur. In analogy to the subcritical pressure range, where various thermodynamic properties, such as the specific heat, the compressibility, etc., change discontinuously or reach a maximum value at the saturation line, numerous authors consider its extension into the supercritical region to be the line for all points, where the thermodynamic properties listed below reach a maximum, for example:

$$\left. \frac{\partial c_p}{\partial P} \right)_T = 0 \quad 2.1$$

$$\left. \frac{\partial c_p}{\partial T} \right)_P = 0 \quad 2.2$$

$$\left. \frac{\partial^2 v}{\partial T^2} \right)_P = 0 \quad 2.3$$

Of course there are many other criteria. Unfortunately each of these lie on different lines. But assuming that their course in the supercritical thermodynamic region does not differ very much from each other, we will choose the third condition to be representative for the saturation line. With other words, we say, that the so called "phase

transition" occurs when  $\partial^2 v / \partial T^2)_p = 0$ . Therefore the thermodynamic process in Figure 3 is as follows: we imagine the fluid to enter at point ①. Between ① and ② it will accumulate thermal energy until in accordance to our previous observations it reaches the "saturation line" and a phase change starts. At point ③ the fluid is a mixture of "liquid" and "vapor."

As a conclusion to our thermodynamic observations, it should be emphasized that only the establishment of the model made a description of the process in a thermodynamic diagram possible.

### 2.2. Kinematics of the System

In the following the kinematics of the simplified model shall be discussed in some detail. Figure 4 shows the density as a function of enthalpy, time and position. The continuous lines describe qualitatively the real conditions in a two-phase flow system. It can be seen that the curves are for small enthalpy values straight lines parallel to the corresponding abscissa. As the fluid gets at subcritical pressures close to the saturation line or at supercritical pressures close to the line for which  $\partial^2 v / \partial T^2)_p = 0$ , the density decreases steadily. Finally its functional dependence on the enthalpy, time or position becomes of hyperbolic character.

If we introduce again in accordance to the assumptions of our model, the simplifications into the graphs of Figure 4, the density distributions experience two important alterations:

(1) The actual density distribution consisting of three different regions (constant, transition and hyperbolic) has been replaced by a

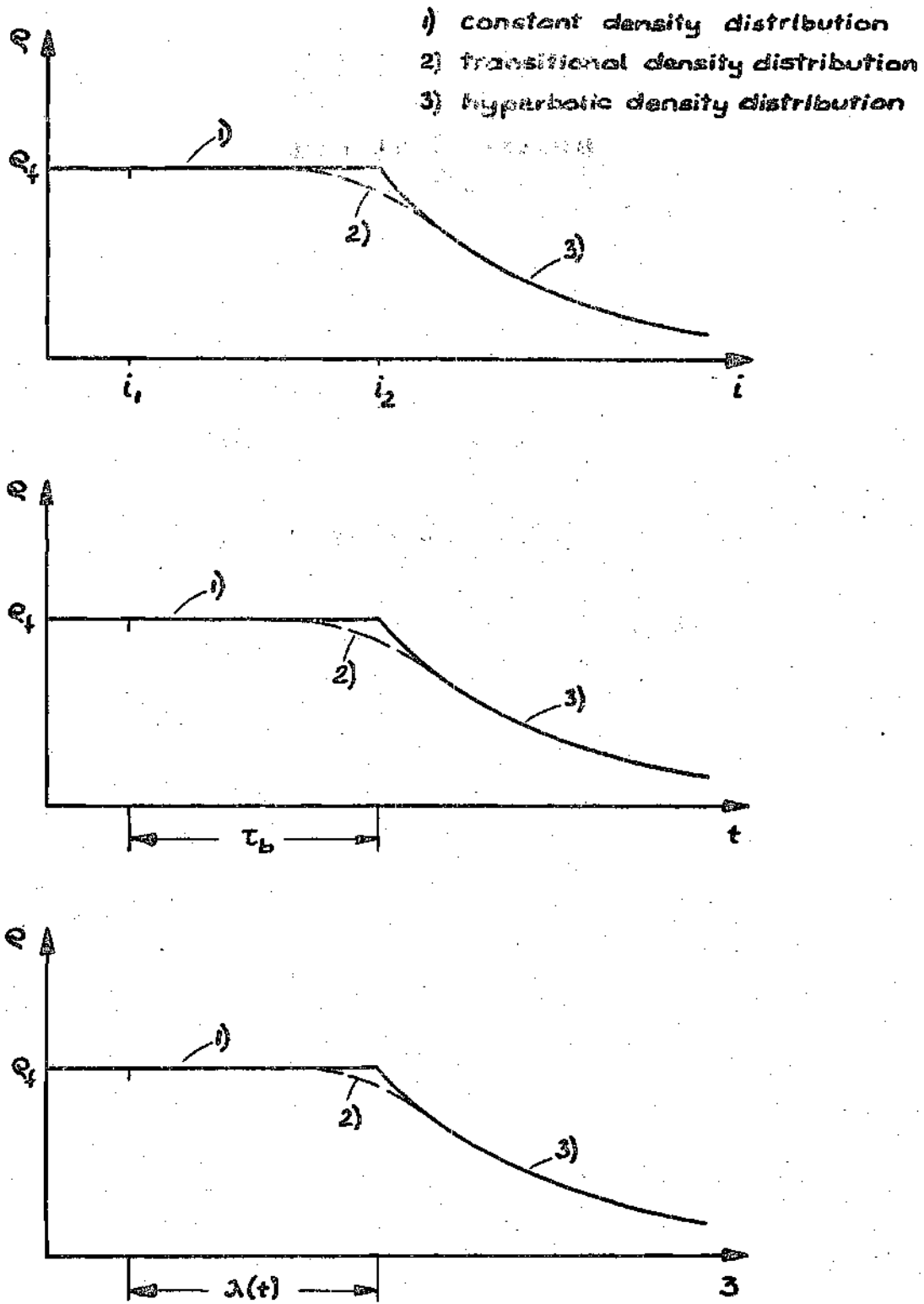


Figure 4. Density as a Function of Enthalpy, Time and Position - "Two-Region" Approximation Showing the Time Lag and the Space Lag

two region approximation.

(2) The two-region density profile consists of one straight line and a hyperbolic function and has a discontinuity at their intersection.

The behavior of a particle from the time it enters the heated section will be therefore as follows: in the first portion of the system, although its temperature increases considerably, the density will remain constant. When the particle reaches saturation conditions, a phase change will occur and from then on its density will decrease exponentially with time. The motion of the particle for steady state conditions through the two-phase flow system depends therefore on two characteristic values:

(1) The time elapsed between the injection of the "heavy" particle in the heated duct and its transformation to the "light" fluid, which will be denoted as the time lag  $\tau_b$ .

(2) The slope of the linear functional relationship between velocity and position in the two-phase region. As will be seen in Chapter IV, the slope, which will be called in analogy from combustion theory reaction frequency, depends only on the system parameters.

For the case that the flow process through the duct is also time dependent, the space lag  $\lambda(t)$ , which indicates the location in the duct, where the transformation from the "heavy" to the "light" fluid takes place, will also have to be given.

### 2.3. Dynamics of the System

According to control theory, the dynamics of a system are best examined by observing the response of the system to a given inlet

perturbation of the inlet velocity, for example, a sinusoidal function. As in the results that Crocco and Cheng (28) obtained from extensive studies in the field of combustion, here we also shall distinguish two different modes of response: random fluctuations and organized or coordinated oscillations.

Random fluctuations will always appear in a system whenever there is no coordination or dependence among the different properties or parameters.

Organized oscillations of a system will be present if there exists a mechanism for intermittent storage and release of some particular form of energy. Such a mechanism for example are the oscillations of pressure, which will affect the saturation temperature thereby inducing oscillations in the rates of evaporation. These, in turn, may induce flow oscillations. Variations of the boiling boundary as a function of the inlet flow, density, and velocity oscillations in the second phase, as well as variable heat transfer coefficients and flow regime changes may also contribute to the formation of such mechanisms. Considering the inlet velocity to be the input of our system and the pressure drop along the duct to be the response, the previously described mechanisms will determine as well the amplitude as the phase lag of the response with respect to the inlet perturbation. Figure 5 shows how two sinusoidal movements can be related time-wise to each other.

It is evident that under certain operational conditions the timing between inlet and outlet could be such that for increasing velocity perturbation the pressure variation decreases or viceversa. In this case, regenerative feedback is present. The response will perform

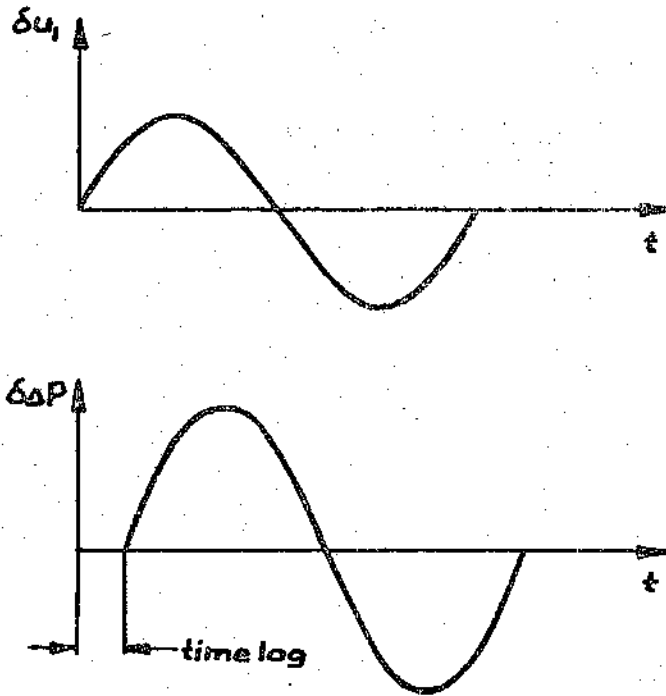


Figure 5. Time Lag Between the Variations of Inlet Velocity and Exit Pressure Drop

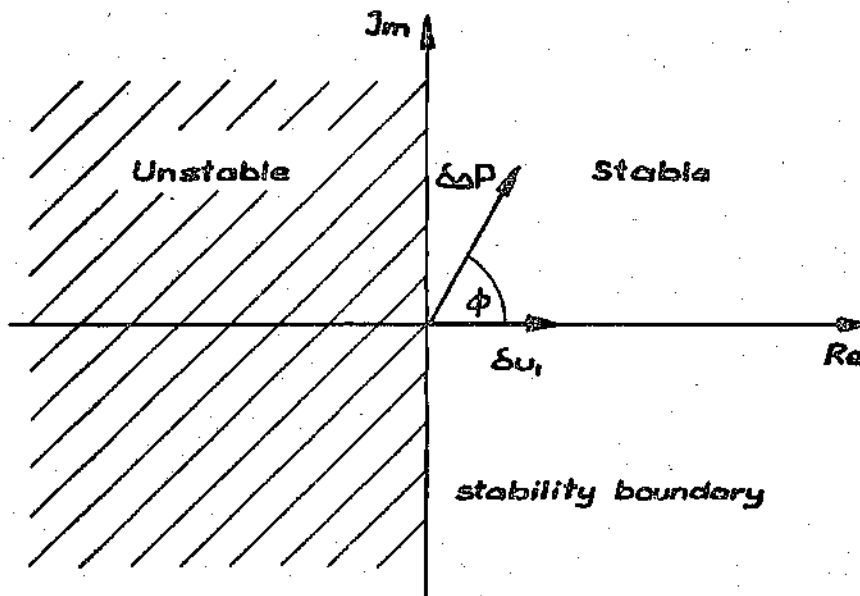


Figure 6. Phase Lag  $\phi$  Between the Variations of Inlet Velocity and Exit Pressure Drop in the Complex Plane and the Stability Boundary



undamped oscillations, because energy is supplied to the system at the proper frequency and phase relation in order to overcome the losses due to various damping effects, as for example friction.

If the phase lag between input and output is equal to  $\pi$  the system will be certainly unstable, because the gradients of both oscillations will always have opposite signs. In practice small deviations from these operational conditions can fairly well imagined also to be unstable. Therefore the following more rigorous stability criterion will be used in this analysis: system instability will always be present, whenever opposite signs of the gradients of inlet perturbation and outlet response predominate over a whole period. For stability therefore the phase lag  $\phi$  between output and input has to be

$$-\frac{\pi}{2} < \phi < \frac{\pi}{2} \quad 2.4$$

In a complex plane, plotting the inlet on the real axis, the output will have to be on the right hand side of the imaginary axis. Figure 6 shows this graphically.

Before we proceed to present the method of solution, let us point out one very important feature of our analysis: in the first three sections of this chapter, we presented a model and its operational behavior, which will be used in this analysis to study the pertaining problem. Here we assumed that for unperturbed flow conditions, the two-phase flow is at a certain position also time independent. In reality it is known that in flow boiling several physical effects exist that are highly time dependent. Among these we can cite

nucleation, formation and detachment of bubbles, the behavior of the different flow regimes and mainly their transitions to each other, variations of pressure with flow conditions and finally changes of the heat transfer coefficient. In other words our system was considered on the whole to be time independent, but several properties like density, pressure, enthalpy and velocity profiles were varying with time locally without influencing the overwhole behavior of the system. These local variations can also have an oscillatory character. They represent again potential organized oscillations and therefore under certain operational conditions they might influence decisively the dynamic response of the system. By introducing a simplifying model, we will have to keep in mind that all these small scale effects will not be taken care of in our analysis.

## 2.4. Method of Solution

### 2.4.1 The Differential Method

The simplified system introduced in sections 1, 2 and 3 of this chapter can actually be subdivided in two subsystems with a moving boundary. The first subsystem will be the liquid phase and the second one the two phase region. To analyze the dynamic behavior of the whole system, or more specifically the functional relationship between pressure drop and inlet velocity perturbation, the three general field equations and corresponding constitutive equations will be applied to each subsystem. Therefore the method of solution can be outlined as follows (see Figure 7):

The inlet velocity of the subsystem ①, which represents the

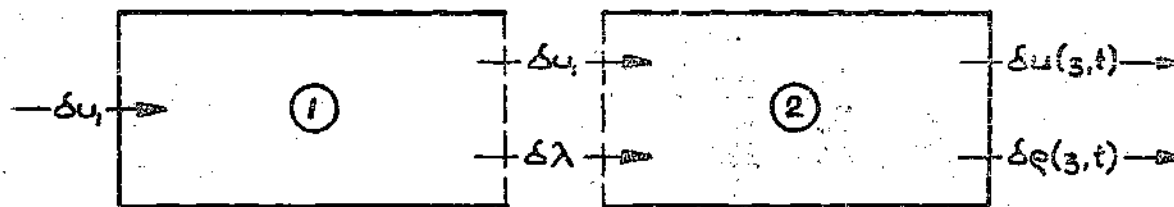


Figure 7. Block Diagram of the System and its Two Component Subsystems

"heavy" fluid region, will be perturbed. As the density is constant, the velocity can be obtained immediately out of the continuity equation. By integrating the energy equation in which the velocity has to be introduced, we obtain the boiling boundary  $\lambda(t)$ , which at the same time represents the boundary of the first subsystem. Therefore we can say that out of the first subsystem we obtained two responses: the velocity of the liquid and the movement of the boiling boundary. These two outputs will be the input of the second subsystem, for which we will have to assign an appropriate expression for the equation of state, depending whether the system is supposed to work at sub- or supercritical conditions. By solving simultaneously the continuity and energy equation, we get the velocity distribution. Introducing this expression back into the continuity equation and taking into account for the moving boiling boundary  $\lambda(t)$ , the density variations along the duct will be obtained. With the velocity and density in both subsystems known, the momentum equation will be evaluated to get an expression for the pressure drop variations. The exact solution of this problem was treated extensively by Serov, Teletov, Boure, Zuber and Ishii and Zuber. The present work therefore only offers a qualitative analysis. The reason why such an extensive theoretical investigation was performed was to study physical phenomena, which will permit a detailed analysis of advantages and disadvantages of the integral method.

#### 2.4.2. The Integral Method

Integral methods of analysis have found ample applications in the mechanics of continua. In heat transfer and fluid mechanics a great variety of problems appeared, where the use of the differential

equations of change delivered very complicated solutions. By integrating these equations over a finite volume of the system, thereby obtaining overall balances of mass, momentum and energy, information on the gradients inside the system is lost and only relations between the properties at the inlet and outlet can be given. But still in numerous cases, the power and simplicity of the integral method has been proven. In fluid dynamics for example satisfactory results can be obtained in the evaluation of the local friction coefficient for the flat plate in an incompressible flow assuming in the boundary layer a third order velocity distribution that satisfies the boundary conditions.

In our problem of two-phase flow instabilities, the integral method will be used exclusively in the treatment of the energy and momentum equations of the second phase. The evaluation of the first phase and the velocity profile in the second phase will be performed by using the exact solutions, obtained by Serov, Teletov, Boure, Zuber and Ishii and Zuber (22, 25, 26, 1, 20), in order to optimize the approximation of the integral method.

#### 2.4.3. Stability Analysis

To avoid extensive computation procedures a simplified stability criterion, first used in the analysis of Ishii and Zuber (20), will be applied. After non-dimensionalizing the obtained stability equation, a stability plane will be set up, to show the effects, which various parameters (such as mass flow rate, subcooling, power input, etc.) have on flow stability. Finally a comparison with previous work, mainly the theoretical analysis of Ishii and Zuber (20) and experimental data, will allow a careful judgement of the integral method, presented in this analysis.

## CHAPTER III

## DYNAMICS OF THE SINGLE-PHASE REGION

3.1. The Governing Equations

The single-phase region will be defined as the channel length extending from the inlet plenum to the boiling boundary, at which the mixed mean enthalpy is at saturation. Any occurrence of subcooled boiling in this region will be neglected and it will be assumed that the fluid in this region is incompressible. The problem will be formulated in terms of three field conservation equations and a constitutive equation of state. For a one-dimensional situation, the single-phase region is described in terms of the continuity equation

$$\frac{\partial \rho}{\partial t} + u \frac{\partial \rho}{\partial z} + \rho \frac{\partial u}{\partial z} = 0 \quad 3.1$$

the energy equation

$$\frac{\partial i}{\partial t} + u \frac{\partial i}{\partial z} = \frac{1}{\rho} \frac{q_s}{A_c} \quad 3.2$$

and the momentum equation

$$-\frac{\partial p}{\partial z} = \rho \frac{\partial u}{\partial t} + \rho u \frac{\partial u}{\partial z} + g \rho + \frac{f}{2D} \rho u^2 \quad 3.3$$

Assuming the density to be independent of the temperature and the process to be isobaric, the thermal constitutive equation of state becomes simply

$$\rho = \rho_f = \text{const} \quad 3.4$$

### 3.2. The Equation of Continuity and the Divergence of the Velocity

Introducing equation 3.4 into the continuity equation, we get

$$\frac{\partial u}{\partial z} = 0 \quad 3.5$$

Therefore the divergence of the velocity is equal to zero. By integrating equation 3.5 we obtain an expression for the velocity distribution, which is only a function of time

$$u = u(t) \quad 3.6$$

To analyze the stability problem a small time dependent velocity perturbation  $\delta u_1$  will be superimposed on the steady state inlet velocity  $\bar{u}_1$ . The velocity distribution in the liquid phase thus becomes

$$u_1(t) = \bar{u}_1 + \delta u_1 \quad 3.7$$

The velocity variation  $\delta u$ , will be given in exponential form

$$\delta u = \epsilon e^{st} \quad 3.8$$

where  $s$  is a complex number.

### 3.3. The Energy Equation

#### 3.3.1. Determination of the Boiling Boundary

To obtain the position of the boiling boundary, we integrate the energy equation

$$\frac{\partial i}{\partial t} + u(t) \frac{\partial i}{\partial z} = \frac{q_s}{\rho_f A_c} \quad 3.9$$

The solution of the first-order partial differential equation can be obtained by the method of characteristics. In this case the general solution of equation 3.9 is

$$\psi_2 = f(\psi_1) \quad 3.10$$

where

$$\psi_1(i, t, z) = C_1 \quad \text{and} \quad \psi_2(i, t, z) = C_2 \quad 3.11$$

are solutions of any two independent differential equations which imply the relationships



$$dt = \frac{dz}{u(t)} = \frac{di}{\frac{q \xi}{\rho_f A_c}}$$

3.12

Taking alternately the first and the second equation, the first and the third equation, we obtain the following set

$$\frac{dz}{dt} = u_1(t) \quad 3.13$$

and

$$\frac{di}{dt} = \frac{q \xi}{\rho_f A_c} \quad 3.14$$

Equation 3.13 is an ordinary differential equation of the first order. The integration of this equation, considering the appropriate boundary conditions, will give the position  $z$  of a particle as a function of time. Therefore equation 3.13 describes the kinematics of the fluid in the single-phase region.

Equation 3.14 is also an ordinary first order differential equation and is dependent on such parameters as heat addition, density of the liquid and geometry of the system. Its integration will describe how the enthalpy varies with time and is therefore simply an energy balance, in which the constitutive equation has already been taken into account. To solve equation 3.14 the boundary conditions will have to be specified. Hereto we reconsider the process in a T-s diagram (temperature-entropy) of Figure 8. The fluid enters at

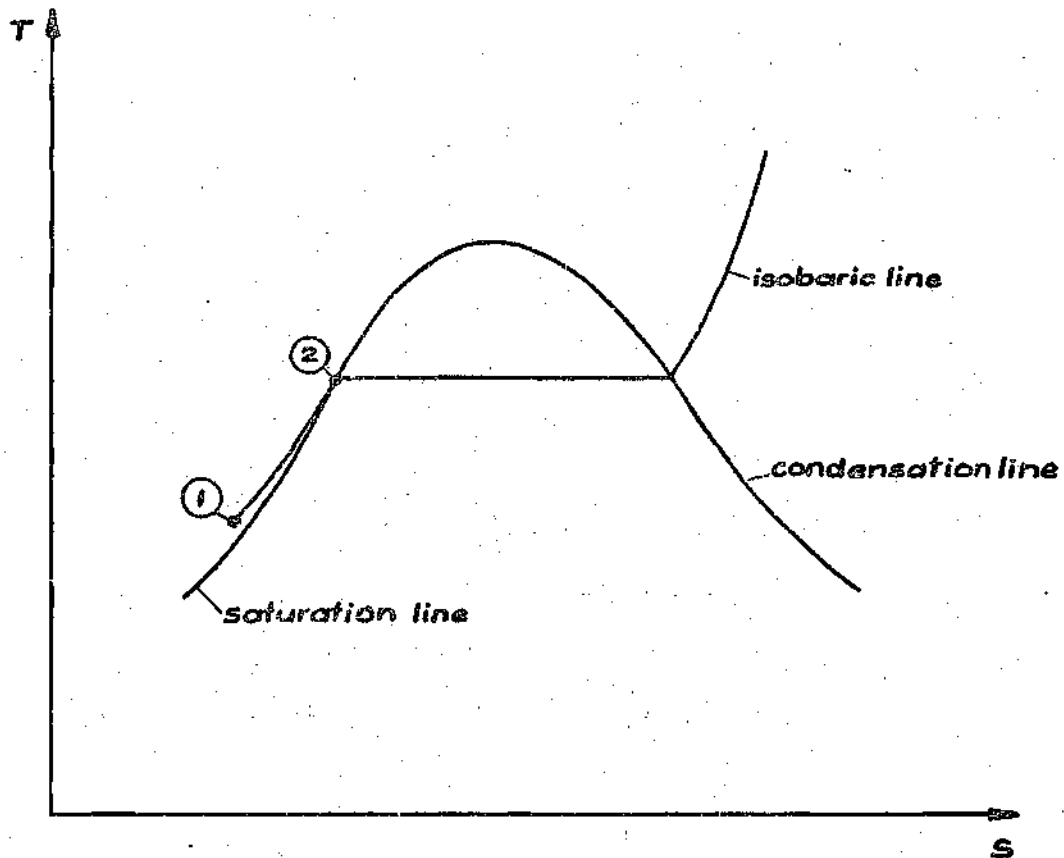


Figure 8. Temperature, Entropy-Diagram with I Isobar and Condensation and Saturation Lines.

point ① with the enthalpy value  $i_1$  and reaches the saturation line at point ②, where the enthalpy is  $i_2$  according to saturation conditions.

By integrating equation 3.14 we obtain the time  $\tau_b$ , which the particle (independent of its velocity or position!) will need to accumulate the necessary amount of thermal energy to reach boiling or saturation conditions. Therefore the boundary conditions for equation 3.14 are

$$\begin{aligned} \text{at } t = 0 \quad i &= i_1 \\ \text{and at } t = \tau_b \quad i &= i_2 \end{aligned} \tag{3.15}$$

Rewriting, integrating and considering the boundary conditions just formulated, equation 3.14 becomes

$$\int_0^{\tau_b} dt = \frac{q_f A_c}{q \xi} \int_{i_1}^{i_2} di \tag{3.16}$$

or

$$\tau_b = \frac{q_f A_c}{q \xi} (i_2 - i_1) \tag{3.17}$$

Once we know the time a particle remains in the liquid phase, by integrating equation 3.13, we get the position of the boiling boundary or the length of the single-phase region

$$\int dz = \int u_1(t) dt + C \quad 3.18$$

or

$$z = \bar{u}_1 t + \frac{\epsilon e^{st}}{s} + C \quad 3.19$$

The boundary conditions

$$z = 0 \quad \text{when} \quad t = \tau - \tau_b \quad 3.20$$

$$\text{and} \quad z = \lambda \quad \text{when} \quad t = \tau \quad 3.21$$

indicate the time  $t = \tau - \tau_b$  at which a specific particle that for  $t = \tau$  becomes saturated, entered the duct. Thus equation 3.21 implies for the constant  $C$  that

$$0 = \bar{u}_1(\tau - \tau_b) + \frac{\epsilon e^{s(\tau - \tau_b)}}{s} + C \quad 3.22$$

or solving for  $C$

$$C = -\bar{u}_1(\tau - \tau_b) - \frac{\epsilon e^{s(\tau - \tau_b)}}{s} \quad 3.23$$

At  $t = \tau$ ,  $z = \lambda$  and equation 3.19 becomes therefore

$$\lambda = \bar{u}_1 \tau_b + \left[ \frac{1 - e^{-s\tau_b}}{s} \right] \epsilon e^{st} \quad 3.24$$

In this equation  $\tau$  is a variable and therefore will be replaced in the following again by  $t$ . If we consider the space lag  $\lambda$  as a sum of a steady-state space lag  $\bar{\lambda}$  and a time-dependent space lag  $\lambda(t)$ , this means

$$\lambda = \bar{\lambda} + \delta\lambda \quad 3.25$$

we obtain finally an expression for the oscillatory movement of the boiling boundary

$$\delta\lambda = \left[ \frac{1 - e^{-s\tau_b}}{s} \right] \delta u_1 \quad 3.26$$

Referring the obtained solution, the following point shall be clearly emphasized: the integration of equation 3.13 was not performed with respect to a fixed time value, but to a time difference  $\tau_b$ . Thus equation 3.26 is valid for every particle, which spends the time  $\tau_b$  in the liquid phase.

### 3.3.2. The Dynamic Behavior of the Boiling Boundary

Equation 3.26 gives the relation between input (=entrance velocity) and output (=moving boiling boundary). The term in brackets is the transfer function. If we assume the inlet perturbation  $\delta u_1$  to be as undamped oscillation and  $s=i\omega$ , the equation for  $\delta \lambda$  becomes herewith

$$\delta \lambda = - \frac{i \epsilon e^{i \omega t}}{\omega} \left[ 1 - e^{-i \omega \tau_b} \right] \quad 3.27$$

Separating the inlet perturbation  $\delta u_1$  into a real and an imaginary component

$$\delta u_1 = \epsilon e^{i \omega t} = \epsilon \left[ \cos \omega t + i \sin \omega t \right] \quad 3.28$$

and performing the same operation on equation 3.27 (whereby the imaginary part will describe the actual flow conditions, because for time  $t=0$ ,  $\delta u_1$  has also to be zero), we can write the relation between input and output as follows:

$$\delta \lambda = \frac{\epsilon \tau_b}{\omega} \sin \frac{\omega \tau_b}{2} \left[ i \sin \omega \left( t - \frac{\tau_b}{2} \right) + \cos \omega \left( t - \frac{\tau_b}{2} \right) \right] \quad 3.29$$

This equation allows two interesting conclusions:

(1) The absolute value of the boiling boundary perturbation is inversely proportional to the frequency  $\omega$ .

(2) For the case that

$$\omega \tau_b = 2\pi \quad 3.30$$

the boiling boundary will not move at all.

In the following the dependence of  $\delta\lambda$  on the frequency  $\omega$  and the subcooling  $\tau_b$  will be discussed. Figure 9 is an Armand diagram which shows the phase lag and the amplitude of  $\delta\lambda$  with respect to the inlet perturbation  $\delta u_1$  for varying frequency  $\omega$  but constant subcooling  $\tau_b$ . For a time  $t=0$ ,  $\delta u_1$  appears on the real axis. The diagram shows several features:

(a) Large amplitudes of  $\delta\lambda$  are only possible at low frequencies. This can be assumed to be one of the reasons for the appearance of "chugging oscillations."

(b) For frequencies, which satisfy the conditions of equation 3.30,  $\delta\lambda$  is equal to zero. This result will be mainly interesting for further observations in the two-phase region.

(c) The phase lag between  $\delta u_1$  and  $\delta\lambda$  varies from  $-\pi$  to 0.

(d) The amplitude of  $\delta\lambda$  is linear dependent on the time lag  $\tau_b$ :

$$|\delta\lambda| \sim \tau_b |\delta u_1| \quad 3.31$$

(e) The limiting case  $\omega \rightarrow 0$  follows from

$$\begin{aligned} \lim_{\omega \rightarrow 0} |\delta\lambda| &= \lim_{\omega \rightarrow 0} \frac{2\varepsilon}{\omega} \sin \frac{\omega \tau_b}{2} \left( -i \sin \frac{\omega \tau_b}{2} + \cos \frac{\omega \tau_b}{2} \right) \\ &= \tau_b |\delta u_1| \quad 3.32 \end{aligned}$$

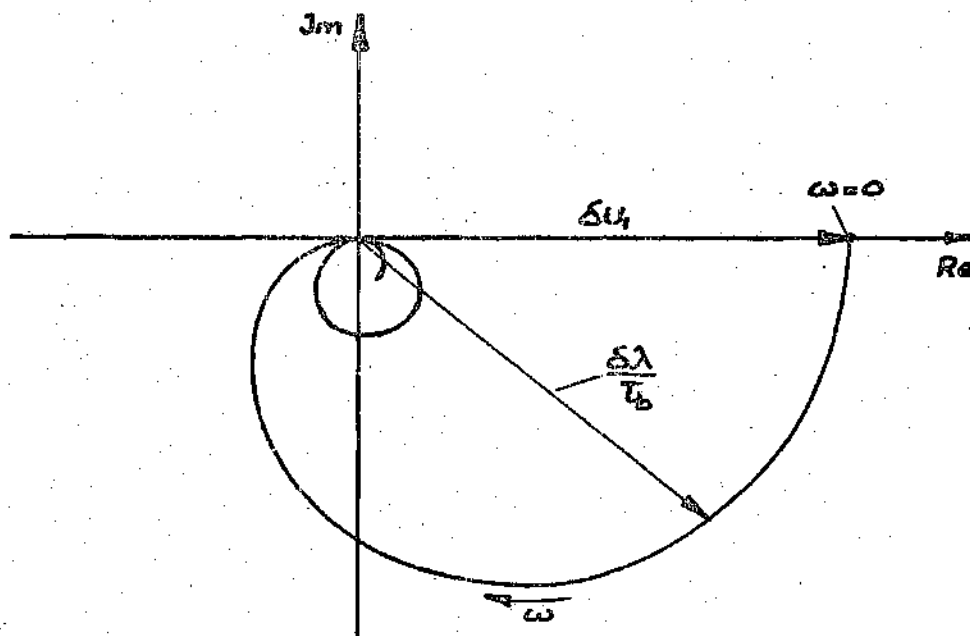


Figure 9. The Boiling Boundary as a Function of the Inlet Velocity Perturbation for Varying Frequencies and Constant Subcooling

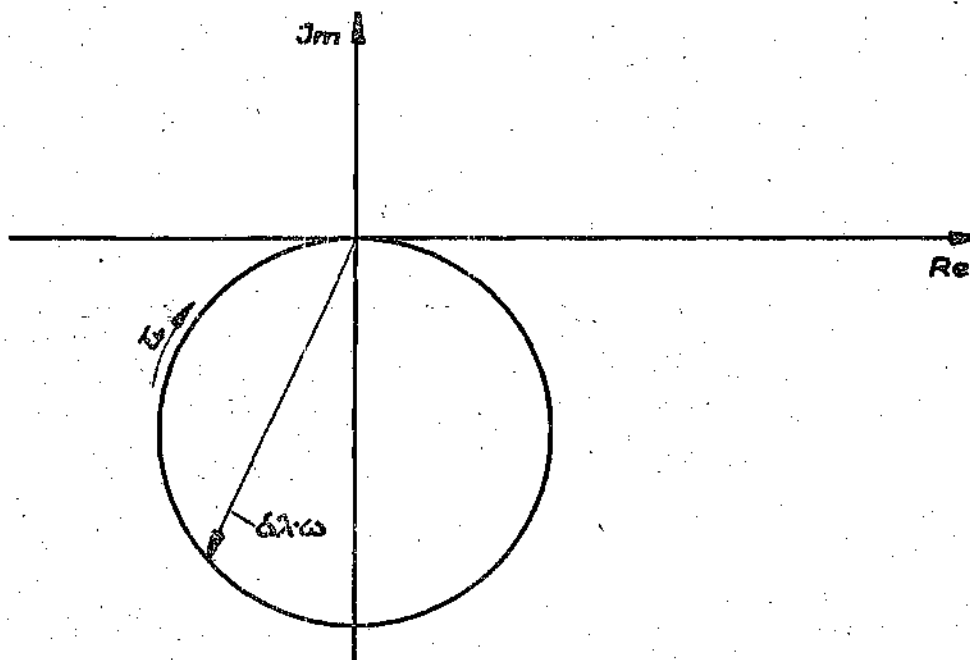


Figure 10. The Boiling Boundary as a Function of the Inlet Velocity Perturbation for Varying Subcooling and Constant Frequencies



Similar observations can be made to analyze the dependence of  $\delta\lambda$  on the time lag  $\tau_b$  at constant frequencies. Figure 10 shows again an Armand diagram, out of which we observe

(a) For a time lag  $\tau_b$  that satisfies equation 3.30, the response will be equal to zero.

(b) The phase lag of  $\delta\lambda$  with respect to  $\delta u_1$  varies between  $-\pi$  and  $0$ .

(c) The amplitude of  $\delta\lambda$  is inversely proportional to the frequency  $\omega$ .

$$|\delta\lambda| \sim \frac{|\delta u_1|}{\omega} \quad 3.33$$

For a better understanding of the behavior of the single-phase region, let us consider the case that the inlet perturbation is a step function. Figure 11 shows the enthalpy distribution (curve a) before the perturbation. Curve b represents steady state conditions after the perturbation occurred. For a given subcooling the time required to reach saturation conditions is given by equation 3.17. The length of the single phase region for an inlet velocity  $\bar{u}_1$  is first

$$\lambda_1 = \frac{\bar{u}_1}{\tau_b} \quad 3.34$$

and for new steady state conditions

$$\lambda_2 = \frac{\bar{u}_2}{\tau_b} \quad 3.35$$

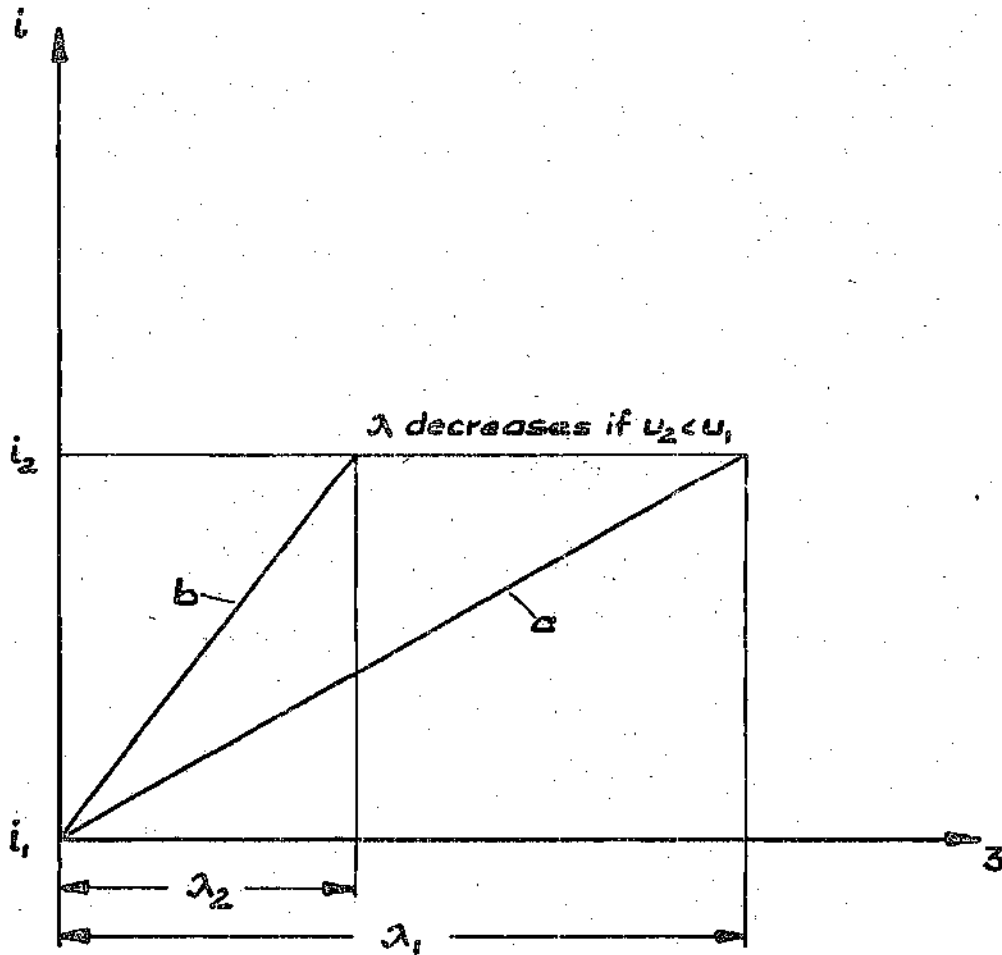


Figure II. Enthalpy Distributions in the Single-Phase Region Before and After a Velocity Step Function Perturbation

where  $\bar{u}_2 < \bar{u}_1$  is the inlet velocity after the perturbation. Therefore the moment the inlet velocity varies, the boiling boundary starts moving (for extensive studies see Ledinegg (12) ) with constant velocity

$$\frac{d\lambda}{dt} = \frac{\lambda_2 - \lambda_1}{\tau_b} \quad 3.36$$

It must be emphasized that there is no dead time or time delay between the occurrence of the perturbation and the moving incipience of the boiling boundary. But of course there is a time delay between the two steady state positions.

#### 3.4. The Momentum Equation

After the preceding thorough study of the behavior of the boiling boundary and the velocity distribution, the differential momentum equation will be integrated. The boundary conditions are

$$\begin{aligned} P &= P_1 & \text{at} & \quad z = 0 \\ P &= P_2 & \text{at} & \quad z = \lambda(t) \end{aligned} \quad 3.37$$

The integration will be performed along the flow direction, taking into account that the density in the single-phase region is assumed to be constant

$$-\int_{P_1}^{P_2} dP = \rho_f \int_0^{\lambda(t)} \left[ \frac{\partial u_1}{\partial t} + u_1 \frac{\partial u_1}{\partial z} + g + \frac{f}{2D} u_1^2 \right] dz \quad 3.38$$

In view of equation 3.5, 3.7 and 3.25 the pressure drop becomes

$$P_1 - P_2 = \rho_f \left[ \frac{\partial(\bar{u}_1 + \delta u_1)}{\partial t} + g + \frac{f}{2D} (\bar{u}_1 + \delta u_1)^2 \right] (\bar{\lambda} + \delta \lambda) \quad 3.39$$

Linearizing and retaining only the first power, we get

$$\begin{aligned} P_1 - P_2 = & \rho_f g \bar{\lambda} + \frac{f}{2D} \rho_f \bar{u}_1^2 + \rho_f \bar{\lambda} \delta u_1 + \frac{f}{2D} \rho_f 2\bar{u}_1 \bar{\lambda} \delta u_1 \\ & + \rho_f g \delta \lambda + \rho_f \frac{f}{2D} \bar{u}_1^2 \delta \lambda \end{aligned} \quad 3.40$$

The inlet pressure drop in accordance with Zuber (1) is

$$P_0 - P_1 = k_i \rho_f u_1^2 \quad 3.41$$

which upon linearization can be expressed as

$$P_0 - P_1 = k_i \rho_f \bar{u}_1^2 + k_i \rho_f 2\bar{u}_1 \delta u_1 \quad 3.42$$

With equation 3.40 we can write the total pressure drop in the single-phase region

$$\begin{aligned}
 P_0 - P_2 = & \rho_f g \bar{\lambda} + \frac{f}{2D} \rho_f \bar{u}_1^2 + k_i \rho_f \bar{u}_1^2 \\
 & + \rho_f \bar{\lambda} s \delta u_1 + \frac{f}{2D} \rho_f 2\bar{u}_1 \bar{\lambda} \delta u_1 + \rho_f g \delta \lambda \\
 & + \rho_f \frac{f}{2D} \bar{u}_1^2 \delta \lambda + k_i \rho_f 2\bar{u}_1 \delta u_1
 \end{aligned}$$

3.43

If we define now the steady state values of the pressure drop due to body forces (gravity) by

$$\overline{\Delta P_{bf}} = g \rho_f \bar{\lambda}$$

3.44

due to friction by

$$\overline{\Delta P_{f2}} = \frac{f}{2D} \bar{\lambda} \rho_f \bar{u}_1^2$$

3.45

and due to the inlet orifice by

$$\Delta P_{oi} = k_i \rho_f \bar{u}_1^2$$

3.46

equation 3.43 becomes

$$\begin{aligned}
 P_0 - P_2 &= \overline{\Delta P_{01}} + \overline{\Delta P_{12}} + \overline{\Delta P_{bf}} + \left\{ \rho_f \bar{\lambda} \right\} \frac{d\delta u_1}{dt} \\
 &+ \left\{ \frac{\partial \overline{\Delta P_{01}}}{\partial \bar{u}_1} + \frac{\partial \overline{\Delta P_{12}}}{\partial \bar{u}_1} \right\} \delta u_1 + \left\{ \frac{\partial \overline{\Delta P_{bf}}}{\partial \bar{\lambda}} + \frac{\partial \overline{\Delta P_{12}}}{\partial \bar{\lambda}} \right\} \delta \lambda
 \end{aligned}$$

3.47

Here again we consider the total pressure drop across the liquid phase as a sum of a steady state and a time dependent pressure drop

$$\Delta P_{02} = \overline{\Delta P_{02}} + \delta \Delta P_{02} \quad 3.48$$

For the time dependent part we get

$$\begin{aligned}
 \delta \Delta P_{02} &= \left\{ \rho_f \bar{\lambda} \right\} \frac{d\delta u_1}{dt} + \left\{ \frac{\partial \overline{\Delta P_{01}}}{\partial \bar{u}_1} + \frac{\partial \overline{\Delta P_{12}}}{\partial \bar{u}_1} \right\} \delta u_1 \\
 &+ \left\{ \frac{\partial \overline{\Delta P_{bf}}}{\partial \bar{\lambda}} + \frac{\partial \overline{\Delta P_{12}}}{\partial \bar{\lambda}} \right\} \delta \lambda
 \end{aligned} \quad 3.49$$

Again the transfer function appears in brackets if we express  $\delta \Delta P_{02}$  as a function of  $\delta u_1$

$$\delta \Delta P_{02} = \left[ \rho_f \bar{\lambda} s + \left\{ \frac{\partial \overline{\Delta P_{01}}}{\partial \bar{u}_1} + \frac{\partial \overline{\Delta P_{12}}}{\partial \bar{u}_1} \right\} + \left\{ \frac{\partial \overline{\Delta P_{bf}}}{\partial \bar{\lambda}} + \frac{\partial \overline{\Delta P_{12}}}{\partial \bar{\lambda}} \right\} \left( \frac{1 - e^{-s\tau_0}}{s} \right) \right] \delta u_1 \quad 3.50$$

This equation can easily render a graphical representation. In an Armand diagram for

$$t = \frac{2\pi}{\omega} n \quad \text{with} \quad n = 0, 1, 2 \quad 3.51$$

the first term appears on the real axis, the second is imaginary and the third term differs in its structure from the transfer function of the boiling boundary only by a constant. The geometrical addition of these components determines the magnitude and phase lag of  $\delta\Delta P_{O_2}$  with respect to  $\delta u_1$ . However the plot of the transfer function will vary considerably if the coefficients, like density  $\rho_f$  or friction factor  $f$ , are changed.

Figure 12 shows the operational conditions for

$$\left\{ \frac{\partial \overline{\Delta P}_{O_1}}{\partial \bar{u}_1} + \frac{\partial \overline{\Delta P}_{I_2}}{\partial \bar{u}_1} \right\} > \left\{ \frac{\partial \overline{\Delta P}_{bf}}{\partial \bar{\lambda}} + \frac{\partial \overline{\Delta P}_{I_2}}{\partial \bar{\lambda}} \right\} \cdot \text{Re} \left( \frac{1 - e^{-s\tau_0}}{s} \right)$$

3.52

With words this inequality says that the value on the left hand side is bigger than the term in brackets times the real part of the boiling boundary transfer function on the right hand side. In this case the phase lag between the response  $\delta\Delta P_{O_2}$  and the inlet  $\delta u_1$  is never bigger than  $\frac{\pi}{2}$  and the system is, according to section 2.3 in Chapter II, stable.

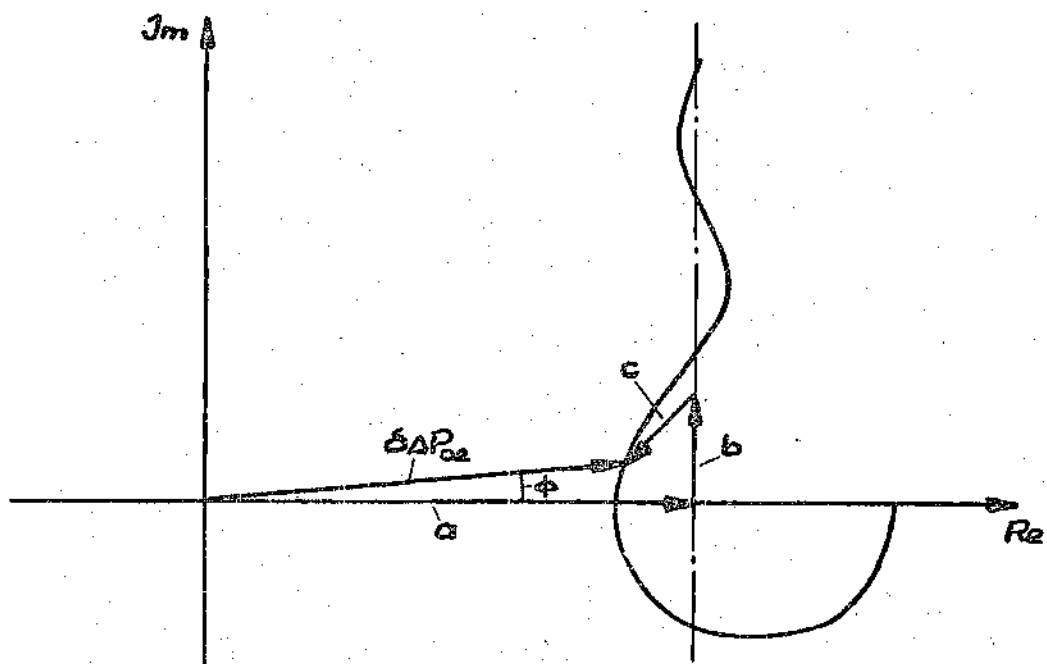


Figure 12. Pressure Drop Variations for Large Inlet Flow Restrictions  $k_1$

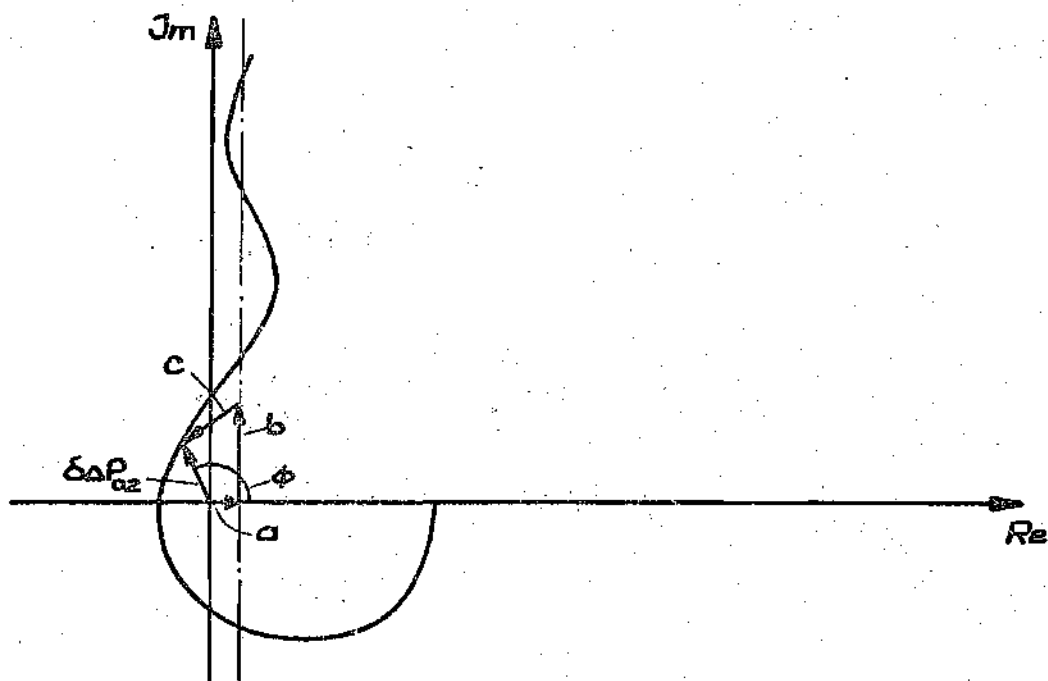


Figure 13. Pressure Drop Variations for Small Inlet Flow Restrictions  $k_1$



In the following we will show under which conditions the single-phase region becomes unstable. Hereto we reverse in equation 3.53 the sign

$$\left\{ \frac{\partial \overline{\Delta P_{01}}}{\partial \bar{u}_1} + \frac{\partial \overline{\Delta P_{12}}}{\partial \bar{u}_1} \right\} < \left\{ \frac{\partial \overline{\Delta P_{14}}}{\partial \bar{\lambda}} + \frac{\partial \overline{\Delta P_{12}}}{\partial \bar{\lambda}} \right\} \cdot \operatorname{Re} \left( \frac{1 - e^{-s\tau_b}}{s} \right) \quad 3.53$$

and analyze whether such a situation can arise under extreme operational conditions. Therefore to make the inequality as big as possible, we set  $k_i = 0$  or  $\overline{\Delta P_{01}} = 0$ . Furthermore we let the perturbation frequency be

$$\omega \approx \frac{3\pi}{2\tau_b} \quad 3.54$$

in order to use the maximum for the real part of the boiling boundary transfer function

$$\operatorname{Re} \left( \frac{1 - e^{-s\tau_b}}{s} \right) = \frac{2\tau_b}{3\pi} \quad 3.55$$

Simplifying the inequality equation 3.53, we get with

$$u_f = \frac{\lambda}{4f}$$

3.56

the equation

$$\frac{2gD}{f \bar{u}_f^2} > 3\pi - 1$$

3.57

Figure 13 shows the transfer function for which this inequality is fulfilled. In this case the phase lag between  $\delta P_{O_2}$  and  $\delta u_1$  can very well be equal to  $\pi$  creating therefore unstable flow conditions.

Out of the present observations the following conclusions can be made:

(a) The operational conditions of the system are stabilized by increasing the inlet flow restriction  $k_i$ .

(b) For sufficient high values of the parameters on the right hand side in the inequality equation 3.52, the pressure perturbations can also become for small frequencies large. This is also easily understandable. If the flow restrictions at the entrance become too large, then the pressure variations are also considerable and the system no longer operates at constant pressure.

(c) For small friction factor  $f$ , small entrance velocity  $\bar{u}_f$ , but large system diameter  $D$ , according to equation 3.57, the single-phase flow region can become unstable.

In Figure 12 and Figure 13 we set

$$a = \left\{ \frac{\partial \bar{\Delta P}_{01}}{\partial \bar{u}_1} + \frac{\partial \bar{\Delta P}_{12}}{\partial \bar{u}_1} \right\}$$

$$b = \rho_f \bar{\lambda} \omega$$

$$c = \left\{ \frac{\partial \bar{\Delta P}_{01}}{\partial \bar{\lambda}} + \frac{\partial \bar{\Delta P}_{12}}{\partial \bar{\lambda}} \right\} \left( \frac{1 - e^{-s\tau_b}}{s} \right)$$

## CHAPTER IV

## DYNAMICS OF THE TWO-PHASE REGION

4.1. The Governing Equations

In this chapter the three field equations describing the conservation of mass, momentum and energy and an appropriate constitutive equation will permit the calculation of the pressure drop in the two-phase region under time dependent conditions. Together with the results obtained in the single-phase region, they will make a qualitative analysis of the pertaining problem possible.

For a one-dimensional formulation, the continuity, energy and momentum equations are given respectively by

$$\frac{\partial \rho}{\partial t} + u \frac{\partial \rho}{\partial z} + \rho \frac{\partial u}{\partial z} = 0 \quad 4.1$$

$$\frac{\partial i}{\partial t} + u \frac{\partial i}{\partial z} = \frac{1}{\rho} \frac{q \dot{E}}{A_c} \quad 4.2$$

$$-\frac{\partial p}{\partial z} = \rho \frac{\partial u}{\partial t} + \rho u \frac{\partial u}{\partial z} + g \rho + \frac{f}{2D} \rho u^2 \quad 4.3$$

Furthermore we need an equation of state. Again we assume an isobaric process. Thereby we decouple the momentum equation from the

energy and the continuity equation. The density is then only a function of the enthalpy and can be written in the form

$$\rho = \rho(i)$$

4.4

As will be shown in the next section of this chapter, such a simplification of the problem limits considerably the range of perturbation frequencies. Moreover the two-phase flow will be homogeneous, excluding herewith the possibility of relative velocities between the phases.

The investigations of the two-phase flow region will start with a discussion of the equation of state and its dependence on the pressure level. Afterwards from continuity and energy equations, the velocity profile will be determined. Introducing this expression back into the continuity equation, the density as a function of time and position will be derived.

#### 4.2. The Equation of State

Before we derive an appropriate equation of state for sub- and supercritical pressures, we will analyze the limiting effect of assuming isobaric flow conditions on the range of perturbation frequencies.

For a one component, homogeneous medium the thermal equation of state

$$d\rho = \left. \frac{\partial \rho}{\partial T} \right|_P dT + \left. \frac{\partial \rho}{\partial P} \right|_T dP$$

4.5

can also be written in the form

$$\frac{dQ}{Q} = -\beta dT + \alpha dP \quad 4.6$$

with the isobaric expansivity

$$\beta = -\frac{1}{Q} \left( \frac{\partial Q}{\partial T} \right)_P \quad 4.7$$

and the isothermal compressibility

$$\alpha = \frac{1}{Q} \left( \frac{\partial Q}{\partial P} \right)_T \quad 4.8$$

Introducing in equation 4.6 the caloric equation of state

$$di = \left( \frac{\partial i}{\partial T} \right)_P dT + \left( \frac{\partial i}{\partial P} \right)_T dP \quad 4.9$$

in the form

$$di = c_p dT + \left. \frac{\partial i}{\partial P} \right|_T dP$$

4.10

and rearranging gives

$$\frac{dR}{R} = -\beta \frac{di}{c_p} + \left[ \alpha + \frac{\beta}{c_p} \left. \frac{\partial i}{\partial P} \right|_T \right] dP$$

4.11

In terms of substantial derivatives we get

$$\frac{1}{R} \frac{DR}{Dt} = -\frac{\beta}{c_p} \frac{Di}{Dt} + \left[ \alpha + \frac{\beta}{c_p} \left. \frac{\partial i}{\partial P} \right|_T \right] \frac{DP}{Dt}$$

4.12

Introducing

$$\left. \frac{\partial i}{\partial P} \right|_T = \frac{1}{R} (1 - T\beta)$$

4.13

Equation 4.12 becomes

$$\frac{1}{\rho} \frac{D\rho}{Dt} = -\frac{\beta}{c_p} \frac{Di}{Dt} + \left\{ \alpha + \frac{1}{\rho} \frac{\beta}{c_p} (1 - T\beta) \right\} \frac{DP}{Dt}$$

4.14

With  $\delta$  as the ratio of the specific heats

$$\delta = \frac{c_p}{c_v}$$

4.15

and the adiabatic compressibility

$$\alpha_s = \frac{1}{\rho} \left( \frac{\partial \rho}{\partial P} \right)_s$$

4.16

we obtain

$$\alpha = \delta \alpha_s = \frac{\delta}{\rho a_s^2}$$

4.17

where  $a_s$  is the velocity of sound defined by

$$a_s = \sqrt{\left( \frac{\partial p}{\partial \rho} \right)_s}$$

4.18



Equation 4.17 in 4.14 gives

$$\frac{1}{\rho} \frac{D\rho}{Dt} = - \frac{\beta}{c_p} \frac{Di}{Dt} + \left\{ (1 - T\beta) \frac{\beta}{c_p} + \frac{\delta}{a_s^2} \right\} \frac{1}{\rho} \frac{DP}{Dt} \quad 4.19$$

For a perfect gas and in the supercritical region

$$\beta = \frac{1}{T} \quad 4.20$$

Therefore we finally obtain

$$\frac{1}{\rho} \frac{D\rho}{Dt} = - \frac{\beta}{c_p} \frac{Di}{Dt} + \frac{\delta}{a_s^2} \frac{1}{\rho} \frac{DP}{Dt} \quad 4.21$$

Out of this equation the following conclusions can be made: for small pressure variations with respect to time the density can be considered to be a function of the enthalpy alone. But hereto the velocity of sound  $a_s$  has also to be assumed high values. Therefore the present analysis will be limited to the investigation of low frequency instabilities in two-phase flow systems, for which the velocity of sound is comparatively high.

For the derivation of an appropriate equation of state, the same approach Zuber (1) formulated, will be used. At subcritical pressures the equation of state can be obtained from basic considerations on two phase mixtures in thermodynamics. There the quality is defined

as the ratio of the vapor phase to the total mass. In terms of the mass flow rates of the vapor phase  $G_g$  and of the liquid phase  $G_f$ , the quality  $x$ , for the case of no relative velocity between the phases, is

$$x = \frac{G_g}{G_f + G_g} \quad 4.22$$

We also know that the specific volume and the enthalpy for such two phase mixtures are given by

$$v = (1-x)v_f + xv_g \quad 4.23$$

and

$$i = (1-x)i_f + xi_g \quad 4.24$$

where  $v_f$ ,  $i_f$  and  $v_g$ ,  $i_g$  are the specific volume and the enthalpy of the liquid and of the vapor respectively. By eliminating the quality  $x$  from equation 4.23 and equation 4.24, we obtain the equation of state for a system working at subcritical pressures

$$v(i) = v_f + \frac{\Delta v_{fg}}{\Delta i_{fg}} (i - i_f) \quad 4.25$$

Differentiating this equation we get the gradient of change

$$\left. \frac{dv}{di} \right)_p = \frac{\Delta v_{fg}}{\Delta i_{fg}} \quad 4.26$$

For supercritical pressures the ideal gas equation was assumed to be the constitutive equation of state in the light fluid. Deriving in this equation the specific volume with respect to temperature

$$dv = \frac{R}{P} dT \quad 4.27$$

and using the corresponding total differential for the enthalpy

$$di = c_p dT \quad 4.28$$

we get by combining both equations

$$\left. \frac{dv}{di} \right)_p = \frac{R}{P c_p} \quad 4.29$$

With the boundary condition

$$v = v_f \quad \text{at} \quad i = i_2 \quad 4.30$$

we obtain by integrating equation 4.29 the equation of state for the "light" fluid region

$$v(i) = v_f + \frac{R}{\rho c_p} (i - i_2) \quad 4.31$$

A comparison of equation 4.25 and equation 4.31 shows us that both equations of state are of the same form. Therefore we can replace them by one equation, which is valid as well at subcritical as at supercritical pressures

$$v(i) = v_f + \left( \frac{dv}{di} \right)_p (i - i_2) \quad 4.32$$

The distinction of both pressure levels will be kept in mind by considering equation 4.26 and equation 4.29.

#### 4.3. The Equation of Continuity and the Divergence of the Velocity

The velocity profile in the two-phase mixture will be obtained again by integrating the divergence of the velocity. Therefore we rewrite the continuity equation in the form

$$\frac{\partial u}{\partial z} = -\frac{1}{\rho} \left[ \frac{\partial \rho}{\partial t} + u \frac{\partial \rho}{\partial z} \right] \quad 4.33$$

To integrate this equation, we reconsider equation 4.4, which states that the density is assumed to be only a function of the enthalpy. The right hand side of equation 4.33 then becomes

$$\frac{\partial e}{\partial t} + u \frac{\partial e}{\partial z} = \frac{de}{di} \left( \frac{\partial i}{\partial t} + u \frac{\partial i}{\partial z} \right) \quad 4.34$$

Introducing the energy equation equation 4.2 in equation 4.34 we get

$$\frac{\partial e}{\partial t} + u \frac{\partial e}{\partial z} = \frac{1}{\rho} \frac{de}{di} \frac{q \xi}{A_c} \quad 4.35$$

Herewith we reconsider again the divergence of the velocity

$$\frac{\partial u}{\partial z} = - \frac{1}{\rho^2} \frac{de}{di} \frac{q \xi}{A_c} \quad 4.36$$

In analogy from chemical reaction systems, we define the right hand side of equation 4.36 to be the reaction frequency

$$\Omega = \left( - \frac{1}{\rho^2} \frac{de}{di} \right) \frac{q \xi}{A_c} = \frac{dv}{di} \frac{q \xi}{A_c} \quad 4.37$$

and we get

$$\frac{\partial u}{\partial z} = \Omega \quad 4.38$$

This equation states that the divergence of the velocity in the two-phase region is equal to the volumetric rate of formation of the "light" fluid per unit volume.

A comparison of equation 4.37 with equation 4.26 and equation 4.29 gives that  $\Omega$  will be for sub- and supercritical pressures a constant. The integration of equation 4.38 is therefore independent of the pressure level. With the boundary condition

$$u = \bar{u}_1 + \delta u_1 = \bar{u}_1 + \varepsilon e^{st} \quad \text{at} \quad z = \lambda(t) \quad 4.39$$

we get for the velocity distribution in the two-phase region

$$u_g(z, t) = \bar{u}_1 + \Omega(z - \bar{\lambda}) + \varepsilon e^{st} - \Omega \frac{\varepsilon e^{st}}{s} (1 - e^{-s\tau_b}) \quad 4.40$$

Equation 4.40 can be written in two different ways and each of them will allow us interesting conclusions:

The first one expresses the velocity  $u_g(z, t)$  as the sum of a steady state and a perturbed function

$$u_g(z, t) = \bar{u}_1 + \Omega(z - \bar{\lambda}) + \delta u_1 - \Omega \delta \lambda \quad 4.41$$

or

$$u_g(z, t) = \bar{u}_g(z) + \delta u_g(t) \quad 4.42$$

where

$$\bar{u}_g(z) = \bar{u}_1 + \Omega(z - \bar{\lambda}) \quad 4.43$$

is only a function of position  $z$ , and

$$\delta u_g(t) = \delta u_1 - \Omega \delta \lambda \quad 4.44$$

is only a function of time. Thus the inlet perturbation propagates with infinite velocity and is independent of position  $z$ . But at the same time equation 4.44 says that the system reacts immediately to any "input" perturbation. With other words the hydrodynamic conditions at a fixed position  $z$  at the end of the duct will immediately be affected, the moment a perturbation  $\delta u_1$  occurs at the entrance. Figure 14 shows the dependence of  $\delta u_g(t)$  on  $\delta u_1$  as a function of the frequency in an Armand diagram.

The second form of writing equation 4.40 represents the most general expression, because it gives  $u_g(z, t)$  as a function of  $z$  and two time-dependent terms

$$u_g(z, t) = u_1(t) + \Omega(z - \lambda(t)) \quad 4.45$$

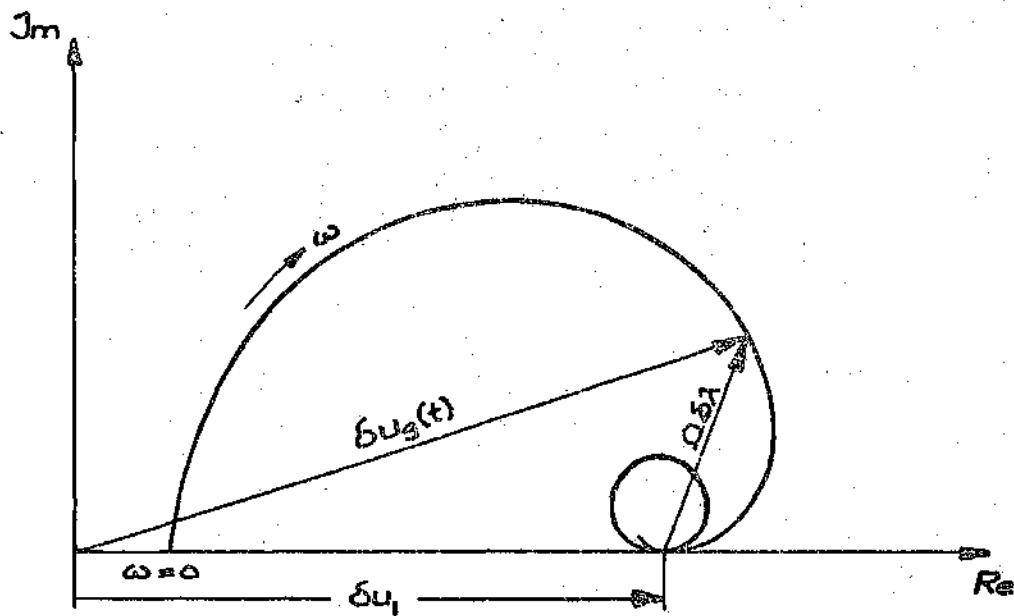


Figure 14. Velocity Perturbation in the Two-Phase Region as a Function of the Inlet Velocity Perturbation

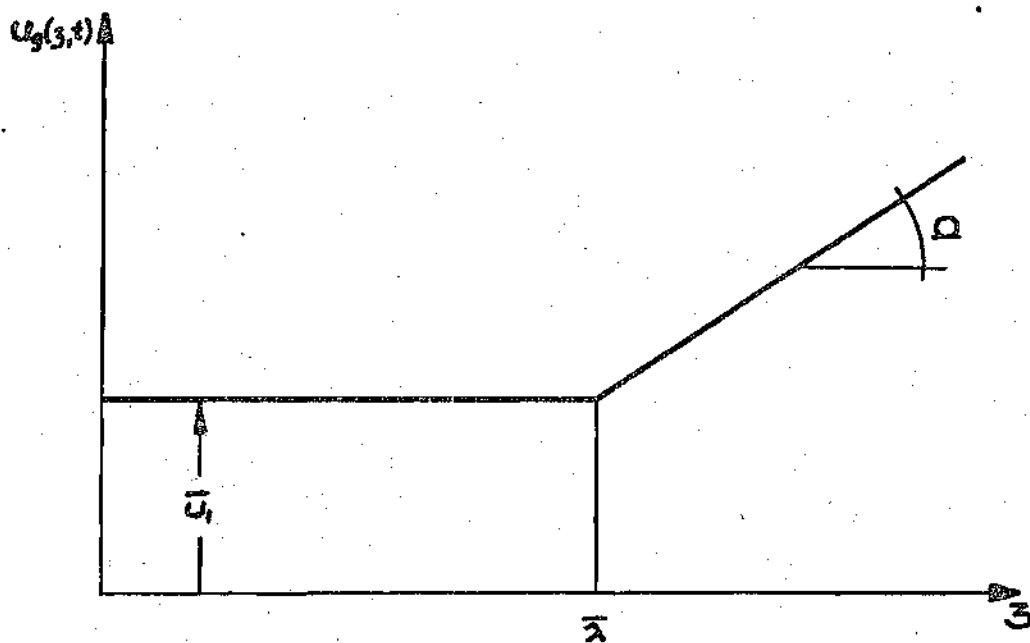


Figure 15. Velocity Distribution for Steady State Conditions



The velocity distribution given in such a form says that the velocity profile along the duct will always consist of two straight lines. The first one is parallel to the abscissa until  $\lambda(t)$ , which means that the velocity in the liquid phase is independent of position, and the second one starts at  $\lambda(t)$ , is connected to the first one and has a slope equal to  $\Omega$  (see Figure 15). Thus, if the perturbation function is an oscillatory movement, then the two straight lines as well as the position of  $\lambda(t)$  will perform oscillations as is indicated in Figure 16.

For a better understanding of the physics of the system, let us perform a stepfunction perturbation: at time  $t$  the inlet velocity  $\bar{u}_1$  changes stepwise and as was described in Chapter III at the same time  $t$  the boiling boundary will start moving with constant velocity towards its new steady state value. But the velocity profile in the two-phase region will move parallel to itself and always linked to  $\lambda(t)$  towards a new steady state position. Figure 17 describes this process for the case that  $\bar{u}_2 > \bar{u}_1$ .

#### 4.4. The Density Distribution

To compute the density perturbation in the two-phase region, two possibilities exist:

(1) To use the energy equation in order to get the enthalpy perturbation and to introduce this expression into the equation of state from which the density perturbation can be obtained. This method has the advantage of providing information referring the enthalpy distribution in the two-phase region.

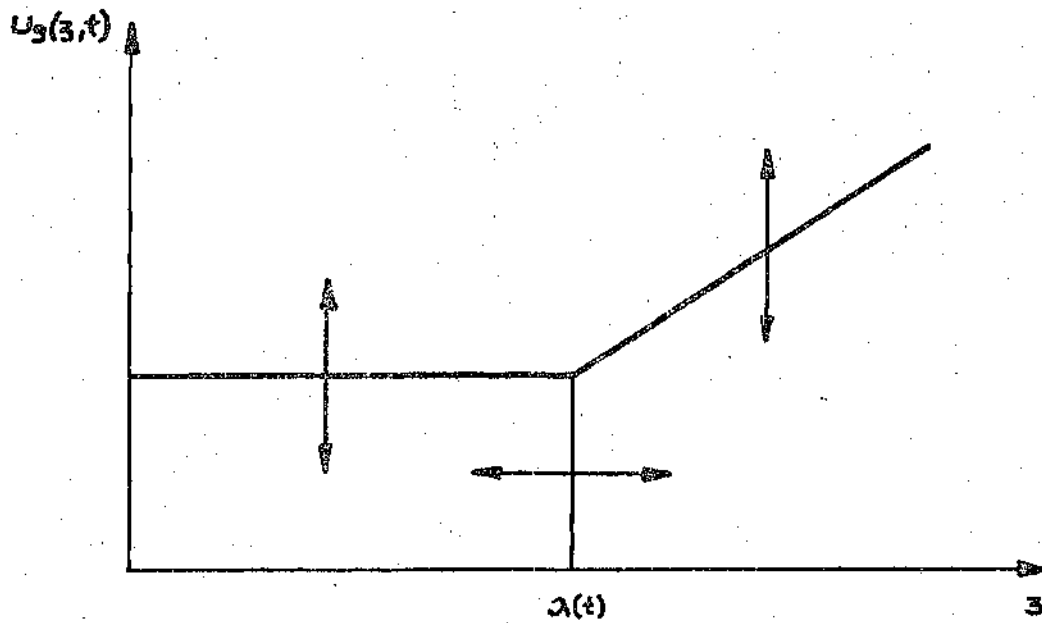


Figure 16. Oscillatory Modes of the Velocity Profile for a Sinusoidal Input

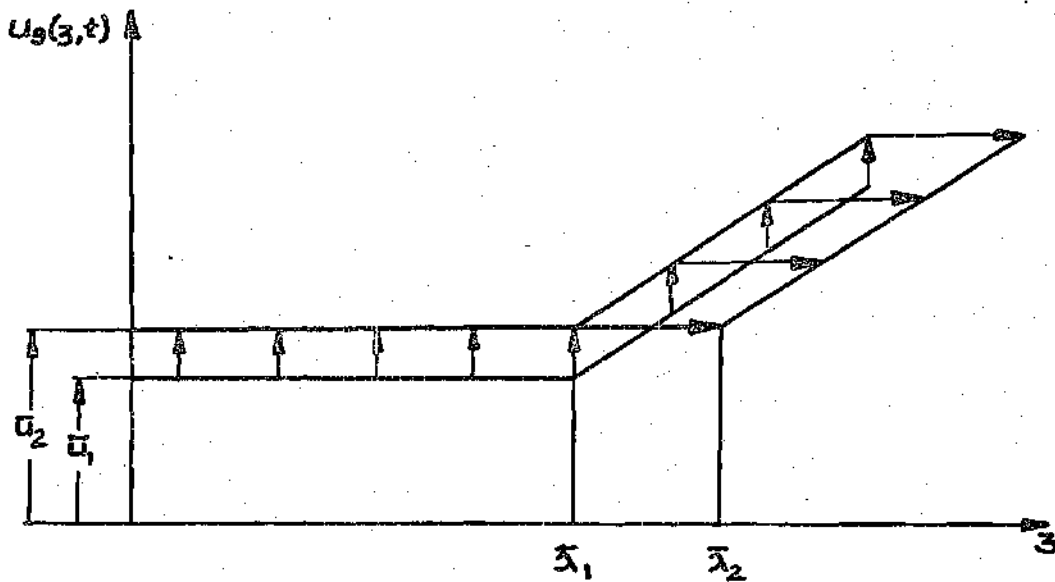


Figure 17. Behaviour of the Velocity Profile for an Inlet Step Function Perturbation.

(2) To use the continuity equation directly. In this case we would not need the energy equation and therefore we also would not get the enthalpy perturbation.

In this analysis the second possibility will be chosen in order to get a solution with the smallest amount of approximations and to make the computational process as short as possible.

If we introduce equation 4.38 into equation 4.1 and rearrange, we get

$$\frac{\partial \varrho}{\partial t} + u \frac{\partial \varrho}{\partial z} = -\varrho \Omega \quad 4.46$$

This equation was first formulated by Serov (21). It is a first order partial differential equation. The solution once more can be obtained by means of characteristics:

$$\varphi_2 = f(\varphi_1) \quad 4.47$$

where

$$\varphi_1(i, t, z) = C_1 \quad \text{and} \quad \varphi_2(i, t, z) = C_2 \quad 4.48$$

are solutions of any two independent differential equations, which imply the relationships:

$$dt = \frac{dz}{u(t)} = \frac{d\varrho}{-\varrho \Omega} \quad 4.49$$

Out of this equation, we obtain the following two equations

$$\frac{dz}{dt} = u(t) \quad 4.50$$

and

$$\frac{dq}{dt} = -\rho\Omega \quad 4.51$$

Here also in agreement with the corresponding equations of Chapter III similar observations can be made. Equation 4.50 describes the kinematic behavior of a particle in the two-phase region (note the difference in the expressions for the velocity!). Equation 4.51 is again an energy balance, in which the constitutive equation has already been taken into account.

First we solve equation 4.50 to get an expression, which gives us the position of a particle in the two-phase region as a function of time. Thus

$$\frac{dz}{dt} = u(t) = u_1 + \Omega(z - \lambda) \quad 4.52$$

or rewriting

$$\frac{dz}{dt} - \Omega z = \bar{u}_1 - \Omega \bar{\lambda} + \delta u_1 - \Omega \delta \lambda \quad 4.53$$

This is a first order differential equation of the type

$$\frac{dz}{dt} + f(t)z = h(t) \quad 4.54$$

and its general solution is

$$z = e^{-\int f(t) dt} \left( \int h(t) e^{\int f(t) dt} dt + C_1 \right) \quad 4.55$$

Applying the general solution to the given velocity distribution, we get

$$ze^{-\Omega t} + \left( \frac{\bar{u}_1}{\Omega} - \bar{\lambda} \right) e^{-\Omega t} - \frac{\epsilon e^{(s-\Omega)t}}{(s-\Omega)} \left( \frac{s-\Omega + \Omega e^{-s\tau_b}}{s} \right) = C_1 \quad 4.56$$

To evaluate the constant  $C_1$ , we consider the boundary condition, which will be given in terms of time differences. At time  $t = \tau$  ( $\tau$  is a variable), the particle is at position  $z = k$ , and at  $t = \tau - \tau_{2k}$  it just entered the two-phase region. Therefore

$$t = \tau$$

$$z = k$$

$$\text{and } t = \tau - \tau_{2k}$$

$$z = \lambda(\tau - \tau_{2k})$$

$$= \bar{\lambda} + \delta\lambda(\tau - \tau_{2k})$$

4.57

Equation 4.56 thus becomes

$$\bar{\lambda} e^{-\Omega(\tau - \tau_{2k})} + \delta\lambda(\tau - \tau_{2k}) e^{-\Omega(\tau - \tau_{2k})} + \left[ \frac{\bar{u}_1}{\Omega} - \bar{\lambda} \right] e^{-\Omega(\tau - \tau_{2k})}$$

$$= \frac{\epsilon e^{(s-\Omega)(\tau - \tau_{2k})}}{(s-\Omega)} \left[ \frac{s - \Omega + \Omega e^{-s\tau_b}}{s} \right] = k e^{-\Omega\tau} + \left[ \frac{\bar{u}_1}{\Omega} - \bar{\lambda} \right] e^{-\Omega\tau}$$

$$= \frac{\epsilon e^{(s-\Omega)\tau}}{(s-\Omega)} \left[ \frac{s - \Omega + \Omega e^{-s\tau_b}}{s} \right]$$

4.58

dividing the equation by  $e^{-\Omega\tau}$  we obtain

$$\bar{\lambda} e^{\Omega\tau_{2k}} + \delta\lambda(\tau - \tau_{2k}) e^{\Omega\tau_{2k}} + \left[ \frac{\bar{u}_1}{\Omega} - \bar{\lambda} \right] e^{\Omega\tau_{2k}} - \frac{\epsilon e^{s(\tau - \tau_{2k})\Omega\tau_{2k}}}{(s-\Omega)} \left[ \frac{s - \Omega + \Omega e^{-s\tau_b}}{s} \right]$$

$$= k + \frac{\bar{u}_1}{\Omega} - \bar{\lambda} - \frac{\epsilon e^{s\tau}}{(s-\Omega)} \left[ \frac{s - \Omega + \Omega e^{-s\tau_b}}{s} \right]$$

4.59

The position  $k$  for a given time difference  $\tau_{2k}$  can be written as a sum of a time independent and time dependent part

$$k = \bar{k} + \delta k \quad 4.60$$

From equation 4.59 the steady state equation can be obtained as follows

$$\bar{\lambda} e^{\Omega \tau_{2k}} + \left( \frac{\bar{u}_1}{\Omega} - \bar{\lambda} \right) e^{\Omega \tau_{2k}} = \bar{k} + \frac{\bar{u}_1}{\Omega} - \bar{\lambda} \quad 4.61$$

or solving for  $\bar{k}$

$$\bar{k} = \bar{\lambda} + \frac{\bar{u}_1}{\Omega} \left( e^{\Omega \tau_{2k}} - 1 \right) \quad 4.62$$

Subtracting equation 4.61 from equation 4.59 we get an expression for

$$\delta k = \frac{1 - e^{-(s-\Omega)\tau_{2k}}}{(s-\Omega)} \delta u_g + e^{-(s-\Omega)\tau_{2k}} \delta \lambda \quad 4.63$$

This equation indicates the deviation in position from  $\bar{k}$  for a particle, which spent a given time  $\tau_{2k}$  in the two-phase region.

During this time the particle accumulated thermal energy in proportion to the added heat. This thermal energy caused a phase change as the medium is at saturation conditions and therefore a decrease of the density. Out of the partial differential equation equation 4.46, we obtained

$$\frac{d\rho}{dt} = -\rho\Omega \quad 4.64$$

With the boundary condition

$$t = \tau - \tau_{2k} \quad z = \lambda(\tau - \tau_{2k}) \quad \rho = \rho_f \quad 4.65$$

and integrating equation 4.64, we get

$$-\frac{1}{\rho} \int_{\rho_f}^{\rho_k} \frac{d\rho}{\rho} = \int_{\tau - \tau_{2k}}^{\tau} dt \quad 4.66$$

or

$$\rho_k = \rho_f e^{-\Omega \tau_{2k}} \quad 4.67$$

This equation represents the density of a particle, which spent the time  $\tau_{2k}$  in the two-phase flow region. The general solution



for the density as a function of time is

$$\rho = \rho_f e^{-\alpha t} \quad 4.68$$

An expression for the density perturbation as a function of  $z$  and  $t$  can be found out of Figure 18 as follows: if we recall that equation 4.63 gives us the deviation for a constant-density position from steady state conditions, then at certain time  $t$ , the density at  $\bar{K} + \delta K$  is equal to the density at  $\bar{K}$  for steady state conditions

$$\rho_{\bar{K}} = \rho_f \frac{\bar{u}_1}{\bar{u}_{\bar{K}}} \quad 4.69$$

At  $K = \bar{K} + \delta K$  for steady state conditions the density is

$$\rho_K = \rho_{\bar{K} + \delta K} = \rho_f \frac{\bar{u}_1}{\bar{u}_{\bar{K}} + \alpha \delta K} \quad 4.70$$

This density value also can be expressed as a sum of a time independent and a time dependent term

$$\rho_K = \bar{\rho}_K + \delta \rho_K \quad 4.71$$

Therefore at time  $t$  we get the density perturbation by subtracting equation 4.70 from equation 4.69

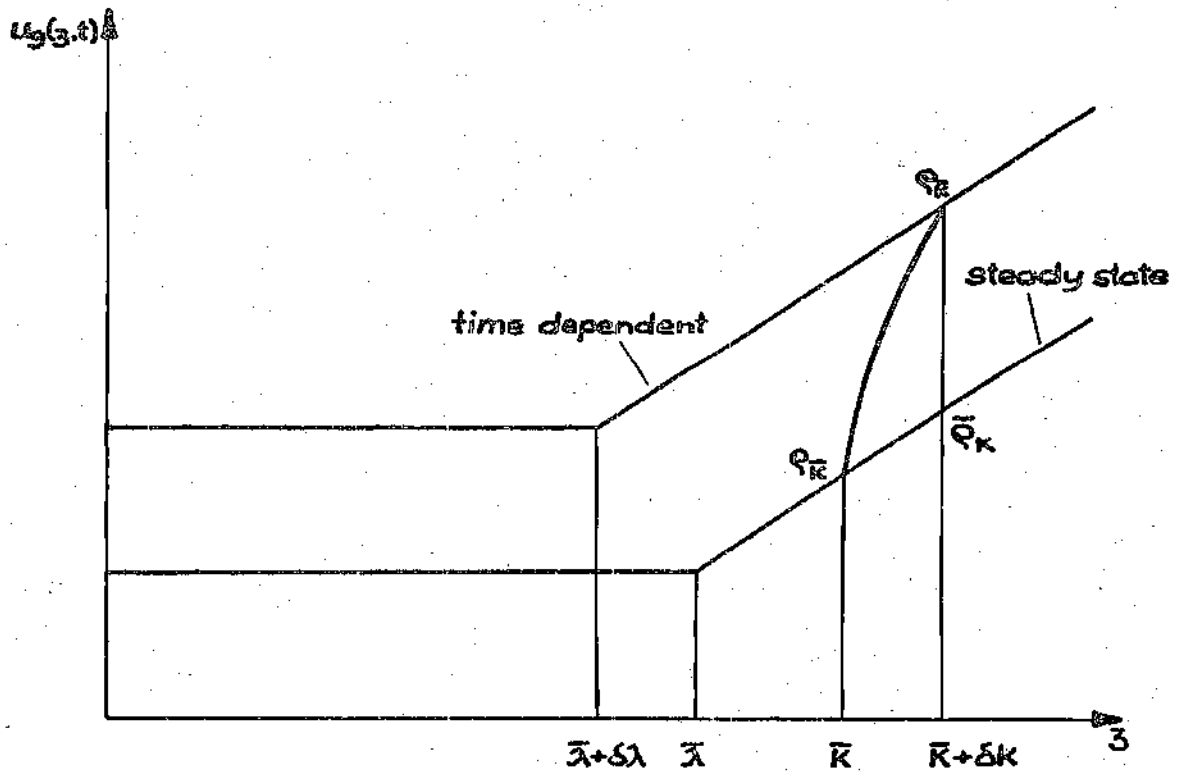


Figure I8. Evaluation of the Density Perturbation out of a Steady State and a Time Dependent Velocity Profile

$$\delta\rho(k, \tau) = \rho_f \frac{\bar{u}_i}{\bar{u}_R} - \rho_f \frac{\bar{u}_i}{\bar{u}_R + \Omega \delta k} \quad 4.72$$

Upon expansion and linearization, this equation becomes

$$\delta\rho(k, \tau) = \rho_f \frac{\bar{u}_i \Omega}{\bar{u}_R^2} \delta k \quad 4.73$$

or using equation 4.63

$$\delta\rho(k, \tau) = \rho_f \frac{\bar{u}_i \Omega}{\bar{u}_R^2} \left( \frac{1 - e^{-(s-\Omega)\tau_{2k}}}{(s-\Omega)} \delta u_g + e^{-(s-\Omega)\tau_{2k}} \delta \lambda \right) \quad 4.74$$

To make this equation independent of the time  $\tau_{2k}$  and therefore to express the density perturbation only as a function of  $k$  and  $\tau$  we replace the exponential terms by

$$e^{-(s-\Omega)\tau_{2k}} = \left( \frac{\rho_f}{\rho_k} \right)^{\frac{\Omega-s}{\Omega}} = \left( \frac{\bar{u}_k}{\bar{u}_i} \right)^{\frac{\Omega-s}{\Omega}} \quad 4.75$$

and rewrite herewith equation 4.74 replacing back  $\tau = t$  and  $k=3$

$$\delta\rho(z,t) = \rho_f \frac{\bar{u}_g \Omega}{\bar{u}_g^2} \left[ \left( \frac{1 - \left( \frac{\bar{u}_g}{\bar{u}_i} \right)^{\frac{\Omega-s}{\Omega}}}{(s-\Omega)} \right) \delta u_g(t) + \left( \frac{\bar{u}_g}{\bar{u}_i} \right)^{\frac{\Omega-s}{\Omega}} \delta \lambda \right] \quad 4.76$$

This is the final expression for the density perturbation in the two-phase region. The equation makes the following observations possible:

(a) The amplitude of the density perturbation decreases inversely proportional to the square of the velocity.

(b) The phase lag between the velocity perturbation  $\delta u_i$ , and the density perturbation depends on the position  $z$  and on the time the particle spent in the two-phase flow region. If we express as a function of the inlet perturbation  $\delta u_i$ , equation 4.76 becomes

$$\delta\rho = \left[ \rho_f \frac{\bar{u}_g \Omega}{\bar{u}_g^2} \left\{ \left( \frac{1 - \left( \frac{\bar{u}_g}{\bar{u}_i} \right)^{\frac{\Omega-s}{\Omega}}}{(s-\Omega)} \right) - \Omega \left( \frac{1 - \left( \frac{\bar{u}_g}{\bar{u}_i} \right)^{\frac{\Omega-s}{\Omega}}}{(s-\Omega)} \right) \left( \frac{1 - e^{-s\tau_b}}{s} \right) + \left( \frac{\bar{u}_g}{\bar{u}_i} \right)^{\frac{\Omega-s}{\Omega}} \left( \frac{1 - e^{-s\tau_b}}{s} \right) \right\} \right] \delta u_i$$

In this equation the expression in brackets gives us the phase lag between  $\delta u_1$  and  $\delta p$ . If the perturbation frequency  $\omega$  is small, then the phase lag of the response as a function of position  $z$  will also remain small. But if the frequency  $\omega$  is large, the phase lag all along the duct will also be considerable and we observe the presence of density waves. Figure 19 and Figure 20 describe qualitatively both cases in an Armand diagram. These density waves can also be presented along the duct. Figure 21 shows the case of low frequencies and Figure 22 of high frequencies.

In Figure 19 and Figure 21 we see that depending on the time the situation can arise that nearly at all positions  $z$  along the duct the density value is above or under the corresponding steady state density distribution, causing big momentum variations. This effect will be emphasized by the fact that for small perturbation frequencies the boiling boundary reacts heavily, causing therefore additionally big momentum changes in the single-phase region. Although they are a precondition for incipient instability, they are not sufficient. As was discussed in Chapter II, it will depend mainly on the timing between velocity perturbation and pressure drop whether sustained or amplified oscillations occur.

For high frequencies (Figure 20 and Figure 22), the density distribution will oscillate around the steady state curve, thus compensating any momentum change.

The physical observations so far described in this section excluded the influence of the velocity distributions on the system stability. Of course it is not easy to predict how much they contribute to the

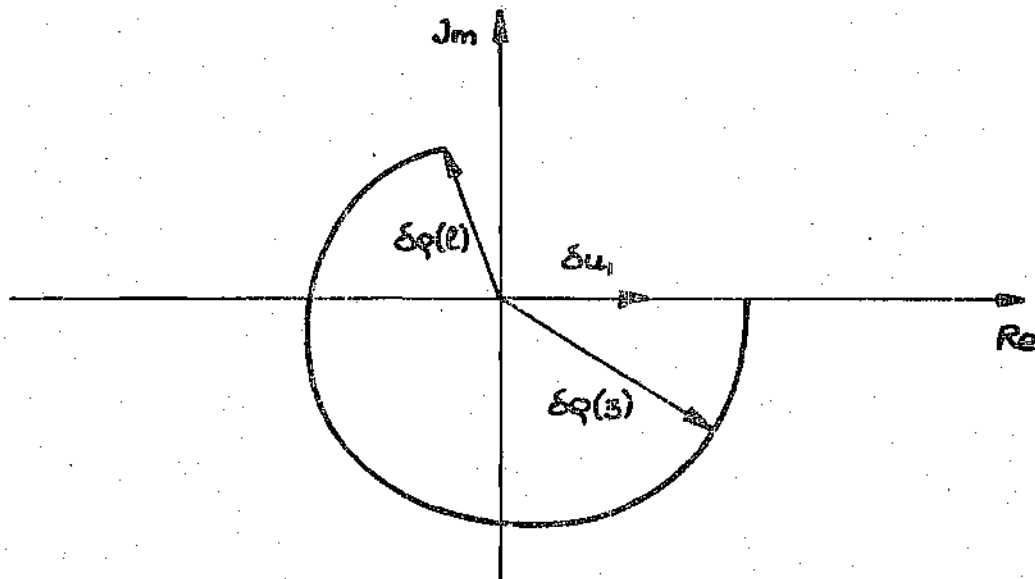


Figure 19. Density Distribution in a Complex Plane for Small Frequencies at a Specific Time

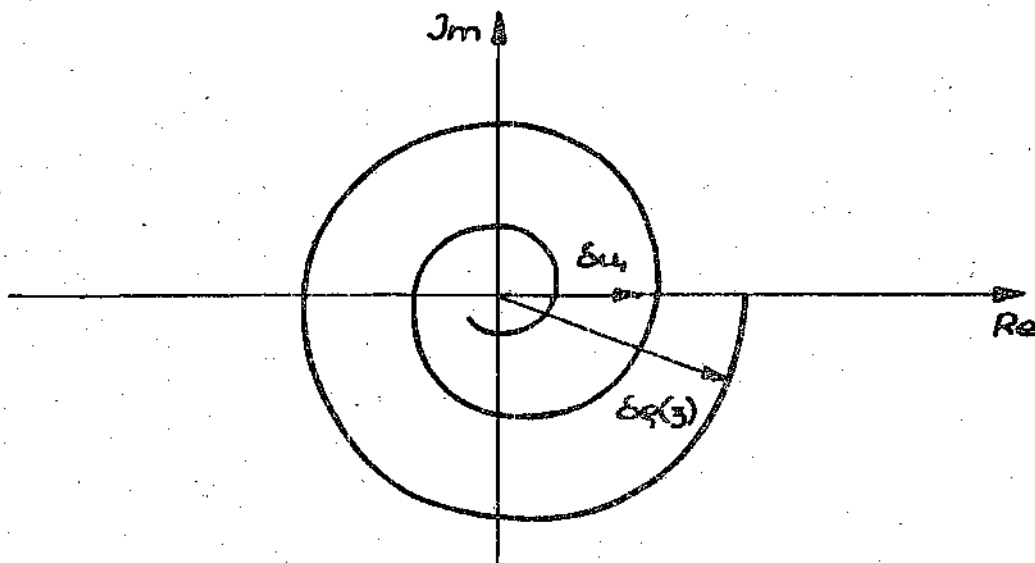


Figure 20. Density Distribution in a Complex Plane for Large Frequencies at a Specific Time

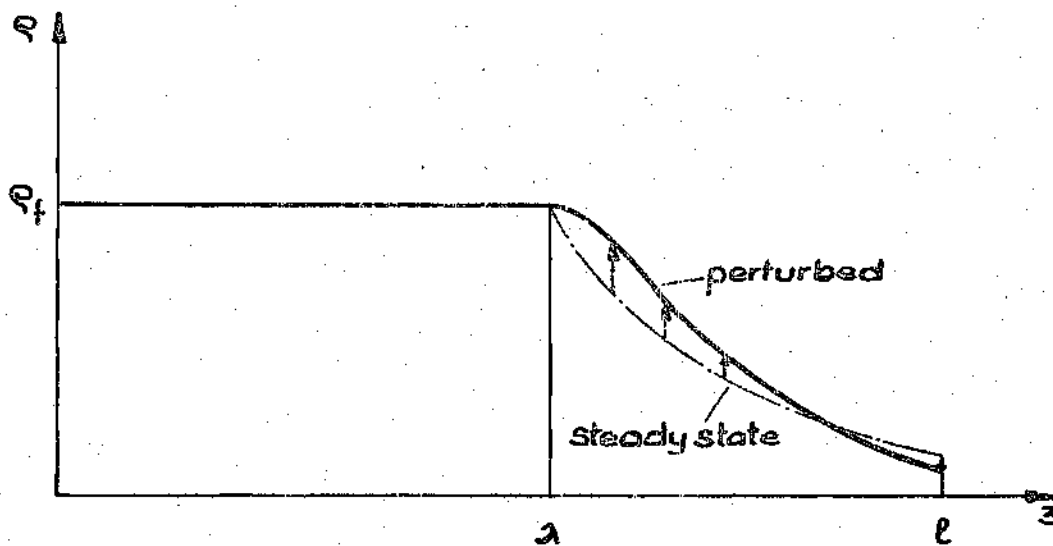


Figure 21. Density Distribution for Small Frequencies as a Function of Position

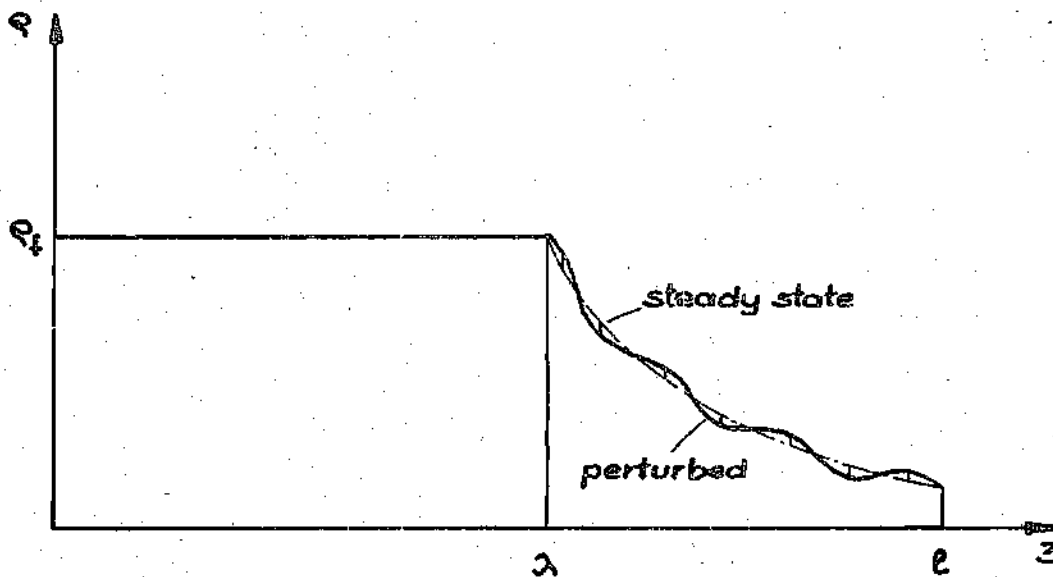


Figure 22. Density Distribution for High Frequencies as a Function of Position

observed flow instabilities. However Yadigaroglu and Bergles (19) report in their analysis that unstable flow oscillations were observed to have a period of approximately twice the transient time of the medium at steady state conditions. As this is very much in agreement with the mathematically obtained results, the assumptions that instabilities at low frequencies are mainly due to the behavior of the density variations seems very reasonable.

The present discussions on the density in the two-phase region will be concluded with an alternative derivation of equation 4.74 and equation 4.76. If we set, as was done by Zuber (1), Ishii and Zuber (20) and Boure (26, 27), the boundary and initial conditions to be

$$i - i_2 = 0 \quad \text{at} \quad t = \tau_2 \quad 4.78$$

$$i - i_2 = 0 \quad \text{at} \quad z = \lambda(\tau_2) = \bar{\lambda} + \epsilon e^{s\tau_2} \left( \frac{1 - e^{-s\tau_0}}{s} \right) \quad 4.79$$

and apply them to equation 4.56 and equation 4.57 we obtain

$$e^{-\Omega(t-\tau_2)} \left\{ \bar{u}_g(z) - \frac{\Omega}{s-\Omega} \delta u_g(t) \right\} = \bar{u}_1 + \left[ e^{-\Omega(t-\tau_2)} \right]^{\frac{s}{\Omega}} \left\{ \Omega \delta \lambda - \frac{\Omega}{s-\Omega} \delta u_1(t) \right\} \quad 4.80$$

This equation can be expressed as

$$e^{-\Omega(t-\tau_2)} \left\{ \bar{u}_g(z) - \frac{\Omega}{s-\Omega} \delta u_g \right\} = \bar{u}_1 - \left\{ \frac{\Omega}{s-\Omega} e^{-s\tau_2} \delta u_1 \right\} \left\{ e^{-\Omega(t-\tau_2)} \right\}^{\frac{s}{\Omega}} \quad 4.81$$



Here we write

$$\left\{ e^{-\Omega(t-t_2)} \right\}^{\frac{s}{\Omega}} = \left\{ \frac{\rho}{\rho_f} \right\}^{\frac{s}{\Omega}} = \left\{ \frac{\bar{\rho}(z)}{\rho_f} \right\} \left\{ 1 + \frac{s}{\Omega} \frac{\delta \rho}{\bar{\rho}(z)} \right\}^{\frac{s}{\Omega}}$$

4.82

and equation 4.81 becomes after rearranging

$$\left\{ \frac{\bar{\rho}(z)}{\rho_f} + \frac{\delta \rho}{\rho_f} \right\} \left\{ \bar{u}_g(z) - \frac{\Omega}{s-\Omega} \delta u_g(t) \right\} =$$

4.83

$$= \bar{u}_1 - \left\{ \frac{\Omega}{s-\Omega} e^{-s\tau_{12}} \delta u_1 \right\} \left\{ \frac{\bar{\rho}(z)}{\rho_f} \right\}^{\frac{s}{\Omega}} \left\{ 1 + \frac{s}{\Omega} \frac{\delta \rho}{\bar{\rho}(z)} \right\}$$

linearizing this equation we finally get for the density perturbation

$$\frac{\delta \rho}{\rho_f} = \left\{ \frac{\bar{u}_1}{\bar{u}_g(z)} \right\}^2 \frac{\Omega}{s-\Omega} \left\{ \frac{\delta u_g(t)}{\bar{u}_1} - e^{-s\tau_{12}} \left\{ \frac{\bar{u}_1}{\bar{u}_g(z)} \right\}^{\frac{s}{\Omega}-1} \frac{\delta u_1}{\bar{u}_1} \right\}$$

4.84

The equality of this result, extensively derived by Zuber (1), Ishii and Zuber (20) and Boure (26, 27), with equation 4.76 can easily be verified.

#### 4.5. Steady State Relations in the Two-Phase Region

As was done by Zuber (1), the momentum equation will be expressed in terms of several steady state relations for the velocity and density in the two-phase region.

The average velocity is defined by

$$\langle u_g \rangle = \frac{1}{e-\bar{\lambda}} \int_0^{e-\bar{\lambda}} \bar{u}_g(z) dz \quad 4.85$$

Using equation 4.43 we obtain

$$\langle u_g \rangle = \bar{u}_1 + \frac{\Omega(e-\bar{\lambda})}{2} = \frac{\bar{u}_3 + \bar{u}_1}{2} \quad 4.86$$

The log mean velocity is defined by

$$u_{em} = \frac{\bar{u}_3 - \bar{u}_1}{\ln \frac{\bar{u}_3}{\bar{u}_1}} = \frac{\Omega(e-\bar{\lambda})}{\ln \frac{\bar{u}_3}{\bar{u}_1}} \quad 4.87$$

If we introduce the log mean density in the "light" fluid region

$$\rho_{em} = \frac{\rho_3 - \rho_1}{\ln \frac{\rho_3}{\rho_1}} \quad 4.88$$

we get herewith the mean velocity

$$u_m = \frac{\rho_f \bar{u}_f}{\rho_m} \quad 4.89$$

Additionally we define an average density by

$$\langle \rho_g \rangle = \frac{1}{l - \bar{\lambda}} \int_0^{l - \bar{\lambda}} \bar{\rho}(z) dz \quad 4.90$$

From equation 4.62 and equation 4.67 and setting there  $\bar{\kappa} = 3$ ,  
the steady state density distribution is

$$\frac{\rho(z)}{\rho_f} = \frac{\bar{u}_1}{\bar{u}_1 + \Omega(z - \bar{\lambda})} \quad 4.91$$

Herewith we obtain in equation 4.78

$$\langle \rho_g \rangle = \frac{\rho_f \bar{u}_f}{\Omega(l - \bar{\lambda})} \ln \frac{\bar{u}_3}{\bar{u}_1} = \frac{\rho_f \bar{u}_f}{\bar{u}_{em}} \quad 4.92$$

Finally with equation 4.79 we define a mean density

$$\rho_m = \frac{\rho_f \bar{u}_f}{\langle u_g \rangle} \quad 4.93$$

#### 4.6. The Momentum Equation

With the steady state relations introduced in section 4.5 and velocity and density profiles in the two-phase region known, the differential pressure drop equation can easily be integrated straight forward. This was extensively done by Zuber (1). Here only an outline of his results will be given.

With the boundary conditions specified by:

$$P = P_2 \quad \text{at} \quad z = \lambda(t)$$

$$P = P_3 \quad \text{at} \quad z = l \quad 4.94$$

the integrated momentum equation becomes

$$-\int_{P_2}^{P_3} dP = \int_{\lambda(t)}^l \left\{ \rho \frac{\partial u}{\partial t} + \rho u \frac{\partial u}{\partial z} + g\rho + \frac{f}{2D} \rho u^2 \right\} dz \quad 4.95$$

Equation 4.95 will be evaluated term by term:

##### 4.6.1. The Inertia Term

The inertia term in the momentum equation is given by

$$\Delta P_I = \int_{\lambda(t)}^l \rho \frac{\partial u}{\partial t} dz \quad 4.96$$

Simplifying and linearizing the integral becomes

$$\Delta P_I = \int_{\lambda(t)}^l \bar{\rho} \frac{\partial \delta u_y(t)}{\partial t} dz \quad 4.97$$

and after performing the integration, we get

$$\Delta P_I = (s - \Omega + \Omega e^{-st_b}) \frac{\rho_f \bar{u}_f}{\Omega} \ln \frac{\bar{u}_3}{\bar{u}_1} \delta u_1 \quad 4.98$$

In view of the definition for the average density and of the equation for the velocity perturbation equation 4.44, the inertia term can be expressed as

$$\Delta P_I = (l - \bar{\lambda}) \langle \rho_g \rangle \frac{d \delta u_g}{dt} \quad 4.99$$

#### 4.6.2. The Convective Acceleration Term

The convective acceleration term in equation 4.95 is given by

$$\Delta P_a = \int_{\lambda(t)}^l \rho u \frac{\partial u}{\partial z} dz \quad 4.100$$

Simplifying and linearizing, the integral becomes

$$\Delta P_a = \Omega \int_{\lambda(t)}^l \left( \bar{\rho} \bar{u}_g(z) + \bar{\rho} \delta u_g(t) + \bar{u}_g(z) \delta \rho \right) dz \quad 4.101$$

Its integration gives

$$\begin{aligned} \Delta P_a = & G \Omega (l - \bar{\lambda}) - G \Omega \varepsilon e^{st} \frac{1 - e^{-s\tau_b}}{s} + \\ & + G \ln \frac{\bar{u}_3}{\bar{u}_1} \varepsilon e^{st} \frac{s - \Omega + \Omega e^{-s\tau_b}}{s} + \\ & + G \ln \frac{\bar{u}_3}{\bar{u}_1} \varepsilon e^{st} \frac{\Omega}{s - \Omega} \frac{s - \Omega + \Omega e^{-s\tau_b}}{s} - \\ & - G \varepsilon e^{st} e^{-s\tau_b} \left( \frac{\Omega}{s - \Omega} \right)^2 \left\{ 1 - e^{-s(\tau_3 - \tau_1)} \frac{\bar{u}_3}{\bar{u}_1} \right\} \end{aligned} \quad 4.102$$

We obtain the steady state acceleration pressure drop by

letting  $\varepsilon = 0$  :

$$\overline{\Delta P_a} = G \Omega (l - \bar{\lambda}) \quad 4.103$$

Inserting this expression into equation 4.102 the convective acceleration term becomes

$$\Delta P_a = \overline{\Delta P_a} - \frac{\overline{\Delta P_a}}{(l-\lambda)} \delta\lambda + \frac{\overline{\Delta P_a}}{\bar{u}_{em}} \delta u_g +$$

$$+ \frac{\Omega}{s-\Omega} \frac{\overline{\Delta P_a}}{\bar{u}_{em}} \delta u_g - \frac{\Omega}{s-\Omega} \frac{\overline{\Delta P_a}}{\bar{u}_i} e^{-s(\tau_3-\tau_1)} \delta u_i$$

4.104

#### 4.6.3. The Gravitational Term

The gravitational term in the momentum equation is given by

$$\Delta P_{bg} = \int_{\lambda(t)}^l g \rho dz$$

4.105

Simplifying, the integral becomes

$$\Delta P_{bg} = \int_{\lambda(t)}^l [g\bar{\rho} + g\delta\rho] dz$$

4.106

and its integration gives

$$\Delta P_{bg} = g \frac{\rho_f \bar{u}_f}{\Omega} \ln \frac{\bar{u}_3}{\bar{u}_1} - g \rho_f \varepsilon e^{st} \left( \frac{1 - e^{-s\tau_0}}{s} \right) +$$

$$+ g(l - \bar{\lambda}) \frac{\rho_f}{\bar{u}_3} \varepsilon e^{st} \frac{\Omega}{s - \Omega} \frac{s - \Omega + \Omega e^{-s\tau_0}}{s} - \frac{\Omega}{s - \Omega} \frac{g(l - \bar{\lambda}) \langle \rho_g \rangle}{\bar{u}_1} e^{-s(\tau_3 - \tau_1)} \delta u_1$$

4.107

Again if we let  $\varepsilon = 0$ , we obtain the steady state gravitational pressure drop

$$\overline{\Delta P_{bg}} = g(l - \bar{\lambda}) \langle \rho_g \rangle$$

4.108

Herewith equation 4.107 becomes

$$\Delta P_{bg} = \overline{\Delta P_{bg}} - \frac{\Delta P_{bg}}{(l - \bar{\lambda})} \frac{\bar{u}_{em}}{\bar{u}_1} \delta \lambda + \frac{\Omega}{s - \Omega} \frac{\overline{\Delta P_{bg}}}{\bar{u}_m} \delta u_g -$$

$$- \frac{\Omega}{s - \Omega} \frac{\overline{\Delta P_{bg}}}{\bar{u}_1} e^{-s(\tau_3 - \tau_1)} \delta u_1$$

4.109



#### 4.6.4. The Frictional Pressure Drop

The frictional term in the momentum equation is given by

$$\Delta P_{23} = \int_{\lambda(t)}^l \frac{f}{2D} \rho u^2 dz \quad 4.110$$

Simplifying and linearizing the integral becomes

$$\Delta P_{23} = \frac{f}{2D} \int_{\lambda(t)}^l \left\{ \bar{\rho} \bar{u}_g^2 + 2\bar{\rho} \bar{u}_g(z) \delta u_g(t) + \bar{u}_g^2(z) \delta \rho \right\} dz \quad 4.111$$

and its integration gives

$$\begin{aligned} \Delta P_{23} = & \frac{f(l-\bar{\lambda})}{2D} \rho_f \bar{u}_f \left[ \bar{u}_1 + \frac{\Omega(l-\bar{\lambda})}{\alpha} \right] - \frac{f}{2D} \rho_f \bar{u}_f^2 \epsilon e^{st} \left( \frac{1 - e^{-s\tau_b}}{s} \right) \\ & + 2 \frac{f(l-\bar{\lambda})}{2D} \rho_f \bar{u}_f \epsilon e^{st} \frac{s - \Omega + \Omega e^{-s\tau_b}}{s} + \frac{\Omega}{s - \Omega} \frac{f(l-\bar{\lambda})}{2D} \rho_f \bar{u}_f \epsilon e^{st} \frac{s - \Omega + \Omega e^{-s\tau_b}}{s} \\ & - \frac{\Omega}{s - \Omega} \frac{f(l-\bar{\lambda})}{2D} \rho_f \bar{u}_f \left[ \bar{u}_1 + \frac{\Omega(l-\bar{\lambda})}{\alpha} \right] \frac{e^{-s(\tau_3 - \tau_1)}}{\bar{u}_1} \epsilon e^{st} \end{aligned} \quad 4.112$$

Out of this equation we obtain the steady state frictional pressure drop by letting  $\varepsilon = 0$ . Thus

$$\overline{\Delta P}_{23} = \frac{f(l-\bar{\lambda})}{2D} \rho_f \bar{u}_f \left( \bar{u}_1 + \frac{\Omega(l-\bar{\lambda})}{2} \right) = \frac{f(l-\bar{\lambda})}{2D} \rho_f \bar{u}_f \langle u_g \rangle \quad 4.113$$

Equation 4.112 in terms of the expression equation 4.113 becomes

$$\begin{aligned} \Delta P_{23} = \overline{\Delta P}_{23} - \frac{\overline{\Delta P}_{23}}{(l-\bar{\lambda}) \langle u_g \rangle} \bar{u}_1 \delta \lambda + 2 \frac{\overline{\Delta P}_{23}}{\langle u_g \rangle} \delta u_g \\ + \frac{\Omega}{s-\Omega} \frac{\overline{\Delta P}_{23}}{\langle u_g \rangle} \delta u_g - \frac{\Omega}{s-\Omega} \frac{\overline{\Delta P}_{23}}{\bar{u}_1} e^{-s(\tau_3-\tau_1)} \delta u_1 \end{aligned} \quad 4.114$$

#### 4.6.5. The Exit Pressure Drop

The effect of the exit pressure drop will be included in the momentum equation equation 4.95. Defining by  $k_e$  a coefficient, which accounts for all the exit pressure losses, we formulate the exit pressure drop as follows

$$P_3 - P_4 = \Delta P_{34} = k_e \rho_3 u_3^2 \quad 4.115$$

Simplifying and linearizing we get

$$\Delta P_{34} = k_e G \bar{u}_3 + 2k_e G \delta u_g + \frac{\Omega}{s-\Omega} k_e G \delta u_g - \frac{\Omega}{s-\Omega} \rho_f \bar{u}_3 e^{-s(\tau_3-\tau_1)} \delta u_1 \quad 4.116$$

For  $\varepsilon = 0$ , the steady state exit pressure drop becomes

$$\overline{\Delta P_{34}} = k_e G \bar{u}_3 \quad 4.117$$

Consequently equation 4.116 can be expressed as

$$\Delta P_{34} = \overline{\Delta P_{34}} + 2 \frac{\overline{\Delta P_{34}}}{\bar{u}_3} \delta u_g + \frac{\Omega}{s-\Omega} \frac{\overline{\Delta P_{34}}}{\bar{u}_3} \delta u_g - \frac{\Omega}{s-\Omega} \frac{\overline{\Delta P_{34}}}{\bar{u}_1} e^{-s(\tau_3-\tau_1)} \delta u_1 \quad 4.118$$

#### 4.6.6. The Integrated Momentum Equation

The sum of equation 4.99, 4.104, 4.109, 4.114 and 4.118 gives the total pressure drop across the two-phase flow region

$$\begin{aligned}
P_2 - P_4 &= \overline{\Delta P_a} + \overline{\Delta P_{bg}} + \overline{\Delta P_{23}} + \overline{\Delta P_{34}} \\
&+ \left\{ (e - \bar{\lambda}) \langle \rho_g \rangle \right\} \frac{d\delta u_d}{dt} - \\
&- \left\{ \frac{\overline{\Delta P_a}}{(e - \bar{\lambda})} + \frac{\overline{\Delta P_{bg}}}{(e - \bar{\lambda})} \frac{\bar{u}_{em}}{\bar{u}_1} + \frac{\overline{\Delta P_{23}}}{(e - \bar{\lambda})} \frac{\bar{u}_1}{\langle u_g \rangle} \right\} \delta \lambda + \\
&+ \left\{ \frac{\overline{\Delta P_a}}{\bar{u}_{em}} + 2 \frac{\overline{\Delta P_{23}}}{\langle u_g \rangle} + 2 \frac{\overline{\Delta P_{34}}}{\bar{u}_3} \right\} \delta u_g + \\
&+ \frac{\Omega}{s - \Omega} \left\{ \frac{\overline{\Delta P_a}}{\bar{u}_{em}} + \frac{\overline{\Delta P_{bg}}}{\bar{u}_m} + \frac{\overline{\Delta P_{23}}}{\langle u_g \rangle} + \frac{\overline{\Delta P_{34}}}{\bar{u}_3} \right\} \delta u_g - \\
&- \frac{\Omega}{s - \Omega} \left\{ \frac{\overline{\Delta P_a}}{\bar{u}_1} + \frac{\overline{\Delta P_{bg}}}{\bar{u}_1} + \frac{\overline{\Delta P_{23}}}{\bar{u}_1} + \frac{\overline{\Delta P_{34}}}{\bar{u}_1} \right\} e^{-s(t_3 - \tau_1)} \delta u_1 \quad 4.119
\end{aligned}$$

In this equation the steady state pressure drop is

$$\overline{\Delta P_{24}} = \overline{\Delta P_a} + \overline{\Delta P_{bg}} + \overline{\Delta P_{23}} + \overline{\Delta P_{34}} \quad 4.120$$

Subtracting equation 4.120 from equation 4.119 the pressure drop perturbation is

$$\begin{aligned}
\delta \Delta P_{24} = & \left\{ (l - \bar{\lambda}) \langle \rho_g \rangle \right\} \frac{d \delta u_g}{dt} \\
& - \left\{ \frac{\overline{\Delta P_a}}{(l - \bar{\lambda})} + \frac{\overline{\Delta P_{0g}}}{(l - \bar{\lambda})} \frac{\bar{u}_{em}}{\bar{u}_1} + \frac{\overline{\Delta P_{23}}}{(l - \bar{\lambda})} \frac{\bar{u}_1}{\langle u_g \rangle} \right\} \delta \lambda \\
& + \left\{ \frac{\overline{\Delta P_a}}{\bar{u}_{em}} + 2 \frac{\overline{\Delta P_{23}}}{\langle u_g \rangle} + 2 \frac{\overline{\Delta P_{34}}}{\bar{u}_3} \right\} \delta u_g + \\
& + \frac{\Omega}{s - \Omega} \left\{ \frac{\overline{\Delta P_a}}{\bar{u}_{em}} + \frac{\overline{\Delta P_{0g}}}{\bar{u}_m} + \frac{\overline{\Delta P_{23}}}{\langle u_g \rangle} + \frac{\overline{\Delta P_{34}}}{\bar{u}_3} \right\} \delta u_g - \\
& - \frac{\Omega}{s - \Omega} \left\{ \frac{\overline{\Delta P_a}}{\bar{u}_1} + \frac{\overline{\Delta P_{0g}}}{\bar{u}_1} + \frac{\overline{\Delta P_{23}}}{\bar{u}_1} + \frac{\overline{\Delta P_{34}}}{\bar{u}_1} \right\} e^{-s(\tau_3 - \tau_1)} \delta u_1
\end{aligned}$$

4.121

#### 4.6.7. Pressure Drop Variations of the Entire System

Adding equation 3.49 and equation 4.121 we get the pressure drop perturbations of the entire system

$$\begin{aligned}
 \delta \Delta P_{04} = & \left\{ \rho_f \bar{\lambda} \right\} \frac{d\delta u_1}{dt} + \left\{ (e - \bar{\lambda}) \langle \rho_g \rangle \right\} \frac{d\delta u_g}{dt} \\
 & + \left\{ \frac{\partial \bar{\Delta P}_{01}}{\partial u_1} + \frac{\partial \bar{\Delta P}_{12}}{\partial u_1} \right\} \delta u_1 - \\
 & - \left\{ \frac{\bar{\Delta P}_a}{(e - \bar{\lambda})} + \frac{\bar{\Delta P}_{bg} \bar{u}_{em}}{(e - \bar{\lambda}) \bar{u}_1} + \frac{\bar{\Delta P}_{23} \bar{u}_1}{(e - \bar{\lambda}) \langle u_g \rangle} - \frac{\partial \bar{\Delta P}_{bf}}{\partial \bar{\lambda}} - \frac{\partial \bar{\Delta P}_{12}}{\partial \bar{\lambda}} \right\} \delta \lambda \\
 & + \left\{ \frac{\bar{\Delta P}_a}{\bar{u}_{em}} + 2 \frac{\bar{\Delta P}_{23}}{\langle u_g \rangle} + 2 \frac{\bar{\Delta P}_{34}}{\bar{u}_3} \right\} \delta u_g + \\
 & + \frac{\Omega}{s - \Omega} \left\{ \frac{\bar{\Delta P}_a}{\bar{u}_{em}} + \frac{\bar{\Delta P}_{bg}}{\bar{u}_m} + \frac{\bar{\Delta P}_{23}}{\langle u_g \rangle} + \frac{\bar{\Delta P}_{34}}{\bar{u}_3} \right\} \delta u_g - \\
 & - \frac{\Omega}{s - \Omega} \left\{ \frac{\bar{\Delta P}_a}{\bar{u}_1} + \frac{\bar{\Delta P}_{bg}}{\bar{u}_1} + \frac{\bar{\Delta P}_{23}}{\bar{u}_1} + \frac{\bar{\Delta P}_{34}}{\bar{u}_1} \right\} e^{-s(\tau_3 - \tau_1)} \delta u_1
 \end{aligned}$$

4.122

This equation is very complicated. Its solution could be obtained by means of computers, but this goes beyond the scope of this analysis. A very detailed investigation was performed by Zuber (1). The present

analysis will be limited to the discussion of physical phenomena, to facilitate in the following chapter the application of the integral method. Several interesting qualitative observations can be made on this result.

A great deal of experimental and theoretical work has shown that two-phase flow systems become unstable in the low frequency range. In equation 4.122 for such a situation the phase lag between  $\delta P_{o4}$  and  $\delta u$ , would be at least larger than  $\frac{\pi}{2}$  and for the most critical conditions even equal to  $\pi$ . Such instabilities have been called in the literature "chugging oscillations." But beside them, numerous experimental investigations have yielded that at high frequencies the system can also become unstable. These detrimental higher mode oscillations have been denominated "acoustical" or "screaming" instabilities.

In section 4.2 of this chapter we proved that the present analysis is only valid in the low frequency range, if we assume isobaric flow conditions. However in the following, we will ignore this restriction to study qualitatively the high frequency domain.

In Chapter III we found that for

$$\omega \rightarrow \infty \quad |\delta \lambda| \rightarrow 0 \quad 4.123$$

Moreover if  $\omega \rightarrow \infty$

$$\frac{1}{\Omega - s} \rightarrow 0 \quad 4.124$$

Finally, because of equation 4.123 if  $\omega$  becomes large

$$\delta u_g(t) \rightarrow \delta u_1 \quad 4.125$$

If we apply these observations to equation 4.122 and rearrange, the equation reduces to

$$\begin{aligned} \delta \Delta P_{04} = & \left\{ \frac{\overline{\partial \Delta P_{01}}}{\partial \bar{u}_1} + \frac{\overline{\partial \Delta P_{12}}}{\partial \bar{u}_1} + \frac{\overline{\partial \Delta P_{23}}}{\langle u_g \rangle} + \frac{\overline{\partial \Delta P_{34}}}{\bar{u}_3} - \right. \\ & \left. - \Omega(e - \bar{\lambda}) \langle \rho_g \rangle \right\} \delta u_1 + \left\{ \rho_f \bar{\lambda} + (e - \bar{\lambda}) \langle \rho_g \rangle \right\} s \delta u_1 \\ & + \Omega e^{-s \tau_b} (e - \bar{\lambda}) \langle \rho_g \rangle \delta u_1 \end{aligned} \quad 4.126$$

Here again similar to Figure 12, the final result can be represented in an Armand diagram. The inlet velocity will be plotted on the real axis.

The first term in equation 4.126 is positive if

$$\frac{\overline{\partial \Delta P_{01}}}{\partial \bar{u}_1} + \frac{\overline{\partial \Delta P_{12}}}{\partial \bar{u}_1} + \frac{\overline{\partial \Delta P_{23}}}{\bar{u}_{em}} + \frac{\overline{\partial \Delta P_{23}}}{\langle u_g \rangle} + \frac{\overline{\partial \Delta P_{34}}}{\bar{u}_3} > \Omega(e - \bar{\lambda}) \langle \rho_g \rangle \quad 4.127$$

If we consider the second term, which is purely imaginary and proportional to the frequency  $\omega$ , to predominate in comparison with the other two terms, equation 4.126 becomes simply



$$\delta \Delta P_{04} = \left\{ \rho_f \bar{\alpha} + (\rho - \bar{\alpha}) \langle \rho_g \rangle \right\} s \delta u_1$$

4.128

Figure 23 shows that for high frequencies the phase lag between  $\delta \Delta P_{04}$  and  $\delta u_1$  is  $\frac{\pi}{2}$ , and the system is, according to the stability criterion formulated in Chapter II, still stable. But experimental research has led to the conclusion that for stability the timing between the inlet perturbation and the response is no longer of importance. Therefore it is believed that in the high frequency domain instabilities occur much more because of large pressure variations. These are necessary to account for the inertia forces, which increase directly proportional with the frequency  $\omega$ . We conclude that the present observations are not allowed according to equation 4.21. But still they were made to analyze the course of the transfer function for increasing frequencies.

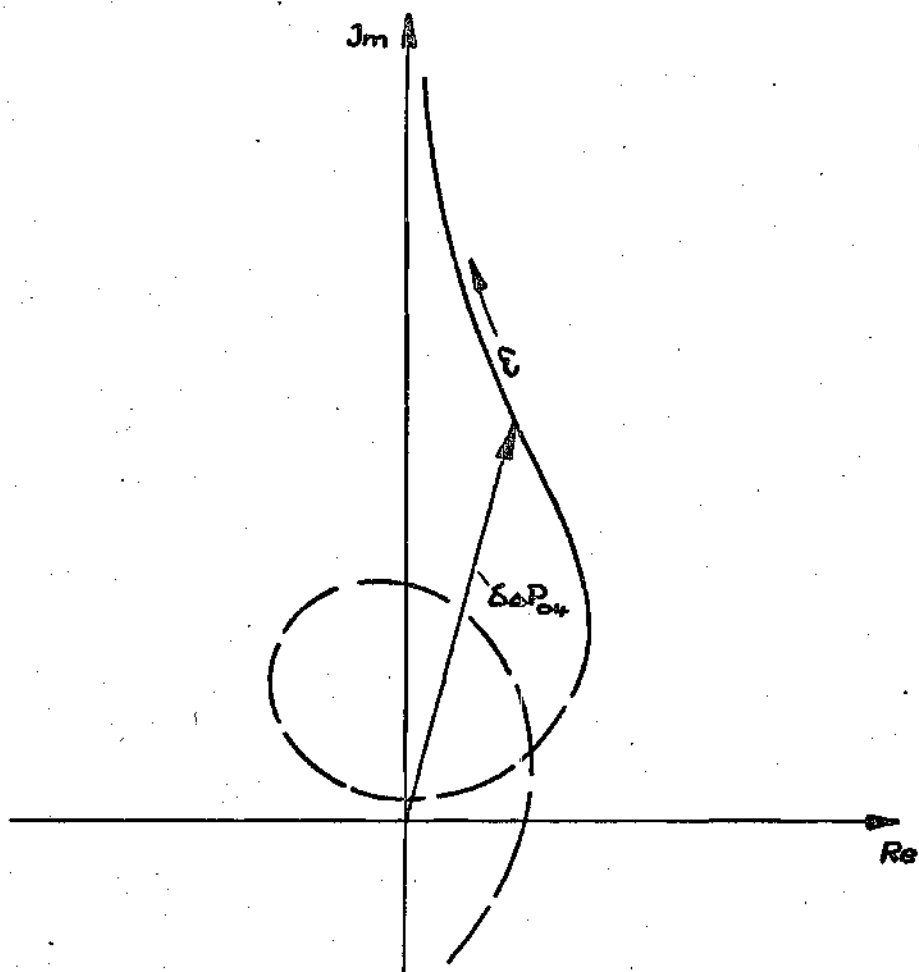


Figure 23. Total Pressure Variations for Higher Frequencies

## CHAPTER V

## ANALYSIS OF TWO PHASE FLOW INSTABILITIES

## BY MEANS OF AN INTEGRAL METHOD

5.1. General Considerations

As was described in Chapter II, the main purpose of the integral method is to simplify the calculation procedure of a theoretical analysis if it becomes too tedious without sacrificing to a certain accuracy of the results.

The previous two chapters showed that the complexity of the pertaining problem in this analysis evidently justifies the application of such an approximate method. It is now the question in which way shall the mathematical analysis be simplified.

The treatment of the single phase region, which was presented in Chapter III, did not represent major difficulties. In Chapter IV the same can be said referring the evaluation of the velocity distribution in the two phase region. However, here considerably more effort was necessary to find an expression for the density variations and afterwards in integrating the momentum equation. To examine best the influence of the integral approach and to minimize the inaccuracies, which inevitably appear by using simplifying techniques, it seems reasonable to limit its application to the evaluation of density and pressure drop fluctuations in the "light" fluid.

The density variations can be evaluated in two ways: by means of energy and constitutive equation or through the continuity equation. Both methods will be treated here to find a general and mainly simple expression for its further use in this analysis.

The pressure drop variations will be determined by simply averaging the momentum equation and introducing in this expression the velocity distribution derived in Chapter IV and the equation for the density obtained by means of the integral method.

Adding the corresponding formulas for the single and the two-phase region, the overall pressure drop of the entire system will follow and the characteristic equation will be specified. Herewith, using a simple stability criteria, a stability plane will be set up to show the effects, which various parameters (such as mass flow rate, subcooling, power input, etc.) have on flow stability. Finally a comparison with previous work, mainly the theoretical analysis of Ishii and Zuber and experimental data, will allow a careful judgement of the integral method presented in this analysis.

## 5.2. The Integrated Density Variations in the Two Phase Region

### 5.2.1. Integral Approach Methods

There are basically two different procedures to derive the overall or integrated density changes as a function of time in the two-phase region.

One possibility is to integrate first the energy equation with respect to position to determine the enthalpy variation, which afterwards through the constitutive equation gives us the density perturbation.

The second way will be to integrate directly the continuity equation. This procedure is a much shorter one and therefore it is expected to offer better results.

The present analysis will follow both methods in detail to find out how generally the integral method works on such a stability problem, and to determine out of both a representative expression for the overall density variation in the two-phase region.

### 5.2.2. Overall Density Variations by Means of Energy and Constitutive Equation

If we introduce the general constitutive equation 4.23 and the expression for the velocity distribution equation 4.33 into the energy equation 4.2, we get

$$\frac{\partial i}{\partial t} + \left[ \bar{u}_g(z) + \delta u_g(t) \right] \frac{\partial i}{\partial z} = \left[ \frac{1}{\rho_f} + \left( \frac{dv}{di} \right)_p (i - i_2) \right] \frac{q \xi}{A_c} \quad 5.1$$

Taking the enthalpy  $i_2$  at the transition point for reference and in view of the definition of the reaction frequency, we rewrite equation 5.1 as

$$\frac{\partial (i - i_2)}{\partial t} + \left[ \bar{u}_g(z) + \delta u_g(t) \right] \frac{\partial (i - i_2)}{\partial z} = \frac{q \xi}{\rho_f A_c} + \Omega (i - i_2) \quad 5.2$$

Its integration with respect to  $z$  from  $\lambda$  to  $l$  gives

$$\int_{\lambda}^l \frac{\partial(i-i_2)}{\partial t} dz + \int_{\lambda}^l \bar{u}_g(z) \frac{\partial(i-i_2)}{\partial z} dz + \int_{\lambda}^l \delta u_g(t) \frac{\partial(i-i_2)}{\partial z} dz = \frac{q \xi}{\rho_f A_c} \int_{\lambda}^l dz + \Omega \int_{\lambda}^l (i-i_2) dz$$

5.3

In this equation we analyze each term:

First integral on the left hand side of equation 5.3: using

Leibniz's rule, the integral becomes

$$\int_{\lambda}^l \frac{\partial(i-i_2)}{\partial t} dz = \frac{\partial}{\partial t} \int_{\lambda}^l (i-i_2) dz$$

5.4

This equation expresses physically the time dependence of all the thermal energy stored in the two phase region with respect to the enthalpy level  $i_2$ . The dependence can be fixed by assuming appropriate enthalpy profiles. Here three of them shall be discussed:

(1) The roughest approximation would be to take an average enthalpy value along the duct and to consider only the length  $(l-\lambda)$  to be a function of time. In this case equation 5.4 becomes

$$\frac{\partial}{\partial t} \int_{\lambda}^l (i-i_2) dz = - \frac{i_3 + i_2}{2} \frac{d\lambda}{dt}$$

5.5

(2) A much better and physically more understandable approximation can be reached, if we assume for the enthalpy distribution the steady state solution

$$i - i_2 = \frac{q \xi}{\rho_f \bar{u}_1 A_c} (z - \lambda) \quad 5.6$$

Introducing equation 5.6 into equation 5.4, integrating with respect to  $z$  and differentiating with respect to time, we get

$$\int_{\lambda}^{\ell} \frac{\partial(i - i_2)}{\partial t} dz = \frac{q \xi}{\rho_f \bar{u}_1 A_c} (\bar{\lambda} - \ell) \frac{d\delta \lambda}{dt} \quad 5.7$$

(3) The best determination of equation 5.4 will be achieved by assuming that the enthalpy distribution is always a straight line, in accordance to the steady state solution, but with the boiling boundary and the entrance velocity  $u_1$  being a function of time. In this case the steady state solution is

$$i - i_2 = \frac{q \xi}{\rho_f u_1(t) A_c} (z - \lambda(t)) \quad 5.8$$

Integrating, writing all the time dependent variables as a sum of a steady state and a perturbed quantity, expanding and linearizing

we finally get

$$\int_{\lambda(t)}^l \frac{\partial(i-i_2)}{\partial t} dz = \frac{q\varepsilon}{\rho_f \bar{u}_f A_c} \left[ (\bar{\lambda} - l) \frac{d\delta\lambda}{dt} - \frac{(l-\lambda)^2}{2\bar{u}_f} \frac{d\delta u_1}{dt} \right]$$

5.9

A comparison shows that equation 5.7 is contained in equation 5.9. Therefore in our following computations equation 5.9 will be used, and once an expression for the density variations has been found, the influence of the additional term, which appears by using equation 5.8 as an enthalpy profile, will be discussed.

Second integral on the left hand side of equation 5.3: this integral can easily be transformed into an enthalpy-dependent expression:

$$\int_{\lambda(t)}^l \bar{u}_g(z) \frac{\partial(i-i_2)}{\partial z} dz = \int_{(i-i_2)}^{(i-i_2)} \bar{u}_g(z) \partial(i-i_2)$$

5.10

Introducing the steady state velocity distribution, the integral in this equation can be divided into two parts, of which one can be evaluated immediately:



$$\int_{\lambda(t)}^l \bar{u}_g(z) \frac{\partial(i-i_2)}{\partial z} dz = \bar{u}_1(i_e - i_2) + \Omega \int^{i-i_2} (l-\lambda) d(i-i_2)$$

5.11

Third integral on the left hand side of equation 5.3: as the velocity perturbation in the two phase-flow region is independent of , we obtain

$$\int_{\lambda(t)}^l \delta u_g(t) \frac{\partial(i-i_2)}{\partial z} dz = \delta u_g(t) (i_e - i_2)$$

5.12

First integral on the right hand side of equation 5.3: the integration gives simply

$$\frac{q \xi}{\rho_f A_c} \int_{\lambda}^l dz = \frac{q \xi}{\rho_f A_c} (l - \lambda)$$

5.13

Second integral on the right hand side of equation 5.3: using the steady state equation in the form

$$d(i-i_2) = \frac{q \xi}{\rho_f \bar{u}_1 A_c} d(z-\lambda)$$

5.14

we get

$$\Omega \int_{\lambda}^{\ell} (i-i_2) d_3 = \Omega \frac{\rho_f \bar{u}_1 A_c}{q \xi} \int^{i-i_2} (i-i_2) d(i-i_2)$$

5.15

and introducing again the steady state solution for  $(i-i_2)$ , we transform this equation into

$$\Omega \int_{\lambda}^{\ell} (i-i_2) d_3 = \Omega \int^{i-i_2} (\ell-\lambda) d(i-i_2)$$

5.16

Equation 5.9, 5.11, 5.12, 5.13 and 5.16 in equation 5.3 give the general integrated energy equation

$$\frac{q \xi}{\rho_f A_c} \left[ (\bar{\lambda} - \ell) \frac{d\delta\lambda}{dt} - \frac{(\ell - \lambda)^2}{2\bar{u}_1} \frac{d\delta u_1}{dt} \right] + \bar{u}_1 (i_e - i_2) + (i_2 - i_2) \delta u_2(t) = \frac{q \xi}{\rho_f A_c} (\ell - \lambda)$$

5.17

solving for the enthalpy and rearranging

$$i_e - i_2 = \frac{q \xi}{\rho_f A_c} \left( \frac{(l - \bar{\lambda}) - \delta \lambda + \frac{1}{\bar{u}_1} \left[ (l - \bar{\lambda}) \frac{d\delta \lambda}{dt} + \frac{(l - \bar{\lambda})^2}{2\bar{u}_1} \frac{d\delta u_1}{dt} \right]}{\bar{u}_1 + \delta u_2(t)} \right)$$

5.18

removing the time dependent function from the denominator into the denominator and writing for

$$l - \bar{\lambda} = \frac{\bar{u}_e - \bar{u}_1}{\Omega}$$

5.19

equation 5.18 becomes

$$i_e - i_2 = \frac{q \xi}{\rho_f A_c} \frac{1}{\Omega} \frac{\bar{u}_3 - \bar{u}_1}{\bar{u}_1} + \frac{q \xi}{\rho_f A_c} \left\{ -\frac{1}{\Omega} \frac{\bar{u}_3 - \bar{u}_1}{\bar{u}_1^2} \delta u_2(t) - \frac{1}{\bar{u}_1} \delta \lambda + \frac{1}{\Omega} \frac{\bar{u}_3 - \bar{u}_1}{\bar{u}_1^2} \frac{d\delta \lambda}{dt} + \frac{(\bar{u}_3 - \bar{u}_1)^2}{2\Omega^2 \bar{u}_1^3} \frac{d\delta u_1}{dt} \right\}$$

5.20

The enthalpy difference ( $i_e - i_2$ ) can be expressed as a sum of a steady state and a perturbed quantity:

$$i - i_2 = \overline{i - i_2} + \delta(i - i_2)$$

5.21

in which

$$\overline{i - i_2} = \frac{q \xi}{\rho_f \bar{u}_f A_c} (l - \bar{\lambda}) \quad 5.22$$

and

$$\delta(i - i_2) = \frac{q \xi}{\rho_f A_c} \left\{ -\frac{1}{\Omega} \frac{\bar{u}_3 - \bar{u}_1}{\bar{u}_1^2} \delta u_f(t) - \frac{1}{\bar{u}_1} \delta \lambda + \frac{\bar{u}_3 - \bar{u}_1}{\Omega \bar{u}_1^2} \frac{d\delta \lambda}{dt} + \frac{\bar{u}_3 - \bar{u}_1}{2\Omega^2 \bar{u}_1^3} \frac{d\delta u_1}{dt} \right\} \quad 5.23$$

Equation 5.23 gives us the enthalpy perturbation in the two-phase region. Using the constitutive equation in the form

$$\frac{\rho_f}{\rho(i)} = 1 + \Omega \frac{\rho_f A_c}{q \xi} (i - i_2) \quad 5.24$$

or with equation 5.21

$$\frac{\rho_f}{\rho(i)} = 1 + \Omega \frac{\rho_f A_c}{q \xi} \overline{(i - i_2)} + \Omega \frac{\rho_f A_c}{q \xi} \delta(i - i_2) \quad 5.25$$

and solving this equation for  $\rho(i)$ , expanding, linearizing and writing

$$1 + \frac{\rho_f A_c}{\rho_f \xi} (i_e - i_2) = \frac{\bar{u}_3}{\bar{u}_1} \quad 5.26$$

we get

$$\frac{\rho_f(i)}{\rho_f} = \frac{\bar{u}_1}{\bar{u}_3} - \frac{\bar{u}_1}{\bar{u}_3} \left[ \frac{\rho_f A_c}{\rho_f \xi} \frac{\delta(i_3 - i_2)}{\bar{u}_3/\alpha_1} \right] \quad 5.27$$

or with equation 5.23

$$\frac{\rho}{\rho_f} = \frac{\bar{u}_1}{\bar{u}_3} + \frac{\bar{u}_3 - \bar{u}_1}{\bar{u}_3^2} \delta u_1(t) + \frac{\bar{u}_1}{\bar{u}_3^2} \delta \lambda - \frac{\bar{u}_3 - \bar{u}_1}{\bar{u}_3^2} \frac{d\delta \lambda}{dt} - \frac{1}{2} \frac{(\bar{u}_3 - \bar{u}_1)^2}{2\alpha_1 \bar{u}_3^2} \frac{d\delta u_1}{dt} \quad 5.28$$

This equation only as a function of  $\delta u_1$  and  $\delta \lambda$  gives

$$\frac{\rho}{\rho_f} = \frac{\bar{u}_1}{\bar{u}_3} + \frac{\bar{u}_3 - \bar{u}_1}{\bar{u}_3^2} \delta u_1 - \frac{\bar{u}_3 - \delta \bar{u}_1}{\bar{u}_3^2} \delta \lambda - \frac{\bar{u}_3 - \bar{u}_1}{\bar{u}_3^2} \frac{d\delta \lambda}{dt} - \frac{1}{2} \frac{(\bar{u}_3 - \bar{u}_1)^2}{2\alpha_1 \bar{u}_3^2} \frac{d\delta u_1}{dt} \quad 5.29$$

Herewith we got a general result for the density perturbation in the two-phase region. Out of this equation we observe that if the integral in equation 5.4 would have been approached by means of equation 5.6, then only the last term in equation 5.29 would be missing. The equation in this case would be

$$\frac{\rho}{\rho_f} = \frac{\bar{u}_1}{\bar{u}_3} + \frac{\bar{u}_3 - \bar{u}_1}{\bar{u}_3^2} \delta u_1 - \frac{\bar{u}_3 - 2\bar{u}_1}{\bar{u}_3^2} \Omega \delta \lambda - \frac{\bar{u}_3 - \bar{u}_1}{\bar{u}_3^2} \frac{d\delta \lambda}{dt} \quad 5.30$$

Finally the use of the roughest approximation, assuming an average enthalpy value along the duct would have given

$$\frac{\rho}{\rho_f} = \frac{\bar{u}_1}{\bar{u}_3} + \frac{\bar{u}_3 - \bar{u}_1}{\bar{u}_3^2} \delta u_1 - \frac{\bar{u}_3 - 2\bar{u}_1}{\bar{u}_3^2} \Omega \delta \lambda - \frac{i_3 + i_2}{2} \frac{d\delta \lambda}{dt} \quad 5.31$$

The expressions for the density variations in the two-phase flow region derived so far, although they are now only a function of time, appear to be lengthy and unfavorable for a further application in the momentum equation. Therefore a second integral approach will be studied in detail with the purpose of getting simpler expressions.

### 5.2.3. Overall Density Variations by Means of the Continuity Equation

By integrating the continuity equation with respect to  $z$  we get

$$\int_{\lambda}^{\ell} \frac{\partial \rho}{\partial t} dz + \int_{\lambda}^{\ell} d(\rho u) = 0$$

5.32

Using Leibniz's rule the time-dependent integral becomes

$$\frac{\partial}{\partial t} \int_{\lambda}^{\ell} \rho dz = \int_{\lambda}^{\ell} \frac{\partial \rho}{\partial t} dz - \rho \bigg|_{\lambda} \frac{d\lambda}{dt}$$

5.33

Equation 5.33 in equation 5.32, integrating and rearranging gives

$$\rho u \bigg|_{\lambda}^{\ell} = \rho \bigg|_{\lambda} \left( u_{\ell} - \frac{d\lambda}{dt} \right) - \frac{\partial}{\partial t} \int_{\lambda}^{\ell} \rho dz$$

5.34

Here again, similar to the previous integral approach, the time dependent integral can be evaluated in three different ways:

- (1) The assumption of an arithmetic average value for the density

along the duct

$$\rho_a = \frac{\rho_f + \rho_g}{2}$$

5.35

gives the simplest expression

$$\frac{\partial}{\partial t} \int_{\lambda}^l \rho dz = - \frac{\rho_f + \rho_g}{2} \frac{d\lambda}{dt}$$

5.36

(2) A considerably better approximation can be worked out by assuming for the density in the integral the steady state distribution

$$\frac{\rho(z)}{\rho_f} = \frac{\bar{u}_1}{\bar{u}_1 + \alpha(z - \lambda)}$$

5.37

Integrating and dividing by the steady state length of the boiling region, gives us an averaged density for the two-phase region

$$\rho_a = \frac{\rho_f \alpha_f}{\alpha(l - \lambda)} \ln \frac{\bar{u}_3}{\bar{u}_1}$$

5.38



Integrating between the moving boiling boundary  $\lambda(t)$  and the exit position  $l$  and differentiating with respect to time, the integral in equation 5.34 becomes

$$\frac{\partial}{\partial t} \int_{\lambda}^l \rho dz = -\frac{\rho_f \bar{u}_f}{\Omega(l-\lambda)} \ln \frac{\bar{u}_3}{\bar{u}_1} \frac{d\delta\lambda}{dt}$$

5.39

(3) The most accurate approximation will give again the most intricate expression. If in equation 5.38  $u_1$ ,  $u_3$  and  $\lambda$  are a function of time, we get

$$\begin{aligned} \frac{\partial}{\partial t} \left[ \frac{\rho_f u_f}{\Omega} \ln \frac{u_1 + \Omega(l-\lambda)}{u_1} \right] &= \frac{\partial u_1}{\partial t} \frac{\rho_f}{\Omega} \ln \frac{u_1 + \Omega(l-\lambda)}{u_1} - \\ &- \frac{\rho_f}{u_1 + \Omega(l-\lambda)} \left[ u_1 \frac{d\delta\lambda}{dt} + (l-\lambda) \frac{du_1}{dt} \right] \end{aligned}$$

5.40

This equation of course is very complicated and therefore will no longer be commented upon in the following analysis. Therefore to compute the density variations equation 5.39 will be used as this expression is physically the most consistent. Substituting equation 5.39 in equation 5.34 gives

$$\rho u)_3 = \rho_f \left( u_1 - \frac{d\delta\lambda}{dt} \right) + \frac{\rho_f u_1}{\bar{u}_3 - \bar{u}_1} \ln \frac{\bar{u}_3}{\bar{u}_1} \frac{d\delta\lambda}{dt}$$

5.41

If we divide this equation by the exit velocity, expand and write all time dependent terms as a sum of a steady state and a time dependent value, we get

$$\frac{\rho}{\rho_f} = \frac{1}{\bar{u}_3} \left( 1 - \frac{\delta u_g}{\bar{u}_g} \right) \left[ \left( \bar{u}_1 + \delta u_1 - \frac{d\delta\lambda}{dt} \right) + \frac{\bar{u}_1}{\bar{u}_3 - \bar{u}_1} \ln \frac{\bar{u}_3}{\bar{u}_1} \frac{d\delta\lambda}{dt} \right]$$

5.42

Rearranging this expression and retaining only the first order terms gives

$$\frac{\rho}{\rho_f} = \frac{\bar{u}_1}{\bar{u}_3} + \left( \frac{u_3 - u_1}{u_3^2} \right) \delta u_1 + \frac{\bar{u}_1}{\bar{u}_3^2} \frac{d\delta\lambda}{dt} + \frac{1}{\bar{u}_3} \left( \frac{\bar{u}_1}{\bar{u}_3 - \bar{u}_1} \ln \frac{\bar{u}_3}{\bar{u}_1} - 1 \right) \frac{d\delta\lambda}{dt}$$

5.43

For reasons of completeness the solution will be mentioned for the case that the arithmetic average value given by equation 5.35 would have been used. Introducing equation 5.36 into equation 5.34 the final result for the density in the two-phase flow area would be

$$\frac{\rho}{\rho_f} = \frac{\bar{u}_1}{\bar{u}_3} + \left( \frac{\bar{u}_3 - \bar{u}_1}{\bar{u}_3^2} \right) \delta u_1 + \frac{\bar{u}_1}{\bar{u}_3^2} \alpha \delta \lambda + \frac{1}{\bar{u}_3} \left( \frac{\rho_f + \rho_g}{2\rho_f} - 1 \right) \frac{d\delta \lambda}{dt} \quad 5.44$$

The two expressions for the overall density variations in the two phase region obtained in this chapter again appear to be complicated and inappropriate for further use in the momentum equation. In the following section an attempt will be made to evaluate the results so far obtained and to set up a simple equation for the density to facilitate the following computational procedures, as this is one of the main purposes of an integral method.

#### 5.2.4. A Simplified Expression for the Overall Density Variations in the Two-Phase Region

In the present analysis only the most adequate of the equations derived in each previous section of this chapter will be used.

Under the point of view of structural similarity and accuracy in section 5.2.2 we choose equation 5.29 and in section 5.2.3 equation 5.42. Considering only the time dependent part, equation 5.29 becomes

$$\frac{\delta \rho}{\rho_f} = \frac{\bar{u}_3 - \bar{u}_1}{\bar{u}_3^2} \delta u_1 - \frac{\bar{u}_3 - 2\bar{u}_1}{\bar{u}_3^2} \Omega \delta \lambda - \frac{\bar{u}_3 - \bar{u}_1}{\bar{u}_3^2} \frac{d\delta \lambda}{dt} - \frac{1}{\Omega} \frac{(\bar{u}_3 - \bar{u}_1)^2}{2\bar{u}_1 \bar{u}_3^2} \frac{d\delta u_1}{dt}$$

5.45

and equation 5.42

$$\frac{\delta \rho}{\rho_f} = \frac{\bar{u}_3 - \bar{u}_1}{\bar{u}_3^2} \delta u_1 + \frac{\bar{u}_1}{\bar{u}_3^2} \Omega \delta \lambda + \frac{1}{\bar{u}_3} \left( \frac{\bar{u}_1}{\bar{u}_3 - \bar{u}_1} \ln \frac{\bar{u}_3}{\bar{u}_1} - 1 \right) \frac{d\delta \lambda}{dt}$$

5.46

These two expressions derived by means of two different integral approaches have in comparison with equation 4.68, which was derived using a differential method, the peculiarity that they only specify the overall density variation of the entire two-phase flow region. Thus, equation 5.45 and equation 5.46 are only a function of time and no longer of space as in equation 4.68. Its phase lag is only dependent on the inlet perturbations  $\delta u_1$  and  $\delta \lambda$  and the corresponding amplitudes. Furthermore, both of them are inversely proportional to the steady state exit velocity  $\bar{u}_3$ .

The simplification of these two equations to a single representative one will be achieved by comparing the corresponding terms.

The first term is in both cases the same. In the following the assumption will be made that for steady state conditions the exit velocity  $\bar{u}_3$  is considerably larger than the inlet velocity  $\bar{u}_1$  ;

this means that

$$\bar{u}_3 \gg \bar{u}_1 \quad 5.47$$

Herewith the coefficient of the first term becomes

$$\frac{\bar{u}_3 - \bar{u}_1}{\bar{u}_3^2} \approx \frac{1}{\bar{u}_3} \quad 5.48$$

The second term only differs in its amplitude. Figure 24 shows the dependence on the exit steady state velocity. In equation 5.46 its value becomes very small for higher exit velocities as it is inversely proportional to the square of  $\bar{u}_3$ , but it remains always positive. In equation 5.45 for  $\bar{u}_3 > 2\bar{u}_1$ , the amplitude is negative and of the order of the first term. In making a decision, preference will be given to the results obtained out of the integrated continuity equation and because of its smallness there, it will be neglected. We will see later that this term does not affect at all the stability criterion which will be used.

The third term in equation 5.45 has a negative coefficient and can be simplified in the same way as was done for the first term, but in this case we emphasize that the approximate value is smaller than the original

$$-\frac{1}{\bar{u}_3} < -\frac{\bar{u}_3 - \bar{u}_1}{\bar{u}_3^2} \quad 5.49$$

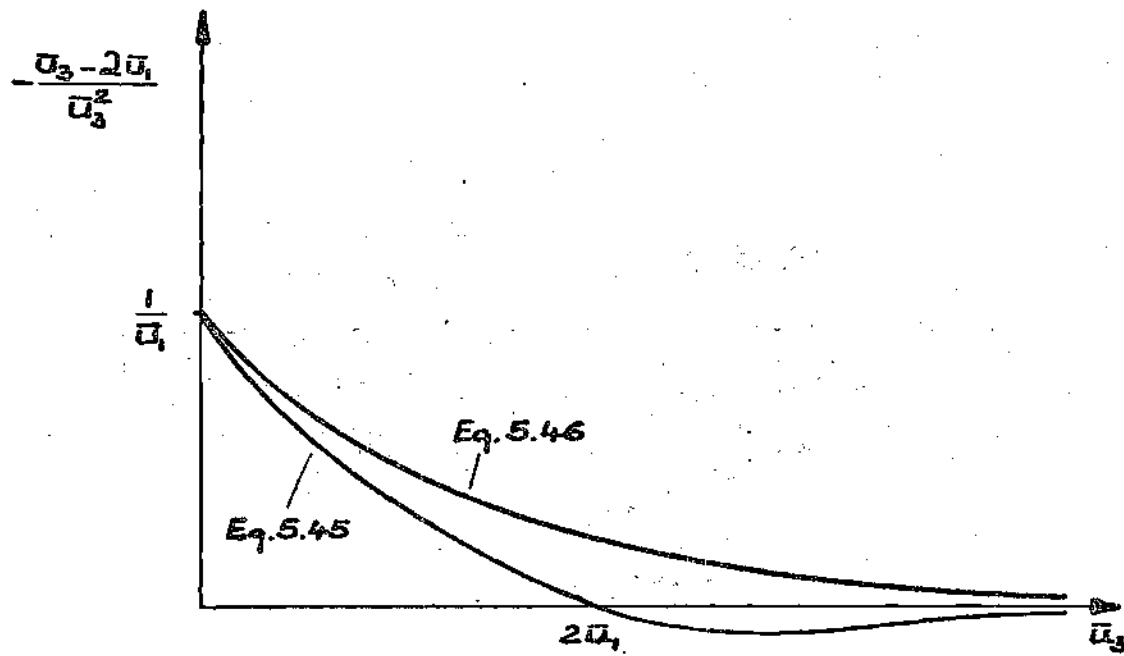


Figure 24. The Second Term in Eq. 5.45 and Eq. 5.46 as a Function of the Exit Velocity

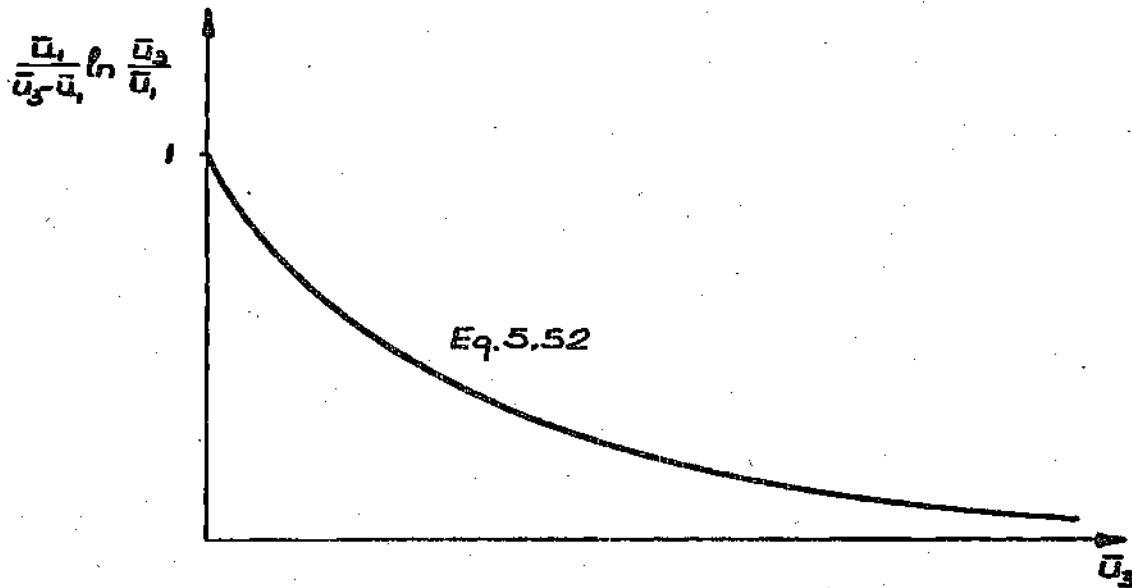


Figure 25. Eq. 5.52 as a Function of the Exit Velocity

Similar observations can be made for equation 5.46. The logarithmic expression becomes for

$$\lim_{\bar{u}_3 \rightarrow \bar{u}_1} \frac{\bar{u}_1}{\bar{u}_3 - \bar{u}_1} \ln \frac{\bar{u}_3}{\bar{u}_1} = 1 \quad 5.50$$

and for  $\bar{u}_3 = \infty$

$$\lim_{\bar{u}_3 \rightarrow \infty} \frac{\bar{u}_1}{\bar{u}_3 - \bar{u}_1} \ln \frac{\bar{u}_3}{\bar{u}_1} = 0 \quad 5.51$$

Figure 25 shows that for  $\bar{u}_3 > \bar{u}_1$ ,

$$\frac{\bar{u}_1}{\bar{u}_3 - \bar{u}_1} \ln \frac{\bar{u}_3}{\bar{u}_1} < 1 \quad 5.52$$

Therefore for the amplitude of the third term, the following inequality can be written

$$\frac{1}{\bar{u}_3} \left( \frac{\bar{u}_1}{\bar{u}_3 - \bar{u}_1} \ln \frac{\bar{u}_3}{\bar{u}_1} - 1 \right) > -\frac{1}{\bar{u}_3} \quad 5.53$$

Assuming

$$\frac{\bar{u}_1}{\bar{u}_3 - \bar{u}_1} \ln \frac{\bar{u}_3}{\bar{u}_1} - 1 \approx -1$$

5.54

the coefficient of the third term becomes equal in both equations 5.45 and 5.46.

The fourth term in equation 5.45 does not appear in equation 5.46 and will be therefore neglected. Herewith we finally write

$$\delta \rho = \frac{\rho_f}{\bar{u}_3} (\delta u_1 - s \delta \lambda)$$

5.55

With equation 3.25 a further simplification is possible

$$\delta \rho = \frac{\rho_f}{\bar{u}_3} e^{-s \tau_b} \delta u_1$$

5.56

As a conclusion to this section, we can say that the integral method has delivered us a very simple expression for the overall density variations in the two-phase region. Because of its structural similarity with equation 4.35 in the following development equation 5.55 will be used.



### 5.3. The Averaged Momentum Equation

To achieve simplicity in evaluating the pressure drop variations of the "light" fluid region, an averaged momentum equation will be used:

$$\Delta P_{23} = (l-\lambda) \frac{\partial}{\partial t} (\rho u)_a + \rho u \left| \frac{d\lambda}{\lambda dt} + \rho u^2 \right|_e - \rho u^2 \Big|_{\lambda} + \frac{f}{2D} (\rho u^2)_a (l-\lambda) + \rho_a g (l-\lambda)$$

5.57

Before we introduce in this equation the expressions for the velocity and density, all the terms will be linearized and expressed as a sum of steady-state and time-dependent values: the change of the total momentum of the fluid in the system with respect to time is

$$(l-\bar{\lambda}) \frac{\partial}{\partial t} (\rho u)_a = (l-\bar{\lambda}) \left[ \bar{\rho}_a \frac{d\delta u_g}{dt} + \bar{u}_a \frac{d\delta \rho}{dt} \right]$$

5.58

The change of momentum in the two-phase flow region because of the moving boiling boundary is taken into consideration by

$$\rho u \Big|_{\lambda} \frac{d\lambda}{dt} = \rho_f \bar{u}_f \frac{d\delta \lambda}{dt}$$

5.59

The rate of momentum eflux and influx by virtue of the bulk fluid motion are

$$\rho \bar{u}^2 \Big|_e = \bar{\rho}_e \bar{u}_e^2 + \bar{u}_e^2 \delta \rho + 2 \rho_f \bar{u}_f \delta u_y$$

$$\rho \bar{u}^2 \Big|_\lambda = \rho_f \bar{u}_f^2 + 2 \rho_f \bar{u}_f \delta u_x$$

5.60

The force of the fluid on the system is

$$\begin{aligned} \frac{f}{2D} (\rho \bar{u}^2)_a (l-\lambda) &= \frac{f}{2D} \left[ \bar{\rho}_a \bar{u}_a^2 + \bar{u}_a^2 \delta \rho + 2 \rho_a \bar{u}_a \delta u_y \right] (l-\bar{\lambda}) \\ &\quad - \frac{f}{2D} \bar{\rho}_a \bar{u}_a^2 \delta \lambda \end{aligned}$$

5.61

and the force of the gravity on the total mass of fluid is

$$\bar{\rho} g (l-\lambda) = \bar{\rho}_a g (l-\lambda) - \bar{\rho}_a g \delta \lambda + g (l-\bar{\lambda}) \delta \rho$$

5.62

We will include the effect of the exit pressure drop in the momentum equation. Defining by  $k_e$  the coefficient for the exit losses, the exit pressure drop can be expressed as

$$\Delta P_{34} = k_e \rho_e \bar{u}_e^2$$

5.63

upon linearization we get

$$\Delta P_{34} = k_e (\bar{\rho}_e \bar{u}_e^2 + \bar{u}_e^2 \delta \rho + 2 \rho_f \bar{u}_f \delta u_g) \quad 5.64$$

Adding equation 5.57 and equation 5.63, we obtain the total pressure drop across the two-phase region

$$\Delta P_{24} = \Delta P_{23} + \Delta P_{34} \quad 5.65$$

Substituting equations 5.58, 5.59, 5.60, 5.61, 5.62 and 5.64 in equation 5.65 gives

$$\begin{aligned} \Delta P_{24} = & (l - \lambda) \left[ \bar{\rho}_a \frac{d\delta u_g}{dt} + \bar{u}_a \frac{d\delta \rho}{dt} \right] + \rho_f \bar{u}_f \frac{d\delta \lambda}{dt} \\ & + \rho_e \bar{u}_e^2 + \bar{u}_e^2 \delta \rho + 2 \rho_f \bar{u}_f \delta u_g - \rho_f \bar{u}_f^2 - 2 \rho_f \bar{u}_f \delta u_l \\ & + \frac{f}{2D} \left[ \bar{\rho}_a \bar{u}_a^2 + \bar{u}_a^2 \delta \rho + 2 \bar{\rho}_a \bar{u}_a \delta u_g \right] (l - \lambda) - \frac{f}{2D} \bar{\rho}_a \bar{u}_a^2 \delta \lambda \\ & + \bar{\rho}_a g (l - \lambda) - \bar{\rho}_a g \delta \lambda + g (l - \lambda) \delta \rho \\ & + k_e \left[ \bar{\rho}_e \bar{u}_e^2 + \bar{u}_e^2 \delta \rho + 2 \rho_f \bar{u}_f \delta u_g \right] \end{aligned} \quad 5.66$$

This equation can also be expressed as

$$\Delta P_{24} = \overline{\Delta P_{24}} + \delta \Delta P_{24} \quad 5.67$$

with

$$\begin{aligned} \overline{\Delta P_{24}} = & \bar{\rho}_e \bar{u}_e^2 - \rho_f \bar{u}_f^2 + \frac{f}{2D} \bar{\rho}_a \bar{u}_a^2 (l-\lambda) \\ & + \bar{\rho}_a g (l-\bar{\lambda}) + k_e \bar{\rho}_e \bar{u}_e^2 \end{aligned} \quad 5.68$$

and rearranging

$$\begin{aligned} \delta \Delta P_{24} = & (l-\bar{\lambda}) \bar{\rho}_a \frac{d\delta u_1}{dt} + \left[ \rho_f \bar{u}_f - (l-\bar{\lambda}) \bar{\rho}_a \Omega \right] \frac{d\delta \lambda}{dt} \\ & + (l-\bar{\lambda}) \bar{u}_a \frac{d\delta \rho}{dt} + \left\{ \bar{u}_e^2 (1+k_e) + \frac{f}{2D} (l-\bar{\lambda}) \bar{u}_a^2 + g(l-\bar{\lambda}) \right\} \delta \rho \\ & + \left\{ \frac{f}{2D} (l-\bar{\lambda}) 2\bar{\rho}_a \bar{u}_a + k_e 2\rho_f \bar{u}_f \right\} \delta u_1 \\ & - \left\{ 2\Omega \rho_f \bar{u}_f + \frac{f}{2D} (l-\bar{\lambda}) 2\Omega \bar{\rho}_a \bar{u}_a + \frac{f}{2D} \bar{\rho}_a \bar{u}_a^2 + \right. \\ & \left. + \bar{\rho}_a g + k_e 2\rho_f \bar{u}_f \Omega \right\} \delta \lambda \end{aligned} \quad 5.69$$

Introducing now the expression obtained in the previous section for the density perturbation and its first derivative, which we write as follows

$$\frac{d\delta\rho}{dt} = \frac{\rho_f}{\bar{u}_g} \left\{ s\delta u_1 - s^2\delta\lambda \right\}$$

5.70

Equation 5.68 becomes

$$\begin{aligned} \delta\Delta P_{24} = & (l-\bar{\lambda})\bar{\rho}_a s\delta u_1 + \left\{ \rho_f \bar{u}_f - (l-\bar{\lambda})\bar{\rho}_a \Omega \right\} s\delta\lambda \\ & + \frac{(l-\bar{\lambda})}{\bar{u}_g} \bar{u}_a \rho_f s\delta u_1 - (l-\bar{\lambda})\bar{u}_a \frac{\rho_f}{\bar{u}_g} s^2\delta\lambda \\ & + \left\{ \bar{u}_e^2 (1+k_e) + \frac{f}{2D} (l-\bar{\lambda})\bar{u}_a^2 + g(l-\bar{\lambda}) \right\} \frac{\rho_f}{\bar{u}_a} \delta u_1 \\ & - \left\{ \bar{u}_e^2 (1+k_e) + \frac{f}{2D} (l-\bar{\lambda})\bar{u}_a^2 + g(l-\bar{\lambda}) \right\} \frac{\rho_f}{\bar{u}_a} s\delta\lambda \\ & + \left\{ \frac{f}{2D} (l-\bar{\lambda}) \Omega \bar{\rho}_a \bar{u}_a + k_e \Omega \bar{\rho}_f \bar{u}_f \right\} \delta u_1 \\ & - \left\{ \Omega \rho_f \bar{u}_f + \frac{f}{2D} (l-\bar{\lambda}) \Omega \bar{\rho}_a \bar{u}_a + \frac{f}{2D} \bar{\rho}_a \bar{u}_a^2 \right. \\ & \left. + \rho_a g + k_e \Omega \rho_f \bar{u}_f \Omega \right\} \delta\lambda \end{aligned}$$

5.71

The total pressure disturbance of the system is the sum of equation 3.47 and equation 5.71:

$$\begin{aligned}
 \delta \Delta P_{04} = & \left\{ \left\{ k_i \rho_f \Delta \bar{u}_i + \frac{f}{2D} \rho_f \Delta \bar{u}_i \bar{\lambda} \right\} + \left\{ \bar{u}_e^2 (1 + k_e) + \frac{f}{2D} (l - \bar{\lambda}) \bar{u}_a^2 \right. \right. \\
 & \left. \left. + g(l - \bar{\lambda}) \right\} \frac{\rho_f}{\bar{u}_e} + \left\{ \frac{f}{2D} (l - \bar{\lambda}) \Delta \bar{\rho}_a \bar{u}_a + k_e \Delta \rho_f \bar{u}_f \right\} \right\} \delta u_i \\
 & + \left[ \rho_f \bar{\lambda} + (l - \bar{\lambda}) \bar{\rho}_a + \frac{(l - \bar{\lambda})}{\bar{u}_3} \bar{u}_a \rho_f \right] \varsigma \delta u_i \\
 & + \left\{ \left\{ \rho_f g + \rho_f \frac{f}{2D} \bar{u}_i^2 \right\} - \left\{ \Delta \rho_f \bar{u}_f + \frac{f}{2D} (l - \bar{\lambda}) \Delta \rho_f \bar{u}_a \right. \right. \\
 & \left. \left. + \frac{f}{2D} \bar{\rho}_a \bar{u}_a^2 + \bar{\rho}_a g + k_e \Delta \rho_f \bar{u}_f \right\} \right\} \delta \lambda \\
 & + \left[ \rho_f \bar{u}_f - (l - \bar{\lambda}) \bar{\rho}_a \right] \varsigma - \left\{ \bar{u}_e^2 (1 + k_e) + \frac{f}{2D} (l - \bar{\lambda}) \bar{u}_a^2 \right. \\
 & \left. + g(l - \bar{\lambda}) \right\} \frac{\rho_f}{\bar{u}_e} \varsigma \delta \lambda + \left[ -(l - \bar{\lambda}) \bar{u}_a \frac{\rho_f}{\bar{u}_3} \right] \varsigma^2 \delta \lambda
 \end{aligned}$$

5.72

This is the final result for the pressure variations as a function of the inlet velocity perturbation, and the corresponding influence coefficients. The equation can also be expressed in terms of steady state pressure drops. For the average values in

the momentum equation 5.57 we use the values defined in equation 4.79 and 4.85. Thus with

$$\bar{u}_a = \langle u_g \rangle$$

$$\bar{p}_a = \langle p_g \rangle$$

5.73

equation 5.72 becomes

$$\begin{aligned} \delta \Delta P_{04} &= \left[ \frac{\partial \overline{\Delta P_{01}}}{\partial \bar{u}_1} + \frac{\partial \overline{\Delta P_{12}}}{\partial \bar{u}_1} + \frac{\bar{u}_3}{\bar{u}_1} \frac{\overline{\Delta P_a}}{\bar{u}_3 - \bar{u}_1} + \left( \frac{1}{\bar{u}_f} + \frac{2}{\bar{u}_3} \right) \overline{\Delta P_{34}} + \right. \\ &+ \left. \left( \frac{2}{\langle u_g \rangle} + \frac{\langle u_g \rangle}{\bar{u}_f \bar{u}_e} \right) \overline{\Delta P_{23}} + \frac{\rho_f}{\langle \rho_g \rangle \bar{u}_3} \overline{\Delta P_{bg}} \right] \delta u_1 \\ &+ \left[ \rho_f \bar{\lambda} + \frac{\overline{\Delta P_a}}{2 \bar{u}_{em}} + \frac{\langle u_g \rangle}{2 \bar{u}_3 \bar{u}_1} \overline{\Delta P_a} \right] \delta u_1 \\ &+ \left[ \frac{\partial \overline{\Delta P_{14}}}{\partial \bar{\lambda}} + \frac{\partial \overline{\Delta P_{12}}}{\partial \bar{\lambda}} - 2 \frac{\overline{\Delta P_a}}{(\bar{e} - \bar{\lambda})} - \left( \frac{2 \rho}{\langle u_g \rangle} - \frac{1}{(\bar{e} - \bar{\lambda})} \right) \overline{\Delta P_{23}} - \right. \\ &- \left. \frac{\overline{\Delta P_{bg}}}{(\bar{e} - \bar{\lambda})} - 2 \rho \frac{\overline{\Delta P_{34}}}{\bar{u}_3} \right] \delta \lambda \\ &+ \left[ \left( \frac{1}{\bar{u}_3 - \bar{u}_1} - \frac{1}{\bar{u}_{em}} \right) \overline{\Delta P_a} - \frac{\bar{u}_3}{\bar{u}_1} \frac{\overline{\Delta P_a}}{\bar{u}_3 - \bar{u}_1} - \frac{\overline{\Delta P_{34}}}{\bar{u}_f} - \right. \\ &- \left. \frac{\bar{u}_a}{\bar{u}_f \bar{u}_e} \overline{\Delta P_{23}} \right] \delta \lambda + \left[ - \frac{\langle u_g \rangle}{\bar{u}_f \bar{u}_3} \frac{\overline{\Delta P_a}}{\rho} \right] \delta^2 \lambda \end{aligned} \quad 5.74$$

## CHAPTER VI

## STABILITY ANALYSIS

6.1. General Considerations

As was commented in Chapter I, unstable conditions in the system will certainly be present if the phase lag between the velocity perturbation and the system pressure drop is equal to half a period of oscillation. In such a situation the gradients of  $\delta u_1$  and of  $\delta \Delta P$  always have an opposite sign. The present theoretical investigation however considers the integral effect and therefore we say that out of a full period, for at least half of it the gradient of inlet and outlet perturbations have to have the same sign. In this case the phase lag between both oscillatory movements is restricted by equation 2.4.

The stability analysis will be performed by using a very simple criterion, first used in the analysis of Ishii and Zuber (20). The results will be plotted in an appropriate stability plane. A parametric study and comparison with experimental data will conclude this analysis.

6.2. A Simplified Stability Analysis

To facilitate the further computational process, we write equation 5.72 in terms of abbreviated influence coefficients

$$\delta \Delta P_{04} = A_1 \delta u_1 + A_2 s \delta u_1 + A_3 \delta \lambda + A_4 s \delta \lambda + A_5 s^2 \delta \lambda$$

6.1



In this equation we set

$$A_1 = \left[ \frac{\partial \overline{\Delta P_{01}}}{\partial \bar{u}_1} + \frac{\partial \overline{\Delta P_{12}}}{\partial \bar{u}_1} + \frac{\bar{u}_3}{\bar{u}_1} \frac{\overline{\Delta P_a}}{\bar{u}_3 - \bar{u}_1} + \left( \frac{1}{\bar{u}_f} + \frac{2}{\bar{u}_3} \right) \overline{\Delta P_{34}} \right. \\ \left. + \left( \frac{2}{\langle u_g \rangle} + \frac{\langle u_g \rangle}{\bar{u}_f \bar{u}_e} \right) \overline{\Delta P_{23}} + \frac{\rho_f}{\langle \rho_g \rangle \bar{u}_3} \overline{\Delta P_{bg}} \right] \quad 6.2$$

$$A_2 = \left[ \rho_f \bar{\lambda} + \frac{\overline{\Delta P_a}}{\Omega \bar{u}_{em}} + \frac{\langle u_g \rangle}{\Omega \bar{u}_3 \bar{u}_1} \overline{\Delta P_a} \right] \quad 6.3$$

$$A_3 = \left[ \frac{\partial \overline{\Delta P_{01}}}{\partial \bar{\lambda}} + \frac{\partial \overline{\Delta P_{12}}}{\partial \bar{\lambda}} - 2 \frac{\overline{\Delta P_a}}{(\bar{e} - \bar{\lambda})} - \left( \frac{2\Omega}{\langle u_g \rangle} - \frac{1}{(\bar{e} - \bar{\lambda})} \right) \overline{\Delta P_{23}} \right. \\ \left. - \frac{\overline{\Delta P_{bg}}}{(\bar{e} - \bar{\lambda})} - 2\Omega \frac{\overline{\Delta P_{34}}}{\bar{u}_3} \right] \quad 6.4$$

$$A_4 = \left[ \left( \frac{1}{\bar{u}_3 - \bar{u}_1} - \frac{1}{\bar{u}_{em}} \right) \overline{\Delta P_a} - \frac{\bar{u}_3}{\bar{u}_1} \frac{\overline{\Delta P_a}}{\bar{u}_3 - \bar{u}_1} - \frac{\overline{\Delta P_{34}}}{\bar{u}_f} - \frac{\bar{u}_a}{\bar{u}_f \bar{u}_e} \overline{\Delta P_{23}} \right] \quad 6.5$$

$$A_5 = \left[ -\frac{\langle u_g \rangle}{\bar{u}_f \bar{u}_3} \frac{\overline{\Delta P_a}}{\Omega} \right]$$

6.6

If we express  $\delta \Delta P_{o4}$  directly as a function of  $\delta u_1$ , equation 6.1 becomes

$$\delta \Delta P_{o4} = \left[ A_1 + s A_2 + \frac{(1 - e^{-s\tau_b})}{s} A_3 + \right. \\ \left. + (1 - e^{-s\tau_b}) A_4 + s(1 - e^{-s\tau_b}) A_5 \right] \delta u_1$$

6.7

Here the terms in brackets represents the transfer function between the input  $\delta u_1$  and the output  $\delta \Delta P_{o4}$ . By rearranging equation 6.7, we obtain the ratio of the oscillatory movements

$$\frac{\delta u_1}{\delta \Delta P_{o4}} = \frac{1}{Q(s)}$$

6.8

with

$$Q(s) = A_1 + s A_2 + \frac{(1 - e^{-s\tau_b})}{s} A_3 + (1 - e^{-s\tau_b}) A_4 \\ + s(1 - e^{-s\tau_b}) A_5$$

6.9

This expression is called the characteristic equation of the system because it determines its behavior towards any perturbation mode, depending only on the system parameters. Figure 26 represents the block diagram of the system. For  $Q(s) = 0$ , equation 6.8 shows that the ratio between input  $\delta u_1$  and output  $\delta \Delta P_{04}$  becomes infinity. Therefore for a given inlet velocity variation, the pressure drop remains constant and the system is stable. In an Armand diagram this situation arises, if the plot of the frequency goes through the origin. But this, in accordance to the stability criterion formulated at the beginning of this section, means that we are crossing the stability boundary. Figure 27 shows qualitatively such a situation for the frequency response in a complex plane.

Figure 28 represents a special situation. Here the frequency plot only touches the stability boundary at the origin. However the same observations are still valid, because a change of the system parameters would immediately lead to conditions similar to these described in Figure 27.

In the following a very simply criterion will be derived to find out the influence of the system parameters on the stability boundary

$Q(s) = 0$ . In equation 6.9 we introduce  $s = i\omega$  and write a common denominator for the whole expression

$$0 = \frac{A_1 \omega + iA_2 \omega^2 - iA_3 [1 - e^{-i\omega t_0}] + A_4 \omega [1 - e^{-i\omega t_0}] + iA_5 \omega^2 [1 - e^{-i\omega t_0}]}{\omega}$$

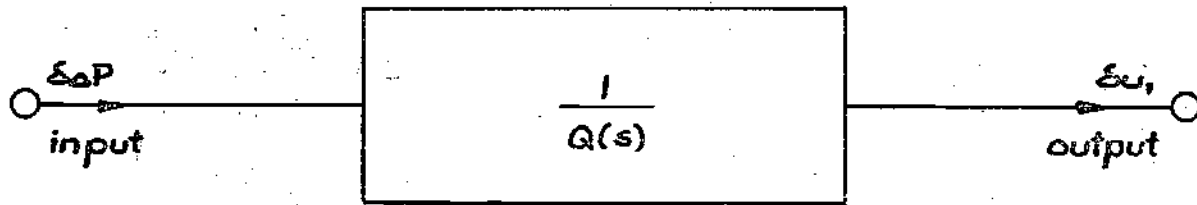


Figure 26. Block Diagram of the System

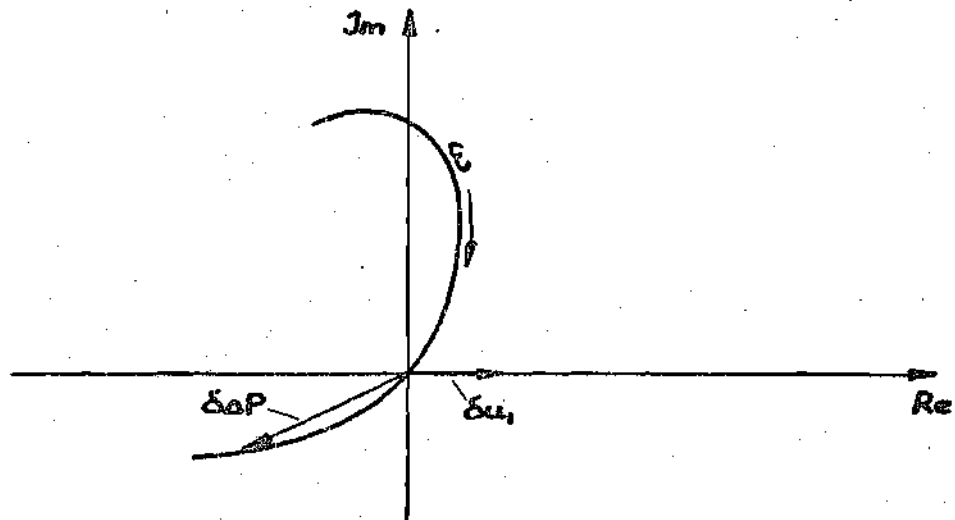


Figure 27. Graphical Representation of the Transfer Function Between Inlet Velocity and Pressure Drop Perturbation

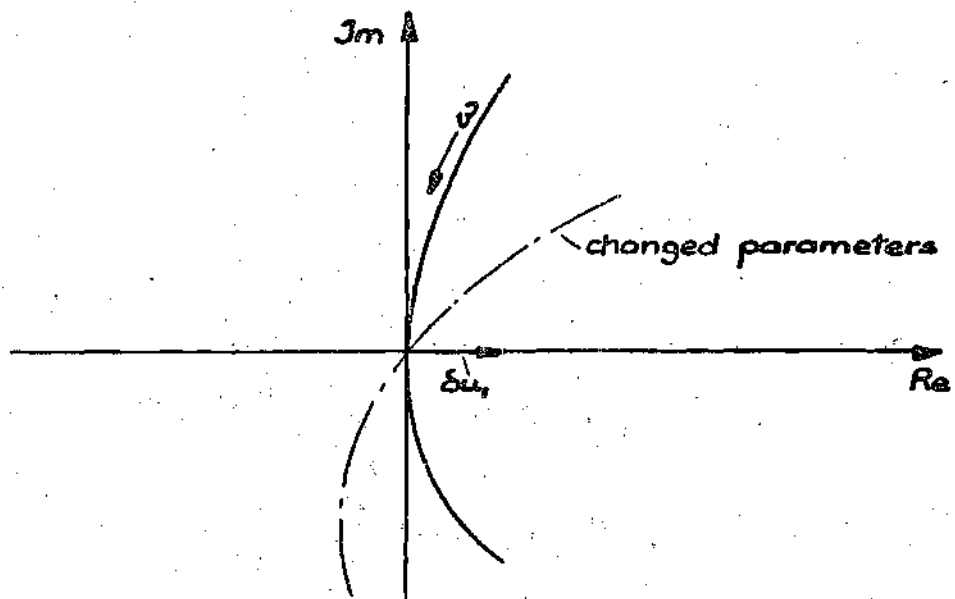


Figure 28. Tangential Course of the Transfer Function and its Dependence on the Parameters

Separating the real and imaginary components, we get

$$0 = \frac{A_{14}\omega - A_4\omega\cos\omega\tau_0 + A_3\sin\omega\tau_0 - A_5\omega^2\sin\omega\tau_0}{\omega} +$$

$$+ \frac{A_4\omega\sin\omega\tau_0 + A_{25}\omega^2 - A_3 + A_3\cos\omega\tau_0 - A_5\omega^2\cos\omega\tau_0}{\omega}$$

6.11

with

$$A_{14} = A_1 + A_4$$

$$A_{25} = A_2 + A_5$$

6.12

The very extensive analysis of Ishii and Zuber (20) showed that the higher orders of  $\omega$  do not influence the course of the stability boundary significantly. Therefore they will be neglected and we obtain for the real part

$$A_3\sin\omega\tau_0 + A_{14}\omega - A_4\omega\cos\omega\tau_0 = 0$$

6.13

and for the imaginary part

$$A_3\cos\omega\tau_0 - A_3 + A_4\omega\sin\omega\tau_0 = 0$$

6.14

Rearranging and using basic relations from trigonometry, these two equations become

$$2 \cos \frac{\omega T_b}{2} \left[ A_3 \sin \frac{\omega T_b}{2} - \omega A_4 \cos \frac{\omega T_b}{2} \right] + (A_{14} + A_4) \omega = 0$$

6.15

and

$$\sin \frac{\omega T_b}{2} \left[ -A_3 \sin \frac{\omega T_b}{2} + A_4 \omega \cos \frac{\omega T_b}{2} \right] = 0$$

6.15

We recall that an unstable situation certainly arises if the phase lag  $\phi$  between input perturbation and output response becomes equal to  $\pi$ . Equation 6.16, the imaginary part of the characteristic equation, gives us hereto the frequencies

$$\omega T_b = 0, 2\pi, 4\pi$$

6.17

and

$$-A_3 \sin \frac{\omega T_b}{2} + A_4 \omega \cos \frac{\omega T_b}{2} = 0$$

6.18

or

$$\tan \frac{\omega \tau_b}{2} = \frac{A_4}{A_3 \tau_b} \frac{\omega \tau_b}{2} \quad 6.19$$

With equation 6.4 and equation 6.5 it can be shown that

$$\frac{A_4}{A_3 \tau_b} > 1 \quad 6.20$$

Figure 29 shows that for

$$\frac{\omega \tau_b}{2} \leq \frac{\pi}{2} \quad 6.21$$

Equation 6.19 has a solution. Therefore instabilities already appear for

$$\omega \tau_b \lesssim \pi \quad 6.22$$

Herewith the integral method and the application of a simplified stability criteria delivered a result which has been repeatedly observed in experimental research: instabilities in two-phase flow systems



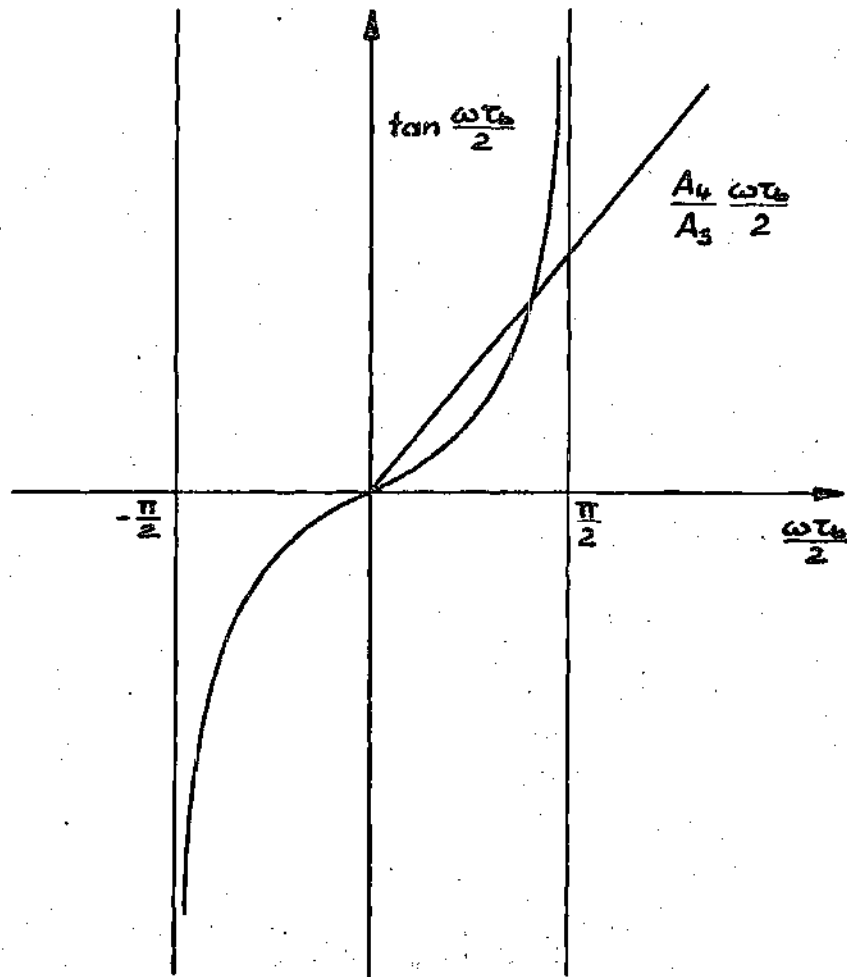


Figure 29. Graphical Solution of Eq.6.19

preferentially occur at low frequencies. In the literature these unstable flow conditions are called chugging oscillations.

Equation 6.18 in equation 6.15 gives the stability boundary

$$A_{14} + A_4 = 0 \quad 6.23$$

In Chapter II we said that for stability the response to a velocity perturbation, which we plot on the real axis, will have to be on the right hand side of the Armand diagram. Thus the real part in equation 6.15 has to be positive or in equation 6.23 it means that

$$A_1 + 2A_4 > 0 \quad 6.24$$

Equation 6.2 and equation 6.5 in equation 6.24 gives

$$\begin{aligned} & \left[ \frac{\partial \overline{\Delta P_{c1}}}{\partial \bar{u}_1} + \frac{\partial \overline{\Delta P_{c2}}}{\partial \bar{u}_1} + \frac{\bar{u}_3}{\bar{u}_1} \frac{\overline{\Delta P_a}}{\bar{u}_3 - \bar{u}_1} + \left( \frac{1}{\bar{u}_f} + \frac{2}{\bar{u}_3} \right) \overline{\Delta P_{34}} \right. \\ & \left. + \left( \frac{2}{\langle u_g \rangle} + \frac{\langle u_g \rangle}{\bar{u}_f \bar{u}_e} \right) \overline{\Delta P_{23}} + \frac{\rho_f}{\langle \rho_g \rangle \bar{u}_3} \overline{\Delta P_{bg}} \right] + 2 \left[ \left( \frac{1}{\bar{u}_3 - \bar{u}_1} - \frac{1}{\bar{u}_{em}} \right) \overline{\Delta P_a} \right. \\ & \left. - \frac{\bar{u}_3}{\bar{u}_1} \frac{\overline{\Delta P_a}}{\bar{u}_3 - \bar{u}_1} - \frac{\overline{\Delta P_{34}}}{\bar{u}_f} - \frac{\bar{u}_a}{\bar{u}_f \bar{u}_e} \overline{\Delta P_{23}} \right] > 0 \end{aligned} \quad 6.25$$

or

$$\left\{ \left\{ k_i \rho_f 2\bar{u}_f + \frac{f}{2D} 2\rho_f \bar{u}_f \bar{\lambda} \right\} + \left\{ \bar{u}_e^2 (1+k_e) + \frac{f}{2D} (e-\lambda) \bar{u}_a^2 + g(e-\bar{\lambda}) \right\} \frac{\rho_f}{\bar{u}_3} \right. \\ \left. + \left\{ \frac{f}{2D} (e-\bar{\lambda}) 2\bar{\rho}_a \bar{u}_a + k_e 2\rho_f \bar{u}_f \right\} + 2 \left\{ \rho_f \bar{u}_f - (e-\bar{\lambda}) \bar{\rho}_a \Omega \right\} \right. \\ \left. - \left\{ \bar{u}_e^2 (1+k_e) + \frac{f}{2D} (e-\bar{\lambda}) \bar{u}_a^2 + g(e-\bar{\lambda}) \right\} \frac{\rho_f}{\bar{u}_3} \right\} > 0$$

6.26

This inequality is independent of the frequency and represents a relation between the different parameters which characterize the system.

### 6.3. Similarity Groups Governing the System

In order to make the results so far obtained independent of a specific geometry of the system and special operational conditions, we will set up in the following a group of dimensionless parameters. These will enable us to generalize our further investigations and to evaluate the quality of the present work in comparison with previous theoretical and experimental research.

Generally in the areas of heat and mass transfer for complete similarity between two systems beside geometrical also kinematic, dynamic (these two are mechanical) and thermal similarity must be fulfilled.

### 6.3.1. Geometric Similarity

Using  $l$  as a length scale we easily nondimensionalize the geometry of the system

$$z^* = \frac{z}{l} \qquad D^* = \frac{D}{l} \qquad 6.27$$

### 6.3.2. Dynamic Similarity

Through a dimensional analysis of the momentum equation the two main dimensionless groups for dynamic similarity can be obtained

The Reynolds Number  $N_{Re}$  :

$$N_{Re} = \frac{\rho_f u_f D}{\mu_f} = \frac{\text{inertia forces}}{\text{frictional forces}} \qquad 6.28$$

The Froude Number  $N_{Fr}$  :

$$N_{Fr} = \frac{\bar{u}_f^2}{gl} = \frac{\text{inertia forces}}{\text{gravity forces}} \qquad 6.29$$

### 6.3.3. Kinematic Similarity

A two-phase flow system with heat addition is a coupled thermo-hydrodynamic problem. As was shown in Chapter II in our simplified system the thermal conditions always determine its kinematics.

Thus kinematic similarity also fulfills thermal similarity. With the reaction frequency  $\Omega$ , we easily non-dimensionalize

The Inlet Velocity

$$\bar{u}_f^* = \frac{\bar{u}_f}{\Omega l} \quad 6.30$$

and

The Outlet to Inlet Velocity Ratio

$$C_r^* = \frac{\bar{u}_f + \Omega(l-\bar{\lambda})}{\bar{u}_f} = 1 + \frac{1-\lambda^*}{\bar{u}_f^*} \quad 6.31$$

Moreover we need two additional parameters to scale the thermal conditions of the fluid at the inlet and the heat addition to the system. Hereto we set up an energy balance

$$q \xi l = \Delta i_{sub} (G_f + G_g) + \Delta i_{fg} G_g \quad 6.32$$

where  $G_f$  and  $G_g$  are the mass flow rates of the liquid and the vapor phase respectively. Therefore the thermal energy added to the duct along its length  $l$  causes the saturation of the total mass flow rate ( $G_f + G_g$ ) and the vaporization of the mass flow rate  $G_g$ .

Rearranging, the following nondimensional equation results

$$\frac{\Delta i_{sub}}{\Delta i_{fg}} = \frac{q \ell}{\rho_f u_f A_c \Delta i_{fg}} - X \quad 6.33$$

with  $X$  defined by equation 4.22 as the quality of the mixture. It shall be mentioned that equation 6.33 could already be used to set up the required similarity groups. However to introduce the reaction frequency  $\Omega$ , we multiply the equation with  $\Delta P / \rho_g$  and obtain

$$N_{sub} = N_{pch} - X \left( \frac{\Delta P}{\rho_g} \right) \quad 6.34$$

Here we wrote

The Subcooling Number  $N_{sub}$  :

$$N_{sub} = \frac{\Delta i_{sub}}{\Delta i_{fg}} \frac{\Delta P}{\rho_g} \quad 6.35$$

The subcooling number  $N_{sub}$  describes the thermodynamic conditions of the fluid at the entrance of the system. Therefore it scales the time, which the fluid entering the duct needs to reach saturation conditions.

The Phase Change Number  $N_{pch}$  :

$$N_{pch} = \frac{q \epsilon l}{A_c \bar{u}_f \Delta i_{fg}} \frac{\Delta \rho}{\rho_g \rho_f} = \frac{\Omega l}{\bar{u}_f} = \frac{l}{\bar{u}_f^*} \quad 6.36$$

The phase change number  $N_{pch}$  scales through the reaction frequency  $\Omega$  the rate of phase change and with  $l/\bar{u}_f$  the residence time of a particle in the duct. Hence it indicates how far the phase change has progressed in a system.

The Boiling Length  $\lambda^*$  :

An energy balance for the liquid phase, solved for  $\lambda$  and scaled with the length  $l$  gives the dimensionless boiling length  $\lambda^*$  :

$$\lambda^* = \frac{\bar{\lambda}}{l} = \frac{\Delta i_{sub} \cdot A_c \rho_f \bar{u}_f}{q \epsilon l} \quad 6.37$$

This parameter can also be obtained subdividing equation 6.35 by equation 6.36

$$\lambda^* = \frac{\bar{\lambda}}{l} = \frac{N_{sub}}{N_{pch}} \quad 6.38$$

The Density Number  $N_\rho$  :

The density number (or ratio) scales the pressure level of the system and thus the fluid properties

$$N_\rho = \rho_g^* = \frac{\rho_g}{\rho_f} \quad 6.39$$

In the following section, the similarity groups presented here will be applied to our simplified stability criterion.

#### 6.4. Dimensionless Stability Criterion

Rearranging, dividing by the steady state mass flux, and introducing an averaged friction factor for the entire system, equation 6.25 becomes

$$\begin{aligned} & 2k_i + 2\frac{f_m}{2D}l + 2k_e + 2\left\{1 - \frac{\rho(l-\bar{x})}{\bar{u}_f + \rho(l-\bar{x})}\right\} \\ & - \left\{ \frac{\bar{u}_f + \rho(l-\bar{x})}{\bar{u}_f} + \frac{f_m}{2D}(l-\bar{x}) \frac{[\bar{u}_f + \rho(\frac{l-\bar{x}}{2})]^2}{\bar{u}_f[\bar{u}_f + \rho(l-\bar{x})]} + g \frac{(l-\bar{x})}{\bar{u}_f[\bar{u}_f + \rho(l-\bar{x})]} \right. \\ & \left. - k_e \frac{\bar{u}_f + \rho(l-\bar{x})}{\bar{u}_f} > 0 \right. \end{aligned} \quad 6.40$$

Applying the similarity groups obtained in section 6.3, equation 6.40 can be rewritten as



$$2k_i + 2 \frac{f_m}{2D^*} + 2k_e > C_r^* (1 + k_e) +$$

$$+ \frac{f_m}{2D^*} (1 - \lambda^*) \frac{\left(\frac{\bar{u}_3 + \bar{u}_1}{2}\right)^2}{\bar{u}_3 \bar{u}_1} + (C_r^* - 1) \frac{\bar{u}_f^*}{C_r^*} \frac{1}{N_{Fr}} - \frac{\rho_s}{C_r^*}$$

6.41

Here we set

$$\frac{\left(\frac{\bar{u}_3 + \bar{u}_1}{2}\right)^2}{\bar{u}_3 \bar{u}_1} \approx \frac{1}{2} N_{pch}$$

6.42

The right hand side of this equation is only a function of the inlet to outlet velocity ratio  $C_r^*$ . However the phase change number  $N_{pch}$  increases linearly with the subcooling number  $N_{sub}$ . The simplification made in equation 6.42 is only valid for small values of  $N_{sub}$  in comparison to  $N_{pch}$ . Figures 33, 34, 35, and 36 show that this is also true for most of the experimental data, thus justifying our assumptions.

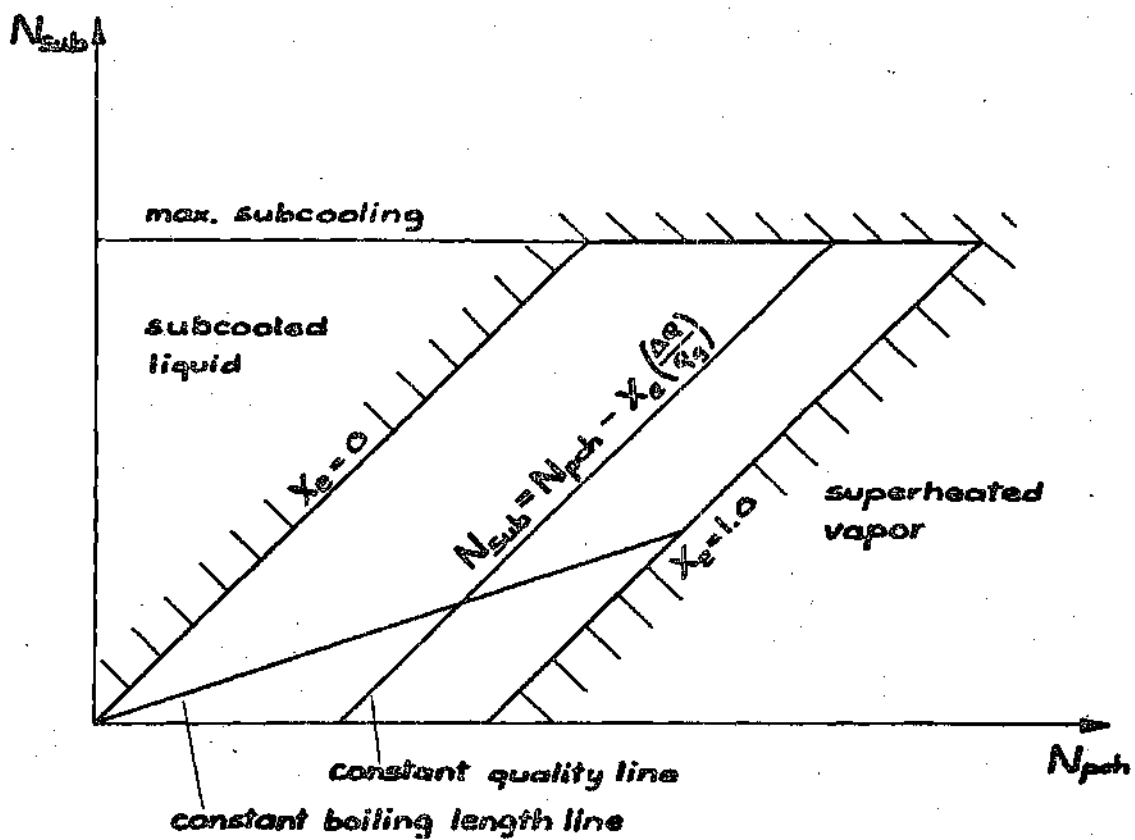


Figure 30. Stability Plane

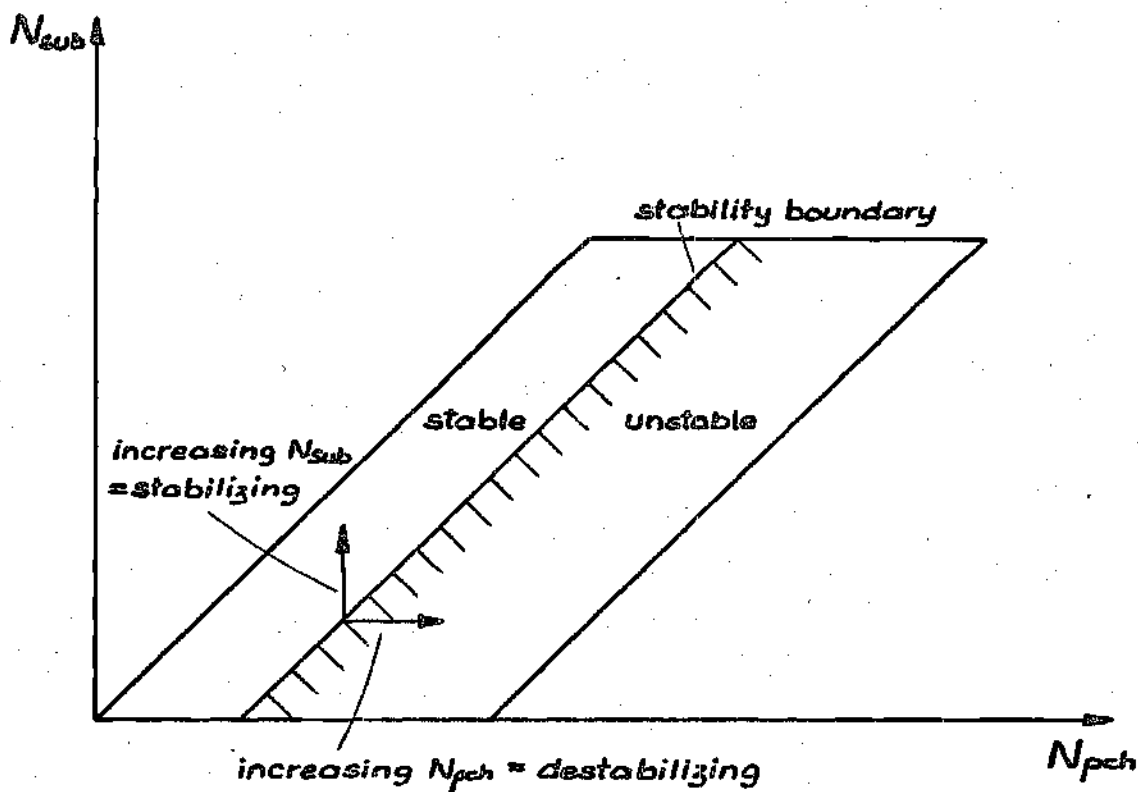


Figure 3I. Influence of the Subcooling Number and Phase Change Number on the Stability of the System

- 1) Increase of system pressure, inlet velocity, inlet flow restriction shifts the line to the right = stabilizes the system
- 2) Increase of friction factor, outlet flow restriction shifts the line to the left = destabilizes the system

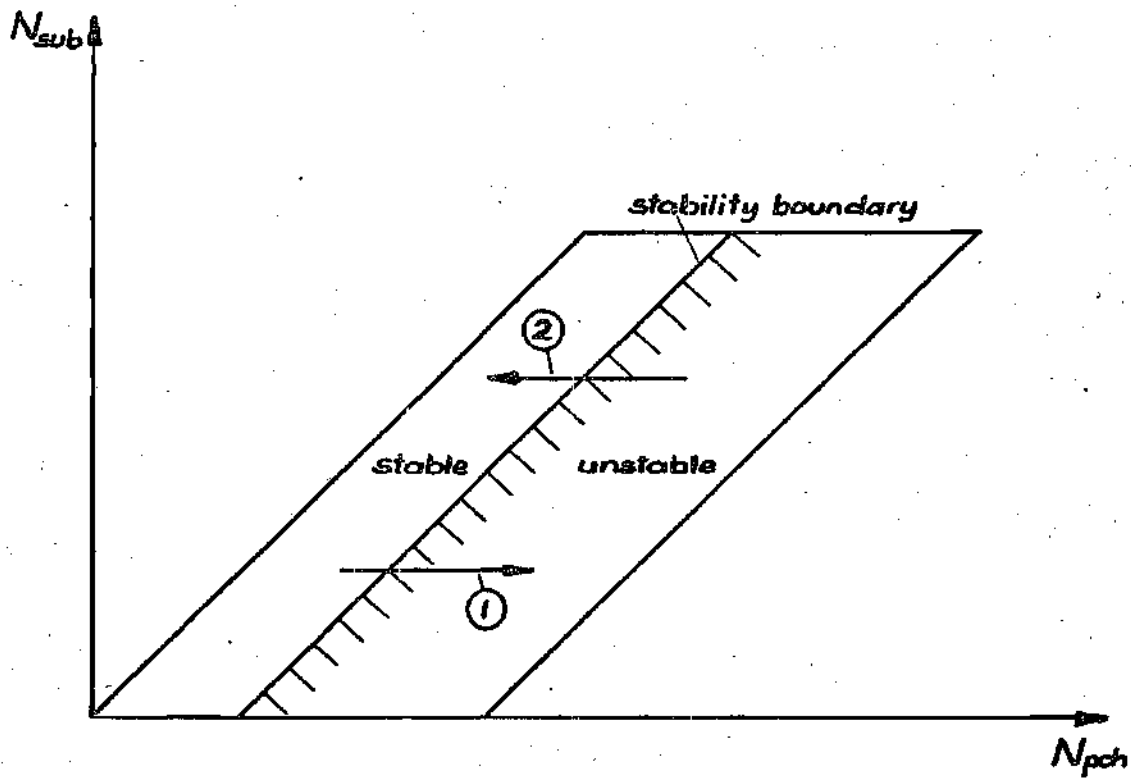


Figure 32. Influence of Several Operational Parameters on the Stability of the System

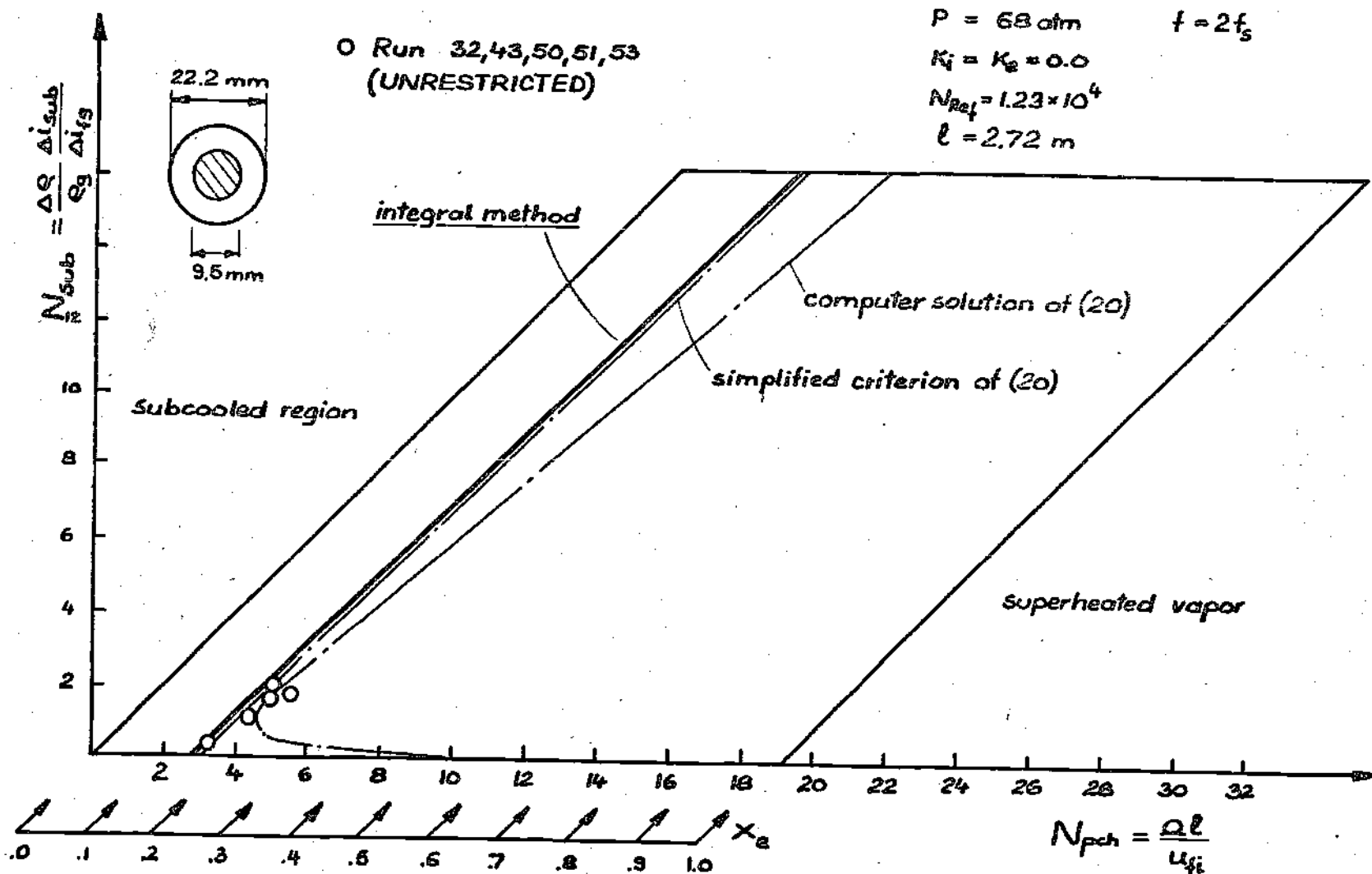


Figure 33. Comparison with Levy's Experiments and the Theory of Ishii and Zuber(20)

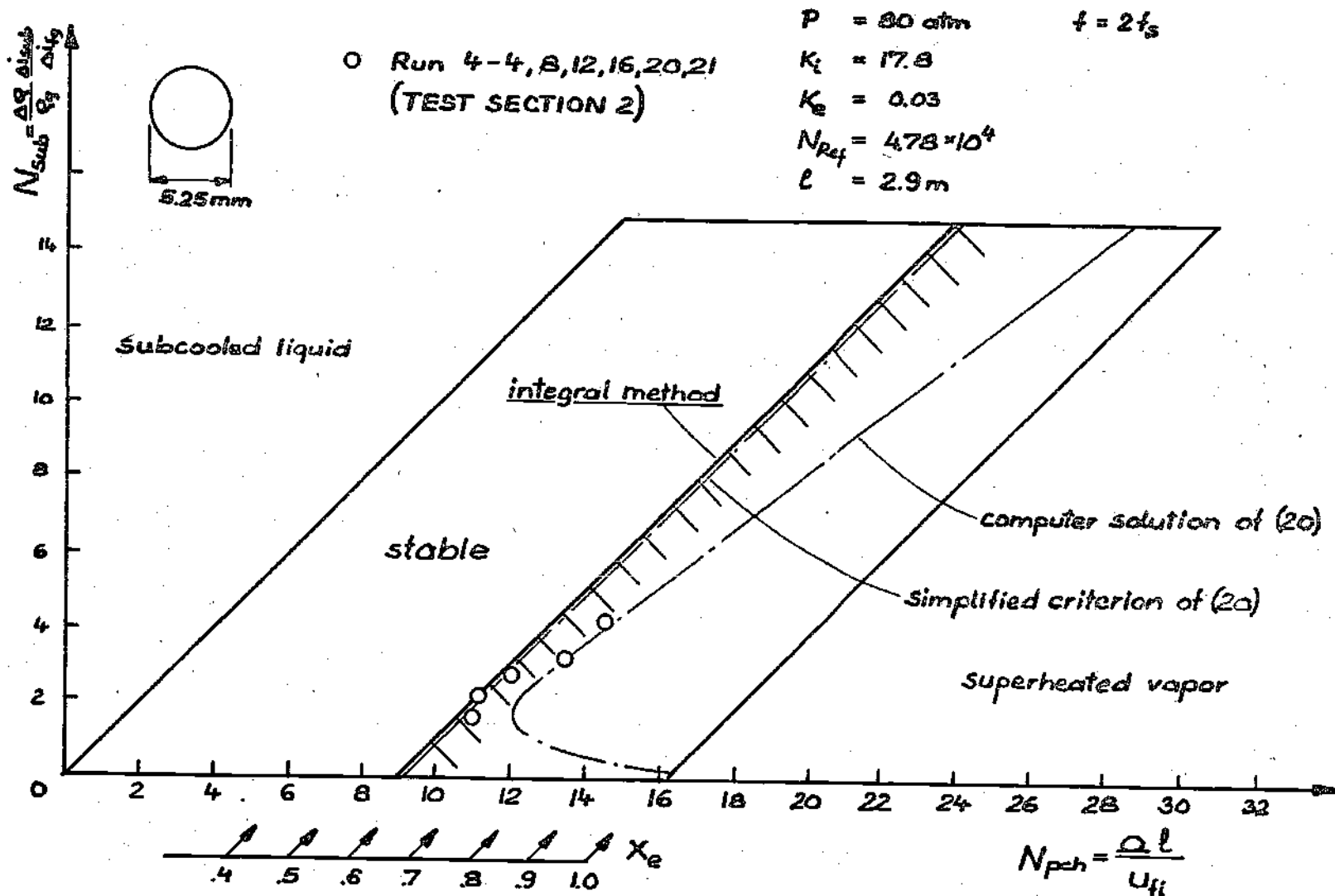


Figure 34. Comparison with Solberg's Experiments and the Theory of Ishii and Zuber(20)

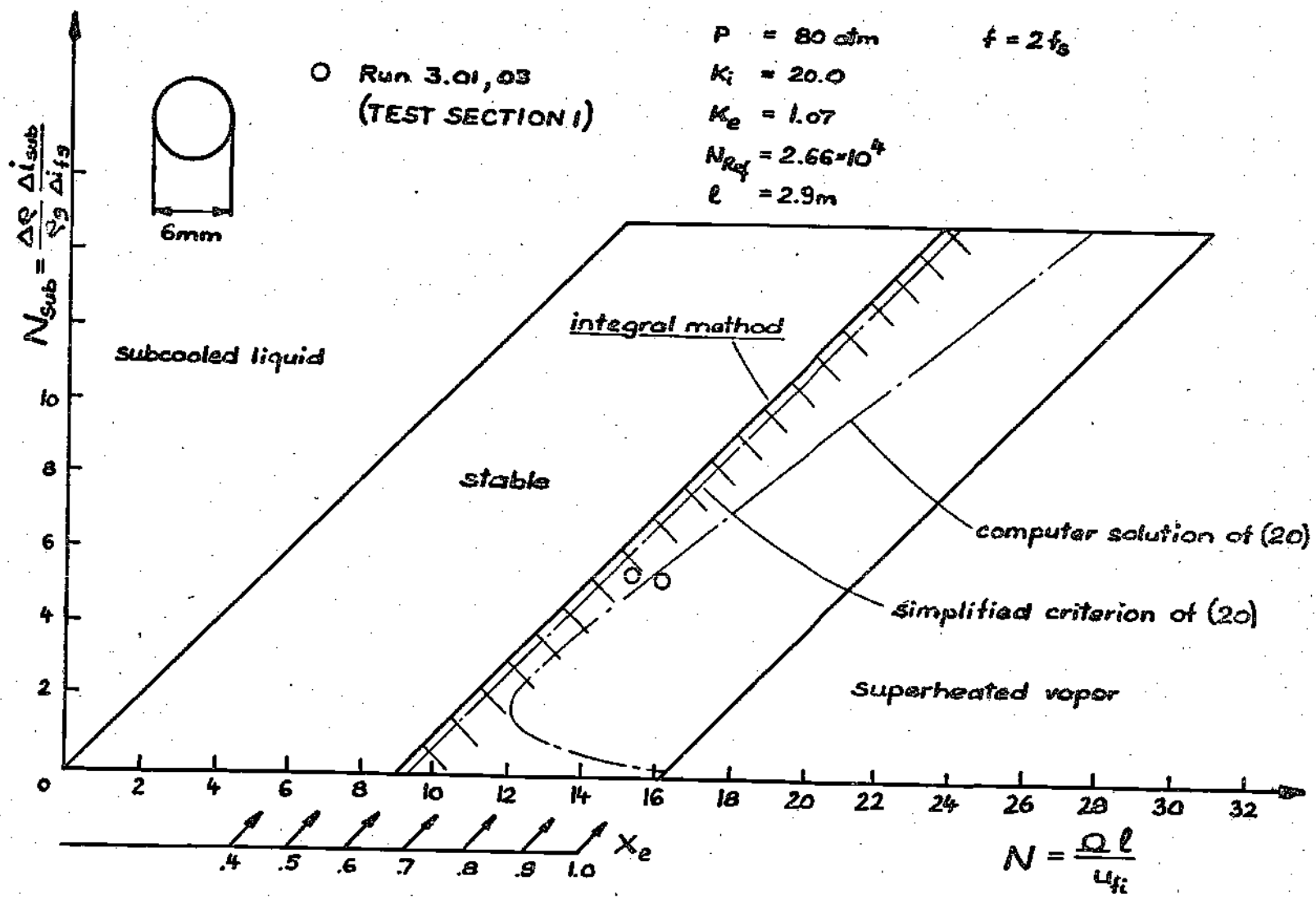


Figure 35. Comparison with Solberg's Experiments and the Theory of Ishii and Zuber(20)

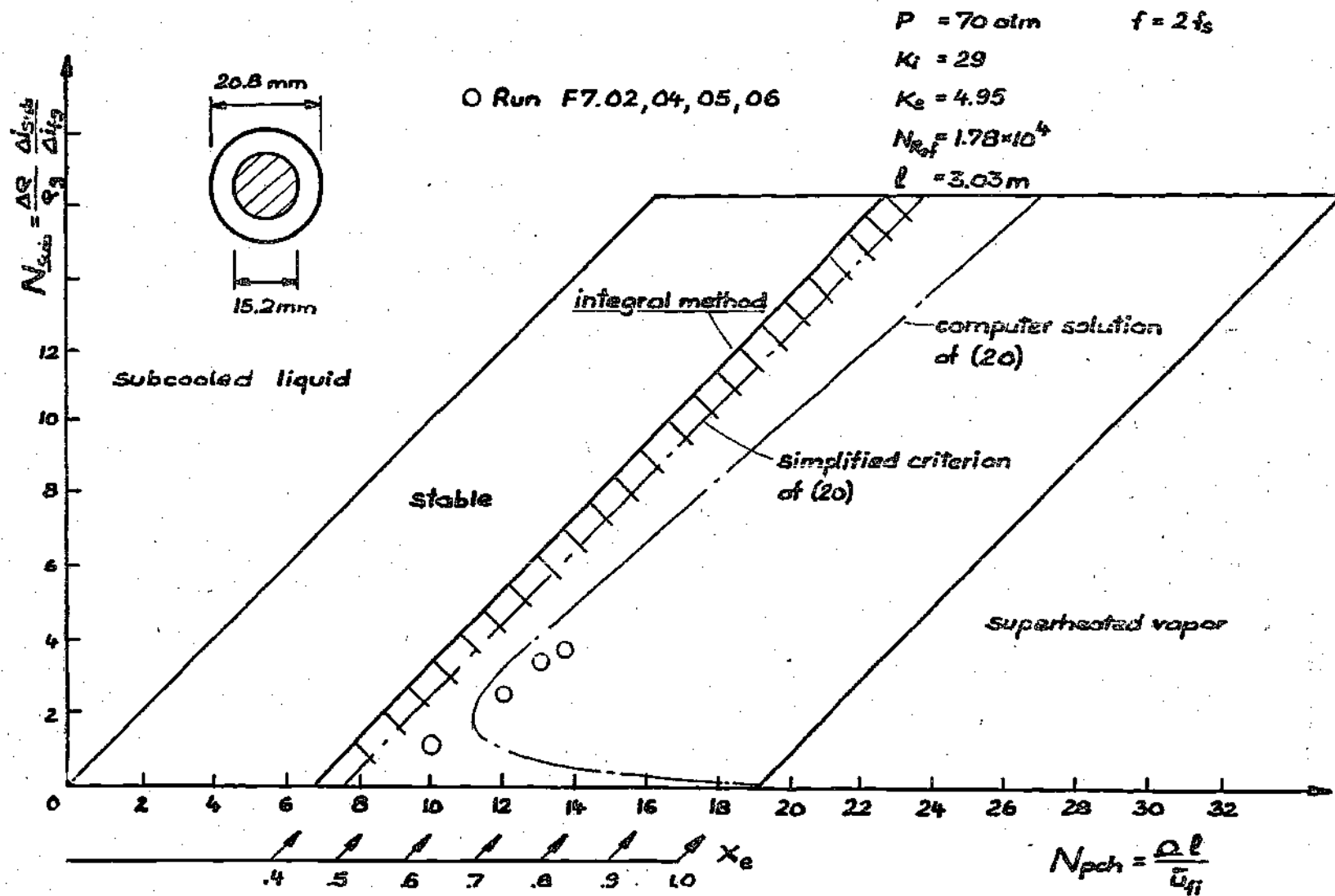


Figure 36. Comparison with FLARE Experiments and the Theory of Ishii and Zuber(20)



With

$$1 - \lambda^* = \frac{C_r^* - 1}{N_{pch}} \quad 6.43$$

neglecting the gravitational forces

$$\frac{\bar{u}_f}{C_r^*} \frac{1}{Z_{Fr}} \approx 0 \quad 6.44$$

and for high  $C_r^*$  values

$$\frac{\bar{u}_f}{C_r^*} \approx 0 \quad 6.45$$

Equation 6.41 finally reduces to

$$C_r^* - 1 < \frac{2 \left\{ k_i + \frac{f_m}{2D^*} + k_e \right\} - (1 + k_e)}{1 + \frac{1}{2} \left\{ \frac{f_m}{2D^*} + 2k_e \right\}} \quad 6.46$$

In the following we shall set up a stability plane and perform a parametric study of the system based on the results just obtained.

### 6.5. The Stability Plane

One of the final purposes of this research is to investigate the influence of different operational variables on the stability of the system. This will be best performed by analyzing the stability criterion equation 6.46 in a two dimensional plane. If we fix the inlet velocity, system pressure and its geometry, we obtain for the coordinates of such a stability plane the subcooling number  $N_{sub}$  and the phase change number  $N_{pch}$ . The subcooling number is always positive but upper bounded by  $\Delta i_s$ , corresponding to the freezing point

$$0 \leq N_{sub} \leq \frac{\Delta i_s}{\Delta i_{fs}} \frac{\Delta Q}{\rho_g}$$

6.47

Moreover from the condition that boiling takes place in the channel, but super-heating of the vapor does not occur, we obtain

$$N_{pch} - \frac{\Delta Q}{\rho_g} < N_{sub} < N_{pch}$$

6.48

Thus the operational domain in the stability plane is bounded. Figure 30 shows these conditions and the relationship between  $N_{sub}$  and  $N_{pch}$  given by equation 6.34 and equation 6.38.

### 6.6. Parametric Analysis of the System

Equation 6.37 in equation 6.38 gives with equation 6.34 and equation 6.45 for stability

$$C_r^* - 1 = X_e \frac{\Delta p}{\rho g} = N_{pch} - N_{sub} < \frac{2 \left\{ k_i + \frac{f_m}{2D^*} + k_e \right\} - (1 + k_e)}{1 + \frac{1}{2} \left\{ \frac{f_m}{2D^*} + 2k_e \right\}}$$

6.49

This expression combines the inequality obtained in section 6.3 with the coordinates of the stability plane. If the operational variables on the right hand side of the inequality are independent of the phase change number  $N_{pch}$  and the subcooling number  $N_{sub}$ , then the functional relationship

$$N_{sub} = f(N_{pch})$$

6.50

is a straight line, which intersects the abscissa for  $N_{sub} = 0$ , thus

$$N_{pch} = \frac{2 \left\{ k_i + \frac{f_m}{2D^*} + k_e \right\} - (1 + k_e)}{1 + \frac{1}{2} \left\{ \frac{f_m}{2D^*} + 2k_e \right\}}$$

6.51

and represents the stability boundary of the system.

A. Influence of  $N_{sub}$  (Subcooling). We consider a system with fixed geometry, Reynolds number  $N_{Re}$ , inlet and outlet flow restrictions  $K_i$  and  $K_e$ , system pressure and also fixed phase change number  $N_{pch}$ . From Figure 31 we see that by increasing the subcooling number  $N_{sub}$ , the point of operation moves away from the stability boundary into the stable domain. Therefore the system has been hereby stabilized.

B. Influence of  $N_{pch}$  (Heat Flux). The same as in A, but now with constant subcooling number  $N_{sub}$ , and increasing  $N_{pch}$  shifts the point of operation into the unstable region.

C. Influence of the System Pressure. An increase of the system pressure does not affect noticeably the parameters on the right hand side of equation 6.51. But the exit quality  $x_e$  decreases, thus stabilizing the flow.

D. Influence of the Inlet Velocity  $\bar{u}_f$ . If in equation 6.51 the inlet and outlet flow restrictions  $K_i$  and  $K_e$  and the friction factor  $f_m$  are independent of the Reynolds number  $N_{Re}$ , then the phase change number  $N_{pch}$  will be the only parameter affected by inlet velocity variations. From equation 6.36 we see that for an increasing inlet velocity  $\bar{u}_f$ , the phase change number  $N_{pch}$  decreases and therefore according to B, the point of operation shifts into the stable region.

E. Influence of the Friction Factor  $f_m$ . An increase of the friction factor  $f_m$  means that the expression on the right hand side

of equation 6.51 decreases. Herewith the stability boundary shifts to the left thereby destabilizing the system.

F. Influence of the Inlet and Outlet Flow Restrictions  $k_i$  and  $k_e$

Analogous to E in equation 6.51 it can easily be verified that the increase of  $k_i$  has a stabilizing effect, whereas the increase of  $k_e$  destabilizes the system.

6.7. Evaluation of the Results

The theoretical investigations presented so far had the main purpose to apply an integral method in the evaluation of instabilities in two-phase flow systems. The results will be compared to the experimental data of Levy (29), Solberg (30), Carver (31) and the theoretical analysis of Ishii and Zuber (20). These authors, as was also done in the present work, particularly examined operational flow conditions at high pressures. Thus they assume the mixture to be in thermal equilibrium, neglect the pressure drop effects on the fluid properties and limit the stability analysis to the low frequency range. Moreover the experimental work was done for both circular and annular tube geometries and for different diameters.

Figures 33, 34, 35, and 36 show that the obtained results are in very good agreement with the mentioned literature (20, 29, 30, 31). Surprising is the similarity of equation 6.51

$$X_e \frac{\Delta \rho}{\rho_g} = N_{pch} - N_{sub} < \frac{2 \left\{ k_i + \frac{f_m}{2D^*} + k_e \right\} - (1 + k_e)}{1 + \frac{1}{2} \left\{ \frac{f_m}{2D^*} + 2k_e \right\}}$$

with the corresponding solution of Ishii and Zuber

$$X_e \frac{\Delta \rho}{\rho_g} = N_{pch} - N_{sub} < \frac{2 \left\{ k_i + \frac{f_m}{2D^*} + k_e \right\}}{1 + \frac{1}{2} \left\{ \frac{f_m}{2D^*} + 2k_e \right\}}$$

6.52

These equations differ within 6 per cent, whereby equation 6.51 is shifted to the left and tends to predict a more unstable system than the measured data and the theoretical work cited at the beginning of this section. Equation 6.51 also does not account for the large stability increase at extremely low subcooling. This effect was not noticed by Levy (29), Solberg (30) and Carver (31), but it was observed by Yadigaroglu and Bergles (19) and also confirmed by the computer solution of Ishii and Zuber (see dotted lines in Figures 33, 34, 35, 36). The actual flow conditions for very small subcooling numbers  $N_{sub}$  are still not known exactly because of experimental difficulties. It is believed that in this region big changes of the phase change number  $N_{pch}$  do occur due to subcooled flow boiling. In this case the phase change proceeds further than for thermal equilibrium and the value of  $N_{pch}$  increases.

The inlet and outlet orifice coefficient  $k_i$  and  $k_e$ , were not given by the experimental data of (29, 30, 31). The present analysis is based on the evaluation of (20), who determined the values from steady state pressure drop equations.

For the friction factor the equation

$$f_m = C_m f_s$$

with  $C_m = 2$  and  $f_s = \frac{0.184}{N_{Re}^{0.2}}$

6.53

was used. The value 2 for  $C_m$  gives a slightly higher pressure drop than the Martinelli and Nelson Correlation. For a smooth pipe the liquid friction factor  $f_s$  is only a function of the Reynolds number  $N_{Re}$ .

As was shown in the present section, the integral method has provided a very satisfactory criterion to avoid unstable operation in the design of two-phase flow systems. However, it should be remembered that the entire analysis was based on linearized field equations. Therefore the theoretically predicted stability boundary only considers incipience instability. Whether unstable flow conditions appear or not will largely depend on the nonlinearities, which were neglected. Nevertheless the agreement between measured and analytically predicted stability boundaries is surprising.

## CHAPTER VII

## SUMMARY AND RECOMMENDATIONS

The analysis is composed of two main parts. The first one presented a differential method based on theoretical investigations of Zuber (1) to study the physics of two-phase flow systems. The second part treated the problem of instabilities in two-phase flow systems by means of an integral method.

Differential Method

An extensive study of the single phase region was made. The mathematical solution was derived as in (1) using the fundamental one-dimensional field equations and the constitutive equation. Additionally, the behavior of the boiling boundary as a function of frequency and subcooling, and of pressure drop as a function of frequency and system parameters was analyzed in detail. The results were plotted in graphs to facilitate the physical understanding. Here it was found for example that large pressure variations can also occur for small frequencies if the inlet flow restriction becomes sufficiently high.

The two-phase region was treated similarly to the first one. Moreover the limitation of the analysis to the low frequency range was proven. The equations of state for a medium at subcritical and supercritical pressures were compared and then generalized to a single one. The velocity distribution in the two-phase region was



derived connecting the continuity and energy equation. In contrast to (1), the density as a function of time and space was obtained by reusing the continuity equation. With density and velocity profiles known, the pressure perturbation followed out of the momentum equation. Again as for phase one, graphical representations were set up, which helped to visualize the physical behavior of the system towards an inlet velocity perturbation. Finally, a qualitative analysis showed that in the high frequency domain instabilities occur because of very large pressure variations, which are necessary to account for the inertia forces of the fluid.

#### Stability Analysis by Means of an Integral Method

To reduce the number of errors, the application of the simplifying integral method was limited to the evaluation of the density variations and the pressure perturbations in the two-phase region.

The overall density changes were determined by integrating with respect to space in two ways:

(1) Introducing the velocity profile directly into the continuity equation, therefore proceeding as was done for the differential method.

(2) Using energy and constitutive equation in accordance to (1). Both solutions were carefully compared and gave a very simple expression for the density perturbation in the second region.

The pressure drop was obtained by averaging the momentum equation and introducing here the velocity profile and the simplified expression for the density.

Out of the pressure drop equation for the entire system, a

characteristic equation was determined.

As in (20) a simple stability criterion was applied to this equation. Neglecting the higher orders of the frequency  $\omega$  a stability analysis was easily accessible. The results obtained are excellent. Although for very complex systems theoretical investigations have the main purpose to help us in understanding the physics and the parametrical behavior of the system itself, the present analysis delivered surprisingly good agreement with experimental data and the very extensive theoretical studies in (20).

#### Recommendations

Because of its many applications in modern technology further research in this area is absolutely necessary. Based on the model used in this work, it is recommended to perform in analogy to this investigation similar stability analysis for the case of heat addition and subcooling variations. Together with the present one a generalized analysis could be made. This means in this case we would consider a simultaneous perturbation of several varying parameters. Writing for the velocity perturbation  $\delta u_1$ , the heat addition variation  $\delta \Omega$  and for the subcooling changes  $\delta \Delta i_{sub}$  we would write an expression for the pressure perturbation in the form

$$\delta \Delta P = Q_1 \delta u_1 + Q_2 \delta \Omega + Q_3 \delta \Delta i_{sub}$$

Here  $Q_1$ ,  $Q_2$ , and  $Q_3$  are the corresponding characteristic equations, or using the scalar product of two vectors

$$\delta \Delta P = \vec{Q} \cdot \vec{\delta C}$$

with

$$\vec{Q} = \begin{pmatrix} Q_1 \\ Q_2 \\ Q_3 \end{pmatrix}$$

as a "characteristic vector" of the system and

$$\vec{\delta C} = \begin{pmatrix} \delta u_1 \\ \delta \varrho \\ \delta \Delta i_{sub} \end{pmatrix}$$

as the generalized "perturbation vector."

## BIBLIOGRAPHY

1. Zuber, N., "An Analysis of Thermally Induced Flow Oscillations in the Near-Critical and Super-Critical Thermodynamic Region," NASA Report No. 8-11422., 1966.
2. Hines, W. S., and Wolf, H., American Rocket Society Journal, v. 32, p. 361, 1962.
3. Cornelius, A. J., and Parker, J. D., 1965 Heat Transfer and Fluid Mechanics Institute, University of California, Los Angeles, 1965.
4. Cornelius, A. J., Argonne National Laboratory, 7032, April 1965.
5. Firstenberg, H., Atomic Energy Commission - US; NDA - 2131 - 12, June, 1960.
6. Thurston, R. S., Los Alamos National Laboratory - 3070, TID - 4500, 1964.
7. Shitzman, M. E., Teplofizika Vysokih Temperatur, V. I., p. 267, 1965.
8. Shitzman, M. E., paper no. 1-59, Second All-Union Conference on Heat and Mass Transfer, Minsk, 1964.
9. Semenkover, I. E., Energomashinostroenie, no. 3, p. 16, 1964.
10. Krasiakova, L. I., and Glusker, B. N., Energomashinostroenie, no. 9, p. 18, 1965.
11. Ledinegg, M., Die Waerme, v. 61, no. 48, p. 891, 1938.
12. Ledinegg, M., "Das Verhalten von Zwangdurchlaufkesseln bei Lastsenderungen," Brennstoff - Waerme - Kraft 12, Nr. 5, p. 197, 1960.
13. Profos, P., Sulzer Technical Review, no. 1, p. 1, 1947.
14. Profos, P., Energie, no. 6, p. 193, 1956.
15. Profos, P., Die Regelung von Dampfanlagen, Springer Verlag, Berlin, 1962.

16. Wallis, G. B., and Heasley, J. H., Journal of Heat Transfer, ASME Trans. Series C, v. 83, 363, 1961.
17. Quandt, E.R., "Analysis and Measurements of Flow Oscillations," Chemical Engineering Progress Symposium, Ser. 57, No. 32, 111-126, 1961.
18. Mayinger, F., and Kastner, W., "Berechnung von Instabilitaeten in Zweiphasenstroemungen," Chemie-Ingenieur-Technik, 40. Jahrgang, p. 1185.
19. Yadigaroglou, G., and Bergles, A. E., "An Experimental and Theoretical Study of Density--Wave Oscillations in Two-Phase Flow," MIT Report No. DSR 74629 - 3, 1969.
20. Ishii, M., and Zuber, N., "Thermally Induced Flow Instabilities in Two-Phase Mixtures," 4th International Heat Transfer Conference, Paris, 1970.
21. Serov, E. P., and Smirnov, O. K., Teplofiziks Vysorih Temperature, v. 2, no. 4, p. 623, 1964.
22. Serov, E. P., "The Operation of Once-Through Boilers in Variable Regimes," Trudy, Moscow Energ. Insi. 11, 1953.
23. Serov, E. P., "Transient Process in Steam Generators," Teploenergetik, vol. 13, 9, p. 50, 1966.
24. Serov, E. P., "Analytical Investigations of the Boundary Conditions for the Formation of Pulsation in Steaming Pipes During Forced Circulation," High Temperature, vol. 3, p. 545, 1965.
25. Teletov, C. G., "The Hydrodynamic Equations of Two-Phase Fluids," Akademia Nauk S.S.S.R., Doklady, vol. 50, p. 99, 1945.
26. Boure, J., Report TT No. 55, Centre d'Etudes Nucleaires de Grenoble, France, 1965.
27. Boure, J., "The Oscillatory Behavior of Heated Channels. An Analysis of Density Effects," C.E.A.R. 3049, Centre d'Etudes Nucleaires de Grenoble, France, 1966.
28. Crocco, L., and Cheng, S. I., "Theory of Combustion Instability in Liquid Propellant Rocket Motors," Pergamon Press, Oxford, 1956.
29. Levy, S., and Beckjord, E. S., "Hydraulic Instability in a Natural Circulation Loop with Net Steam Generation at 1000 psia," G.E.A.P., 3215, General Electric, San Jose, California, July 15, 1959.

30. Solberg, K., "Resultats des Essais d'Instabilities sur la Boucle 'Culine' et Comparisons avec un Codes de Calcul," C.E.N.G., Note 225, Centre d'Etudes Nucleaires de Grenoble, France, 1966.
31. Carver, M. B., "An Analytical Model for the Prediction of Hydrodynamic Instability in Parallel Heated Channels," A.E.C.L., 2681, Atomic Energy Canada Limited, 1968.